Title
microRNA Regulation of Cardiac Development

Author
Morton, Sarah

Publication Date
2008-06-24

Peer reviewed|Thesis/dissertation

MICRORNA REGULATION OF CARDIAC DEVELOPMENT

by

SARAH UHLER MORTON

DISSERTATION

Submitted in partial fulfillment of the requirements for the degree of

DOCTOR OF PHILOSOPHY

in

Biochemistry

in the

GRADUATE DIVISION

of the

University of California, San Francisco

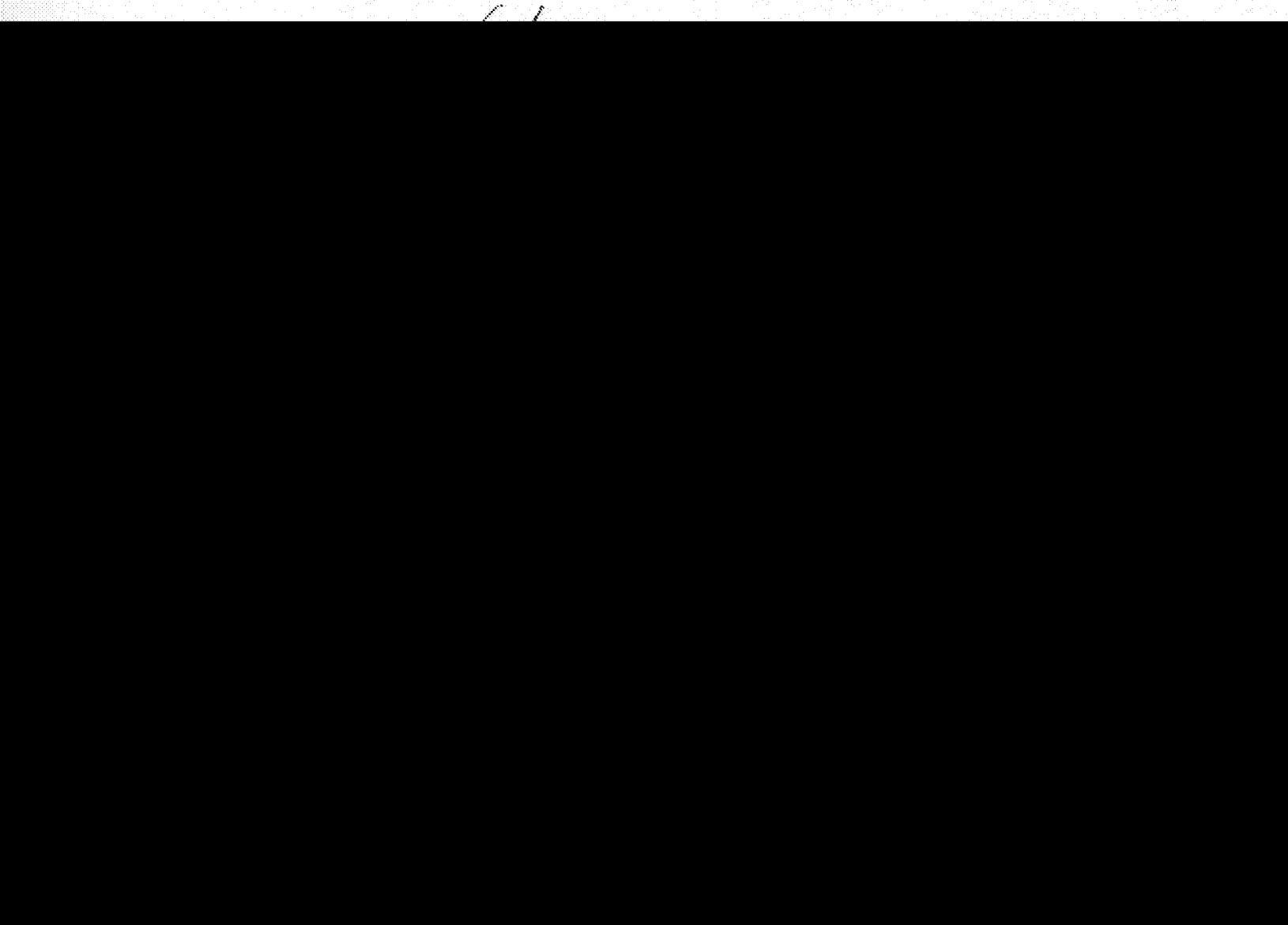

This thesis is dedicated to my husband Jason. The multitudes of reasons for the dedication are best known to him, and include but are not limited to: his unrelenting love, constant support, passion for research and excellent taste in diet pop. Thank you for everything you have done, both those acts I am aware of and the countless kind things that I perhaps haven't yet noticed.

Acknowledgements

When writing a short biographical piece for the Gladstone *Messenger* I had the opportunity to reflect on the early influences in my life that lead to a love of science, and learning more broadly. It is undeniable that my parents are the source of these influences: from electronics sets and microscopes to cross stitching and music, my parents always encouraged me to learn new skills and try new activities, no matter how much accomplishment (or lack thereof) I accrued. Thank you to them for their love and support. Also I would like to thank my brothers, Alan and Thomas, for always making me smile. Sometime even simple smiles can be a bit hard to come across during graduate training.

Academically, I would like to acknowledge first and foremost my mentor, Deepak Srivastava, for his mentorship and support. I have told countless aspiring physician scientists about how you are 'living the dream' and I am lucky to have trained with someone who can excel both at research and in the clinic. I aspire to do the same, and repay your contribution to me with future good work.

I would also like to thank the members of my thesis committee, Michael McManus and Shaun Coughlin, for their guidance and support. They have provided me with scientific and person advice that greatly improved my graduate training. The members of my qualifying exam committee, Michael McManus, Shaun Coughlin, Didier Stainier and Brian Black, also served as wonderful mentors and helped me to improve my research plans.

Many other members of the UCSF community have been instrumental to my research. Kathy Ivey has been a wonderful source of advice and useful critiques; Alecia Muth and Kim Cordes have worked with me to optimize experimental approaches and hypotheses; Vasanth Vedantham and Jason Fish have been wonderful mentors for bench science and career questions; Paul Scherz and Neil Chi have been wonderful collaborators; and Didier Stainier has given freely of his time, advice and zebrafish resources. Bethany Taylor taught me everything I need to know about figure preparation.

Preface

The material presented in Chapter 2 of this dissertation, "miR-138 Is Necessary for Cardiac Patterning" currently under review for publication. The authors were Sarah U. Morton, Paul J. Scherz, Kimberly R. Cordes, Kathy N. Ivey, Didier Y.R. Stainier and Deepak Srivastava.

The material presented in Chapter 3, "miR-202* Is Necessary for Left-Right Patterning", is a work in progress. The co-authors of Chapter 3 are Neil C. Chi, Robin M. Shaw, Kimberly R. Cordes, Didier Y.R. Stainier, Deepak Stainier, and Kathy N. Ivey.

Deepak Srivastava, listed in both publications, directed and supervised the research that forms the basis for the dissertation/thesis. Co-authors other than the research advisor contributed meaningfully to the design of the experiments and to their execution. Sarah Morton lead these two projects, participated in the design of all experiments, and executed a portion of all experiments. The text of the manuscripts was prepared primarily by Sarah Morton and Deepak Srivastava. The work contained in this dissertation is therefore comparable to that contained in a standard dissertation.

_____

Deepak Srivastava

Abstract

microRNAs (miRNAs) are small RNAs known to be necessary for normal development of vertebrates, including development of the heart. miRNAs act primarily through post-transcriptional inhibition of protein expression. Two miRNAs described in this thesis, miR-138 and miR-202*, are shown to be necessary for cardiac development in zebrafish.

miR-138 ensures proper patterning of the cardiac chambers by clearing mRNA transcripts from the ventricle, allowing proper maturation of ventricular cardiomyocytes. Reduction in miR-138 results in cardiac dysfunction and lack of maturation in cardiomyocytes located on the outer curvature of the ventricle. Direct inhibition of Raldh2 protein by miR-138 in the ventricle, resulting in reduced expression of retinoic acid (RA), is necessary to restrict expression of proteins such as Versican to the atrioventricular canal. Interestingly, Versican expression in the ventricle is also directly inhibited by miR-138. Thus miR-138 is demonstrated to be the first miRNA involved in cardiac patterning, and achieves inhibition of Versican expression both directly and indirectly via targeting of Raldh2. The targeting of multiple members of a pathway allows for robust clearance of early ventricular mRNAs.

miR-202*, in contrast, is necessary for both proper development and function of zebrafish hearts. Inhibition of miR-202* in zebrafish embryos leads to randomization of the left-right patterning of the heart, as well as cardiac conduction abnormalities. In cell culture, miR-202* is able to target Pkd2 protein for inhibition; Pkd2 is a calcium channel known to be necessary for specification of the left-right axis in vertebrates. Embryos with knockdown of miR-202* also demonstrate a 2:1

atrioventricular node (AV) block, where the atrium conducts twice for every ventricular conduction. The molecular mechanism for 2:1 AV block remains unknown, but elucidating the targets responsible for the phenotype will give insight into human diseases with similar conduction abnormalities.

In summary, the studies described here identify two miRNAs as being necessary for normal development and/or function of the heart. Future studies further elucidating the role of miR-138 and miR-202* in mammals will provide insight into connections between these miRNAs and human disease.

Table of Contents

Table of Figures

Chapter One:

General Introduction

Part 1: Cardiac Development

The heart is the first organ to function during mammalian development. In humans, congenital heart disease, which occurs in 1% of all live births, is a cause of significant morbidity and mortality (Hoffman, Kaplan et al. 2004). Heart disease, whether congenital or acquired, presents an enormous burden on individuals and society. Though many diseases of the heart and vasculature are multifactorial in origin, we have begun to understand the contribution of single genes, including transcription factors and miRNAs, to many congenital and acquired conditions.

The mature mammalian heart consists of four chambers: a right and left atrium, where blood is received from systemic and pulmonary circulation, respectively; and a right and left ventricle, which sends blood to the pulmonary and systemic circulation, respectively. The atrium and ventricle of each side of the heart are separated by an atrioventricular valve which regulates the flow of blood. In contrast, the mature zebrafish heart consists of only two chambers: a single ventricle and a single atrium, separated by an atrioventricular (AV) canal region, which has a single valve. Though the structure of the hearts differs significantly between zebrafish and mammals, the molecular and cellular events that pattern the heart are largely conserved. Thus a combination of studies in zebrafish and mouse models allows the study of many aspects of heart development relevant to human disease.

Approximately one-third of nonsyndromic congenital heart defects involve the outflow tract of the heart, commonly in the form of a double outlet right ventricle (DORV) or tetrology of Fallot (TOF) (Valdes-Dapena and Gilbert-Barness 2002). Similarly, diseases of the AV canal and its valves, such as mitral valve stenosis, can be congenital or acquired. Understanding the molecular mechanisms that control

development of the heart, especially of the outflow tract and AV canal, will provide insight into why these regions are affected by disease.

Cardiac Progenitor Fields

The chambers of the heart are derived from two different progenitor populations: the first heart field that gives rise to the future atria and left ventricle, and the second heart field that gives rise to the outflow tract and right ventricle (Mjaatvedt, Nakaoka et al. 2001; Cai, Liang et al. 2003) (Figure 1-1). Understanding the migration, specification, and differentiation of the first and second heart fields will further our understanding of how congenital abnormalities arise as the heart develops. As described in the following section, it is at embryonic day (E) 7 that the first heart field forms the cardiac bilateral crescent, which then fuses to form a linear heart tube by E7.5. The second heart field migrates from the pharyngeal mesoderm to the bilateral heart tube by E9.5, as the linear heart tube undergoes looping. The AV canal is derived from the first heart field, and its specification starts as early as E12.5. Though the timing of the morphological events in cardiac development is well characterized, the key molecular signals for heart development are only starting to be understood.

Early Cardiac Development

The cells destined to become the heart are specified early in development. Heart precursors of the first heart field originate bilaterally from the lateral plate mesoderm around the 6th day of mouse embryonic development (Srivastava and Olson 2000). The cardiogenic mesoderm of the first heart field is induced by signals, such as BMP and FGF, from the adjacent anterior endoderm (Schultheiss, Xydas et al. 1995; Schultheiss, Burch et al. 1997; Alsan and Schultheiss 2002). Early on these cardiac progenitor fields begin to express the gene *Nkx-2.5*. The symmetric

fields of cardiac progenitors meet anteriorly by E7, forming the cardiac crescent. Over the next day of development the crescent fuses down its length forming a linear heart tube. Failure of fusion, resulting in cardia bifida, can be caused by mutations in *Foxp4*, which is expressed in the underlying foregut endoderm and acts as a signal for migration of the cardiac progenitor fields (Li, Weidenfeld et al. 2004; Li, Zhou et al. 2004).

Even at this early stage of embryonic development, the atrial and ventricular precursors are distinct populations. Ventricular progenitors are found anterior to the atrial progenitor population along the cardiac crescent. During migration of the bilateral heart fields, there is a gradient of retinoic acid (RA) signaling from posterior to anterior, generated by the posterior mesoderm. RA serves to drive the cardiac progenitors to an atrial fate (Stainier and Fishman 1992). RA also plays an important role in later cardiac development, though it is expressed by the epicardium at that later stage (Stuckmann, Evans et al. 2003).

The zebrafish heart is similarly formed from bilateral fields of mesoderm progenitors, which fuse to form a linear tube by 24 hours post fertilization (hpf). At this point the linear tube is able to circulate blood, but the thinness of the embryo allows for normal development to occur in the absence of cardiac function until 5 days post fertilization. Studies demonstrating the presence of a second heart field in zebrafish have not been published.

Cardiac Looping

The linear heart tube, with ventricular and atrial progenitors oriented on the anterior-posterior axis, undergoes a series of looping events to produce the spatial distribution of chambers found in the adult heart. The left-right axis of the heart is set up by a highly conserved set of genes, including *Nodal*, *Lefty-1*, *Lefty-2* and *Southpaw* (Levin, Johnson et al. 1995; Collignon, Varlet et al. 1996; Meno, Saijoh et

al. 1996). Proper expression of the proteins encoded by these genes is important for overall left-right asymmetry of the body, including the digestive system. Aberrations in the expression of these genes can lead to randomization of left-right asymmetry in the entire organism, including the direction of looping of the heart tube (Kathiriya and Srivastava 2000).

Cardiac looping in zebrafish culminates in a leftward bend between the atrium and ventricle around 32 hpf, positioning the atrium to the right of the ventricle. The AV canal, the future site of the heart valve, is specified by 48 hpf. However, in this process the overall direction of blood from caudal to cranial along the body is not altered. In contrast, the process of cardiac looping in mammals is more extensive, as the heart tube bends 180° on itself, converting the anterior-posterior axis of the heart into a left-right polarity. After the looping is complete, the heart tube is oriented to allow further differentiation of the four chambers of the mammalian heart.

Chamber Morphogenesis

As the chambers of the heart develop, another set of left-right patterning events occur. The atrial progenitors move from a posterior to a left position, while the ventricle moves from anterior towards the right. The chamber identity of left ventricle is associated with Hand1 expression, while the right ventricle expresses Hand2 (Srivastava, Cserjesi et al. 1995). Once the chambers are specified by these restricted patterns of gene expression, there is ballooning of the outer curvature of the heart tube, forming an enlarged space that is the early ventricular chamber (Christoffels, Habets et al. 2000). This ballooning proceeds via asymmetric growth of myocardium, predominantly on the outer curvature of the primitive ventricle. Also particular to the chamber myocytes is the ability to form the trabeculations that

allow efficient contraction of the heart. These trabeculations arise primarily from the outer curvature regions of the heart tube.

Heart cells that occupy portions of the heart tube that do not express the chamber-specific genes are referred to as non-chamber myocardium. Non-chamber myocardium is present at the AV canal and outflow tract of the mouse and zebrafish hearts (Walsh and Stainier 2001; Garrity, Childs et al. 2002). *Tbx2* and *Tbx3* are important genes in repressing the expression of chamber-specific genes, such as *Anf*, in non-chamber myocardium (Ribeiro, 2007). Endocardial cushions, the valve-forming tissue of the heart, form between the atrium and ventricle (Eisenberg and Markwald 1995) from the non-chamber myocardium of the AV canal. It is this valve that allows unidirectional blood flow from the atrium to the ventricle.

Cardiac Outflow Tract

The outflow tract of the heart, which is composed of the aorta and pulmonary artery in the adult heart, is populated by cells from the second heart field that migrate during cardiac looping, at approximately E9.5 in mouse development. Studies mapping the second heart field lineage have used injection of DiI or transgenic expression of LacZ to determine which structures these cells contribute to the adult heart. Second heart field-derived cells are consistently observed in the outflow tract and right ventricle, and studies using *Islet-1*, a gene expressed in the second heart field and other tissues, to drive expression of LacZ also show staining in the interventricular septum and left ventricle (Verzi, McCulley et al. 2005). The migration and differentiation of these cells depend on signaling from the cardiac neural crest, as ablation of the cardiac neural crest leads to deficiencies in migration of cells from the second heart field (Yelbuz, Waldo et al. 2002). Thus it is likely that an aberration in migration and differentiation of the second heart field cause congenital malformations seen in the cardiac outflow tract.

Congenital Cardiac Abnormalities

Many genes have been identified as contributing to inherited or spontaneous abnormalities in cardiac development. Some characterized sets of transcription factors, such as *GATA-4*, *Tbx-5*, *Nkx-2.5*, are known to often co-regulate targets and are also seen to be mutated in many forms of congenital heart disease (Basson, Bachinsky et al. 1997; Goldmuntz, Geiger et al. 2001; Garg, Kathiriya et al. 2003). Many inherited cardiac abnormalities have not yet been linked to a single gene mutation, and it is possible that aberrations in the expression or function of miRNA genes, discussed in the subsequent sections, may play a role in some diseases of cardiac development.

Part 2: microRNA

miRNAs are non-coding RNAs that are highly conserved among vertebrate and invertebrate organisms (Berezikov, Cuppen et al. 2006). There have been hundreds of miRNAs identified in the human, rat, mouse, chicken, and zebrafish genomes, among others. Many of these miRNAs have been shown to be essential for physiological processes such as cardiac development, hematopoeitic lineage differentiation, and reproduction (Wienholds, Koudijs et al. 2003; Thai, Calado et al. 2007; Zhao, Ransom et al. 2007). miRNAs are also seen to be dysregulated in pathologic states such as lymphoma and carcinoma (Lawrie, Gal et al. 2008; Schetter, Leung et al. 2008). Thus the study of these newly-characterized noncoding RNAs will help to advance our understanding of normal development and disease states, potentially leading to new therapeutics (Novina and Chabner 2008; Stenvang and Kauppinen 2008).

miRNA Discovery

miRNAs are 21-23 nucleotide (nt) short RNA molecules that were first discovered through a forward genetic screen in nematodes (Lee, Feinbaum et al. 2004). The first article describing miRNAs, published in 1993, identified *lin-4*, a short RNA, as a negative regulator of the protein encoded by *lin-14* during the first larval stage of *C. elegans* development. The ultimate cloning of short RNAs from the *lin-4* gene indicated that a new, non-coding RNA was in fact responsible for the genetic interactions between the *lin-4* and *lin-14* mutants (Lee, Feinbaum et al. 1993). However, it was not until 2001 that the term microRNA was first used to describe the class of small RNAs characterized by the interaction between a 21-23 nucleotide non-coding RNA and the 3' untranslated region (UTR) of an mRNA transcript (Ruvkun 2001). Three papers, published simultaneously, provided

biochemical and genetic proof for a broad class of small RNAs conserved across multiple species (Lagos-Quintana, Rauhut et al. 2001; Lau, Lim et al. 2001; Lee and Ambros 2001). This initial work also identified many processing steps necessary for miRNA maturation and function. From the first studies of miRNAs in vertebrates the important role of miRNAs in developmental processes was already apparent (Lagos-Quintana, Rauhut et al. 2002; Wienholds, Koudijs et al. 2003).

miRNA Biogenesis

miRNA genes can be found within the open reading frames (ORFs) of other genes, inside either intronic or exonic sequences (Lagos-Quintana, Rauhut et al. 2001; Rodriguez, Griffiths-Jones et al. 2004). Other miRNA genes are intergenic. Regardless of location, miRNAs are transcribed by RNA polymerase III into long, primary miRNA transcripts that can be thousands of bases long (Lee, Kim et al. 2004) (Figure 1-2). These primary miRNAs can contain a single miRNA, or several. One example of a miRNA cluster is the miR-17~92 gene cluster. The genomic locus for miR-17~92 encodes a polycistronic transcript, which results in 7 distinct mature miRNAs when processed.

Once transcribed, a nuclear complex containing Drosha, with an RNAse III domain, and DGCR8, a RNA-binding protein, cleaves the primary miRNA into a shorter hairpin sequence called the pre-miRNA (Lee, Ahn et al. 2003). These 70-90-nt pre-miRNAs are then exported from the nucleus via Exportin 5/RanGTP (Yi, Qin et al. 2003).

In the cytoplasm, the pre-miRNA is cleaved by Dicer to produce a mature miRNA bound to its reverse complement, often referred to as the passenger strand or miRNA* sequence (Lee and Ambros 2001). Both the miRNA and the miRNA* have 2-nt 3’ overhangs in most cases. miRNAs remain bound to Dicer, while the passenger strand is lost and protein subunits are added. The resulting RNA-protein

complex, which contains the miRNA, Dicer and other proteins, is known as the RNA induced silencing compex (RISC). RISC mediates targeting of mRNA by the bound miRNA (Matranga, Tomari et al. 2005), as the mature miRNA bound within RISC can bind to messenger RNA (mRNA) and cause either degradation of the mRNA or inhibit translation.

miRNA-Target Interactions

The binding of mRNA sequences by miRNAs is thought to be mediated by complimentarity between nucleotides 2-7 of the miRNA (known as the seed sequence) and the 3'UTR of the target mRNA in many cases (Lai 2002). Since it has been shown that nucleotides 2-7 of the mature miRNA can dictate specificity of binding, bioinformatic approaches using the seed sequence for target prediction have proven useful (Lewis, Shih et al. 2003; Lewis, Burge et al. 2005; Rajewsky 2006). Bioinformatics algorithms try to predict mRNA targets based on the presence of complementary sequences to the mature miRNA and the secondary structure near the predicted binding sites (Stark, Brennecke et al. 2003). This second characteristic, the structural availability of the miRNA binding site, has been demonstrated to be useful in predicting likely *in vivo* targets (Zhao, Samal et al. 2005). Characterized targets have at least one such binding site, and an accessible 3'UTR sequence that allows endogenous targeting events to occur (Zhao and Srivastava 2007). For instance, if the target site in the 3'UTR is found within a hairpin structure it will not be available for regulation by the miRNA despite the presence of complimentary sequences. The conservation of binding sites between species is also thought to increase the likelihood of an mRNA being a physiologic target of a miRNA (Brennecke, Stark et al. 2005).

After RISC has bound a target miRNA, two overall effects on target mRNA accumulation have been most frequently observed. In some cases, the abundance

of mRNA remains unchanged but translation of the target mRNA is inhibited. In other cases, the abundance of the target mRNA decreases, due either to deadenylation or endonucleolytic cleavage (Yekta, Shih et al. 2004). There have, however, also been recent reports of translational activation of mRNAs bound by miRNAs, in a cell-cycle dependent manner (Vasudevan, Tong et al. 2007; Vasudevan, Tong et al. 2008).

When the amount of mRNA targeted by a miRNA is observed to be unaltered by overexpression of the miRNA, it has been found that the RISC-mRNA interaction leads to localization of the complex to the processing bodies (p-bodies) where translation is inhibited but the mRNA itself is not degraded (Liu, Valencia-Sanchez et al. 2005). These mRNAs no longer fractionate with ribosome subunits, indicating that the mRNA is sequestered from translational activators and other transcriptional machinery while in the p-body (Doench and Sharp 2004). The miRNA-mediated localization of RISC to the p-bodies is also subject to regulation. In some cells there are protein factors that can bind RISC and prevent inhibition, leading to release of the mRNA. For example, the heptaocellular protein HuR is able to interfere with repression of CAT-1 by miR-122 in a reversible fashion (Bhattacharyya, Habermacher et al. 2006).

Other mRNA targets of miRNA regulation are subject to degradation, either by deadenylation or endonucleolytic cleavage (Hutvagner and Zamore 2002; Yekta, Shih et al. 2004). Endolytic cleavage has been demonstrated for miRNA-mRNA interactions with a high degree of complimentarity (Zamore, Tuschl et al. 2000; Yekta, Shih et al. 2004). The initial cleavage event is followed by rapid decay due to the unprotected 5’ and 3’ ends produced. However, endolytic cleavage of mRNA seems to be less common in animals than the 3’ deadenylation of target mRNAs (Giraldez, Mishima et al. 2006; Wu, Fan et al. 2006). The removal of the poly(A) tail is followed by loss of the poly(A) binding protein, which results in decapping (Behm-

Ansmant, Rehwinkel et al. 2006). 5'-exonuclease activity finally causes degradation of the target mRNA.

Regulation of miRNA Abundance

There are many means of miRNA regulation, both demonstrated and potential. It is known that the transcription of some miRNAs is dependent on characterized transcription factors, such as miR-1 transcriptional regulation by serum response factor (SRF) and myocardin (Zhao, Samal et al. 2005). Moreover, some miRNAs are downstream of other miRNAs, such as the dependence of cardiac miR-499 expression on miR-208 expression (van Rooij, Sutherland et al. 2007) ; van Rooij, unpublished).

Regulation of miRNA maturation has been observed for several miRNAs but this phenomenon is not fully understood. pre-miR-138 has been found to be ubiquitously expressed in near-term mouse embryos (Obernosterer, Leuschner et al. 2006). However, the mature form of miR-138 only accumulates to significant amounts in the brain and liver. Efforts to identify the protein factor that regulates processing of miR-138 abundance in mouse are actively underway in several laboratories. Potential protein regulators of this process are being identified by fractionation of active cytoplasmic extracts but the identity of the specific protein or RNA regulators is not yet known. However, and it has recently been reported that one such active cytosolic fraction has been isolated and shown to inhibit *in vitro* processing of pre-miR-138-2 (Obernosterer, unpublished). In another example, lin-28 has been shown to inhibit the processing of another miRNA, let-7, by Dicer both *in vivo* and *in vitro* (Viswanathan, Daley et al. 2008). In stem cells, lin-28 binds to pre-let-7, preventing accumulation of mature let-7 and allowing let-7 target mRNAs to be expressed. During differentiation, lin-28 expression is reduced, thereby allowing let-7 processing and subsequent inhibition of its target mRNAs.

miRNA abundance and target interactions can also be affected by sequence changes mediated by adenosine deaminases active on RNA (ADAR) proteins (Yang, Chendrimada et al. 2006). It has been shown the ADAR edits miR-142 in such as way as to affect both its processing by Dicer and its ability to bind to endogenous target mRNAs. Other sequence modifications, notably 3' uridylation, have also been demonstrated to lead to decreased processing of the pre-miRNA by Dicer (Ebhardt, Thi et al. 2005; Yu, Yang et al. 2005).

Finally, as mentioned above for the example of miR-122, protein cofactors can regulate the interaction between miRNAs and their target mRNAs. Though relatively few examples of this mode of regulation exist, the cell-cycle dependence of miRNA function indicates that more protein regulators of miRNA function may exist. It has been reported that the 3'UTR of tumor necrosis factor alpha (TNF alpha), which contains an AU-rich element (ARE), is translationally activated by miR-369 in response to cellular quiescence via target sites in the ARE (Vasudevan, Tong et al. 2007; Vasudevan, Tong et al. 2008). It remains unknown how the cell cycle is linked to miRNA function, but a protein involved in cell cycle regulation could directly or indirectly modify miRNA or RISC function differentially in S/G2 versus G0.

miRNA Function

Expression of miRNA can be tissue specific, indicating a role in organ development and function. In fact, general miRNA activity has been demonstrated to be necessary for gastrulation, the development of limbs, and many other physiologic processes (Giraldez, Cinalli et al. 2005; Harfe, McManus et al. 2005). However, the larger question of how miRNAs evolved as a regulatory mechanism does not have a clear answer.

What is the primary function of miRNAs? One answer is that miRNAs could be responsible for fine tuning the level of target proteins, thus keeping the amount of

target protein within a very tight range necessary for proper cellular and organismal physiology. This is an expected function served by miRNAs that regulate target mRNAs that are co-expressed in the same cell. One example is miR-214, which is expressed in somites during zebrafish development. miR-214 targets members of the Hedgehog signaling pathway, modulating the activity of the pathway. This modification of Hedgehog signaling by miR-214 results in proper specification of somites to a skeletal muscle fate (Flynt, Li et al. 2007).

In this case, where miRNAs subtly affect the amount of mRNA target, the amount of miRNA expressed in a cell would be titrated in response to the amount of target mRNA. A precedent for this type of regulation is seen in the case of transcriptional regulation of miR-1 in cardiac cells (Zhao, Samal et al. 2005). Though both miR-1 and its targets, SRF and dHAND, are all found in cardiac myocytes at overlapping times, modification of the amount of miR-1 causes profound phenotypes (Kwon, Han et al. 2005; Sokol and Ambros 2005; Yang, Lin et al. 2007). miR-1 likely regulates the expression level of its targets in order to keep the protein accumulation within specific limits; this process is aided by the positive feedback of SRF on the amount of miR-1 transcribed.

An alternative, but not mutually exclusive, hypothesis is that miRNAs dampen transcriptional noise by inhibiting erroneous expression of target mRNAs. This is supported by studies showing that many miRNAs and corresponding target mRNAs are often expressed in separate tissues (Stark, Brennecke et al. 2005). Such a function would also explain why few miRNAs are identified in reverse genetic screening, as the function of the miRNA would only be necessary in instances of stochastic or pathologic misexpression of target mRNAs. For example, the amount of miRNA expressed in the lung throughout development and aging remains remarkably unchanged (Williams, Moschos et al. 2007; Williams, Perry et al. 2007). One interpretation of this finding is that these miRNAs are constitutively expressed to

prevent misexpression of genes that are never intended to be activated in lung tissue. Though many miRNAs undoubtedly perform active functions in development and diseases, there may be many others that are present an insurance policy against stochastic mis-activation of genes.

A third function for miRNAs would be in the switching of cell or organismal state. For example, miRNAs aid in the clearance of maternal mRNAs and thus aid in gastrulation (Wienholds, Koudijs et al. 2003; Mishima, Giraldez et al. 2006). Introduction of a single miRNA, miR-430, rescues the gastrulation defect seen in zebrafish deficient for Dicer. One role of miR-430 is the removal of mRNA transcripts passed on from the mother within the yolk. These maternal mRNAs, such as *nanos*, must be cleared in order for cellular differentiation and maturation processes to occur. I have described a second example of this activity, as described in Chapter 2, where miR-138 is found to clear transcripts from specific regions of the zebrafish heart, thereby aiding in organ patterning.

Part 3: miRNAs in Cardiac Development

Regulation of gene expression by miRNA, via known mechanisms or mechanisms yet to be uncovered, is essential to the development of vertebrate organisms. Recent work has demonstrated that miRNAs are necessary for normal embryonic development in mouse, zebrafish and fly. Most of these studies have been carried out using conditional deletion of Dicer, so non-miRNA-mediated effects of Dicer deletion could theoretically contribute to the observed phenotype. Constitutive deletion of Dicer in mouse and zebrafish leads to embryonic lethality and a failure of germ cell formation (Bernstein, Kim et al. 2003; Wienholds, Koudijs et al. 2003). Additionally, mouse embryonic stem cells without Dicer are deficient in differentiation (Kanellopoulou, Muljo et al. 2005). Tissue-specific deletion of Dicer in mouse limbs showed normal limb patterning with some defects in tissue differentiation and apoptosis (Harfe, McManus et al. 2005). Study of miRNA roles in cardiac development have be studied by conditionally deleting Dicer allele in cardiac progenitors using the *Nkx2.5*-Cre, leading to defects in ventricular myocyte maturation (Zhao, Ransom et al. 2007).

Many miRNAs have been demonstrated to have tissue-specific roles in embryonic and adult animals. Two miRNAs, *miR-1-2* and *miR-208*, have been shown to be necessary for cardiac function via study of mice null for the each of those miRNA genes (van Rooij, Sutherland et al. 2007; Zhao, Ransom et al. 2007). As mentioned earlier there is only one miRNA, *miR-1-2*, that has been shown to be necessary for cardiac development in mouse. The *miR-1-2* null mouse displayed defects in cardiac function, but did not recapitulate fully the ventricular myocyte defects seen in the *Dicer*$^{Fl/Fl}$:*Nkx2.5*-Cre mice. This gap in phenotypes between those two mutant mice indicates that multiple miRNAs are important for cardiac development. Also, gene haploinsufficiencies are known to cause congenital cardiac

malformations in mice and humans, so proper gene dosage is crucial for normal cardiac development. Thus studying the roles of other cardiac-expressed miRNAs, and their mRNA targets, can increase our knowledge of heart development and potential causes of congenital abnormalities.

miR-1

miR-1 has been shown to be specifically expressed in skeletal and cardiac muscle of many organisms. miR-1 is a highly conserved miRNA that is encoded by two loci, producing pre-miR-1-1 and pre-miR-1-2, which both yield the mature miR-1 sequence (Zhao, Samal et al. 2005). miR-1 directs muscle differentiation in fruit fly by targeting the Notch ligand Delta (Kwon, Han et al. 2005). *miR-1-2* deletion demonstrated that *miR-1-2* is necessary for normal cardiac development in the mouse as well (Zhao, Ransom et al. 2007). Serum response factor (SRF) is required for expression of miR-1 in cardiac muscle progenitor cells in both fruit fly and mouse and is known to regulate the balance between progenitor proliferation and differentiation. Mice overexpressing miR-1 have thin-walled ventricles and do not survive beyond E13.5 due to heart failure. In the mouse heart, miR-1 targets Hand2 mRNA, causing translational repression; downregulation of Hand2 decreases ventricular cardiomyocyte expansion (Zhao, Samal et al. 2005). Studies of miR-1 set a precedent for the importance of miRNAs in directing cardiogenic events.

Other potential cardiac miRNAs

In 2005, the Plasterk group published an extensive set of *in situ* hybridization results in zebrafish larvae (Wienholds, Kloosterman et al. 2005). These images contained many tissue-specific miRNA expression patterns, such as miR-138 and miR-145 expression in the cardiac outflow tract of zebrafish embryos at 72 hours post fertilization (hpf). It was this specific expression pattern that led us to initiate

studies of miR-138, the results of which are described in detail in Chapter 2. We found miR-138 to be necessary for cardiac development, including ventricular myocyte maturation, between 24 and 34 hpf in zebrafish, during the time when cardiac looping and chamber maturation are ongoing. miR-138 restricts transcripts, such as *cspg2* and *notch1b*, to the atrioventricular canal and clears them from the ventricle. We found that miR-138 functions to pattern the chambers and valve-regions of the heart by repressing retinoic acid synthesis via the rate-limiting enzyme aldehyde dehydrogenase-1a2 in the ventricle. This domain restriction was reinforced by miR-138-mediated ventricular repression of the gene encoding Versican (*cspg2*), which we found was downstream of retinoic acid signaling.

Once we had characterized one miRNA necessary for cardiac development, we were interested in studying miRNAs that were not yet associated with heart development. To identify miRNAs expressed in the heart during development, we performed miRNA microarrays from heart tissues at many points in mouse development. The arrays revealed miRNAs with varying patterns of expression; some were chamber specific, while others were temporally regulated or ubiquitously expressed. One miRNA, miR-202-5p, was found to be enriched in all ventricular samples, especially at E15.5 and E18.5. Further characterization of the knockdown of miR-202-5p (known as miR-202* in zebrafish) in zebrafish embryos revealed defects in cardiac function and laterality of cardiac looping. These ongoing studies have identified several functional consequences of miR-202* knockdown, and preliminary results indicate that several targets, including Pkd2 and Mapk14, may be responsible for the observed phenotype. Details of our screen and subsequent analysis of miR-202* function in zebrafish are found in Chapter 3.

References

Alsan, B. H. and T. M. Schultheiss (2002). "Regulation of avian cardiogenesis by Fgf8 signaling." Development **129**(8): 1935–1943.

Basson, C. T., D. R. Bachinsky, et al. (1997). "Mutations in human TBX5 cause limb and cardiac malformation in Holt-Oram syndrome." Nat. Genet. **15**(1): 30–35.

Behm-Ansmant, I., J. Rehwinkel, et al. (2006). "MicroRNAs silence gene expression by repressing protein expression and/or by promoting mRNA decay." Cold Spring Harb Symp Quant Biol **71**: 523-30.

Berezikov, E., E. Cuppen, et al. (2006). "Approaches to microRNA discovery." Nat. Genet. **38 Suppl**: S2–S7.

Bernstein, E., S. Y. Kim, et al. (2003). "Dicer is essential for mouse development." Nat. Genet. **35**(3): 215–217.

Bhattacharyya, S. N., R. Habermacher, et al. (2006). "Relief of microRNA-mediated translational repression in human cells subjected to stress." Cell **125**(6): 1111–1124.

Brennecke, J., A. Stark, et al. (2005). "Principles of microRNA-target recognition." PLoS Biol. **3**(3): e85.

Cai, C. L., X. Liang, et al. (2003). "Isl1 identifies a cardiac progenitor population that proliferates prior to differentiation and contributes a majority of cells to the heart." Dev. Cell **5**(6): 877–889.

Christoffels, V. M., P. E. Habets, et al. (2000). "Chamber formation and morphogenesis in the developing mammalian heart." Dev. Biol. **223**(2): 266–278.

Collignon, J., I. Varlet, et al. (1996). "Relationship between asymmetric nodal expression and the direction of embryonic turning." Nature **381**(6578): 155–158.

Doench, J. G. and P. A. Sharp (2004). "Specificity of microRNA target selection in translational repression." Genes Dev. **18**(5): 504–511.

Ebhardt, H. A., E. P. Thi, et al. (2005). "Extensive 3' modification of plant small RNAs is modulated by helper component-proteinase expression." Proc Natl Acad Sci U S A **102**(38): 13398-403.

Eisenberg, L. M. and R. R. Markwald (1995). "Molecular regulation of atrioventricular valvuloseptal morphogenesis." Circ. Res. **77**(1): 1–6.

Flynt, A. S., N. Li, et al. (2007). "Zebrafish miR-214 modulates Hedgehog signaling to specify muscle cell fate." Nat Genet **39**(2): 259-63.

Garg, V., I. S. Kathiriya, et al. (2003). "GATA4 mutations cause human congenital heart defects and reveal an interaction with TBX5." Nature **424**(6947): 443–447.

Garrity, D. M., S. Childs, et al. (2002). "The heartstrings mutation in zebrafish causes heart/fin Tbx5 deficiency syndrome." Development **129**(19): 4635-45.

Giraldez, A. J., R. M. Cinalli, et al. (2005). "MicroRNAs regulate brain morphogenesis in zebrafish." Science **308**(5723): 833–838.

Giraldez, A. J., Y. Mishima, et al. (2006). "Zebrafish MiR-430 promotes deadenylation and clearance of maternal mRNAs." Science **312**(5770): 75-9.

Goldmuntz, E., E. Geiger, et al. (2001). "NKX2.5 mutations in patients with tetralogy of fallot." Circulation **104**(21): 2565–2568.

Harfe, B. D., M. T. McManus, et al. (2005). "The RNaseIII enzyme Dicer is required for morphogenesis but not patterning of the vertebrate limb." Proc. Natl. Acad. Sci. USA **102**(31): 10898–10903.

Hoffman, J. I., S. Kaplan, et al. (2004). "Prevalence of congenital heart disease." Am. Heart J. **147**(3): 425–439.
Hutvagner, G. and P. D. Zamore (2002). "A microRNA in a multiple-turnover RNAi enzyme complex." Science **297**(5589): 2056-60.
Kanellopoulou, C., S. A. Muljo, et al. (2005). "Dicer-deficient mouse embryonic stem cells are defective in differentiation and centromeric silencing." Genes Dev. **19**(4): 489–501.
Kathiriya, I. S. and D. Srivastava (2000). "Left-right asymmetry and cardiac looping: Implications for cardiac development and congenital heart disease." Am. J. Med. Genet. **97**(4): 271–279.
Kwon, C., Z. Han, et al. (2005). "MicroRNA1 influences cardiac differentiation in Drosophila and regulates Notch signaling." Proc. Natl. Acad. Sci. USA **102**(52): 18986–18991.
Lagos-Quintana, M., R. Rauhut, et al. (2001). "Identification of novel genes coding for small expressed RNAs." Science **294**(5543): 853–858.
Lagos-Quintana, M., R. Rauhut, et al. (2002). "Identification of tissue-specific microRNAs from mouse." Curr. Biol. **12**(9): 735–739.
Lai, E. C. (2002). "Micro RNAs are complementary to 3' UTR sequence motifs that mediate negative post-transcriptional regulation." Nat. Genet. **30**(4): 363–364.
Lau, N. C., L. P. Lim, et al. (2001). "An abundant class of tiny RNAs with probable regulatory roles in *Caenorhabditis elegans*." Science **294**(5543): 858–862.
Lawrie, C. H., S. Gal, et al. (2008). "Detection of elevated levels of tumour-associated microRNAs in serum of patients with diffuse large B-cell lymphoma." Br J Haematol.
Lee, R., R. Feinbaum, et al. (2004). "A short history of a short RNA." Cell **116**(2 Suppl): S89-92, 1 p following S96.
Lee, R. C. and V. Ambros (2001). "An extensive class of small RNAs in *Caenorhabditis elegans*." Science **294**(5543): 862–864.
Lee, R. C., R. L. Feinbaum, et al. (1993). "The *C. elegans* heterochronic gene lin-4 encodes small RNAs with antisense complementarity to lin-14." Cell **75**(5): 843–854.
Lee, Y., C. Ahn, et al. (2003). "The nuclear RNase III Drosha initiates microRNA processing." Nature **425**(6956): 415–419.
Lee, Y., M. Kim, et al. (2004). "MicroRNA genes are transcribed by RNA polymerase II." EMBO J. **23**(20): 4051–4060.
Levin, M., R. L. Johnson, et al. (1995). "A molecular pathway determining left-right asymmetry in chick embryogenesis." Cell **82**(5): 803–814.
Lewis, B. P., C. B. Burge, et al. (2005). "Conserved seed pairing, often flanked by adenosines, indicates that thousands of human genes are microRNA targets." Cell **120**(1): 15–20.
Lewis, B. P., I. H. Shih, et al. (2003). "Prediction of mammalian microRNA targets." Cell **115**(7): 787–798.
Li, S., J. Weidenfeld, et al. (2004). "Transcriptional and DNA binding activity of the Foxp1/2/4 family is modulated by heterotypic and homotypic protein interactions." Mol Cell Biol **24**(2): 809-22.
Li, S., D. Zhou, et al. (2004). "Advanced cardiac morphogenesis does not require heart tube fusion." Science **305**(5690): 1619-22.
Liu, J., M. A. Valencia-Sanchez, et al. (2005). "MicroRNA-dependent localization of targeted mRNAs to mammalian P-bodies." Nat. Cell Biol. **7**(7): 719–723.
Matranga, C., Y. Tomari, et al. (2005). "Passenger-strand cleavage facilitates assembly of siRNA into Ago2-containing RNAi enzyme complexes." Cell **123**(4): 607–620.

Meno, C., Y. Saijoh, et al. (1996). "Left-right asymmetric expression of the TGF beta-family member lefty in mouse embryos." Nature **381**(6578): 151–5.
Mishima, Y., A. J. Giraldez, et al. (2006). "Differential regulation of germline mRNAs in soma and germ cells by zebrafish miR-430." Curr Biol **16**(21): 2135-42.
Mjaatvedt, C. H., T. Nakaoka, et al. (2001). "The outflow tract of the heart is recruited from a novel heart-forming field." Dev. Biol. **238**(1): 97–109.
Novina, C. D. and B. A. Chabner (2008). "RNA-Directed Therapy: The Next Step in the miRNA Revolution." Oncologist **13**(1): 1-3.
Obernosterer, G., P. J. Leuschner, et al. (2006). "Post-transcriptional regulation of microRNA expression." Rna **12**(7): 1161–1167.
Rajewsky, N. (2006). "microRNA target predictions in animals." Nat. Genet. **38 Suppl**: S8–S13.
Rodriguez, A., S. Griffiths-Jones, et al. (2004). "Identification of mammalian microRNA host genes and transcription units." Genome Res **14**(10A): 1902-10.
Ruvkun, G. (2001). "Molecular biology. Glimpses of a tiny RNA world." Science **294**(5543): 797-9.
Schetter, A. J., S. Y. Leung, et al. (2008). "MicroRNA expression profiles associated with prognosis and therapeutic outcome in colon adenocarcinoma." Jama **299**(4): 425-36.
Schultheiss, T. M., J. B. Burch, et al. (1997). "A role for bone morphogenetic proteins in the induction of cardiac myogenesis." Genes Dev. **11**(4): 451–462.
Schultheiss, T. M., S. Xydas, et al. (1995). "Induction of avian cardiac myogenesis by anterior endoderm." Development **121**(12): 4203–4204.
Sokol, N. S. and V. Ambros (2005). "Mesodermally expressed *Drosophila* microRNA-1 is regulated by Twist and is required in muscles during larval growth." Genes Dev. **19**(19): 2343–2354.
Srivastava, D., P. Cserjesi, et al. (1995). "A subclass of bHLH proteins required for cardiac morphogenesis." Science **270**(5244): 1995–1999.
Srivastava, D. and E. N. Olson (2000). "A genetic blueprint for cardiac development." Nature **407**(6801): 221–226.
Stainier, D. and M. Fishman (1992). "Patterning the zebrafish heart tube: acquisition of anteroposterior polarity." Dev. Biol. **153**(1): 91–101.
Stark, A., J. Brennecke, et al. (2005). "Animal MicroRNAs confer robustness to gene expression and have a significant impact on 3'UTR evolution." Cell **123**(6): 1133–1146.
Stark, A., J. Brennecke, et al. (2003). "Identification of *Drosophila* MicroRNA targets." PLoS Biol. **1**(3): E60.
Stenvang, J. and S. Kauppinen (2008). "MicroRNAs as targets for antisense-based therapeutics." Expert Opin Biol Ther **8**(1): 59-81.
Stuckmann, I., S. Evans, et al. (2003). "Erythropoietin and retinoic acid, secreted from the epicardium, are required for cardiac myocyte proliferation." Dev. Biol. **255**(2): 334–349.
Thai, T. H., D. P. Calado, et al. (2007). "Regulation of the germinal center response by microRNA-155." Science **316**(5824): 604–608.
Valdes-Dapena, M. and E. Gilbert-Barness (2002). "Cardiovascular causes for sudden infant death." Pediatr Pathol Mol Med **21**(2): 195-211.
van Rooij, E., L. B. Sutherland, et al. (2007). "Control of stress-dependent cardiac growth and gene expression by a microRNA." Science **316**(5824): 575-9.
van Rooij, E., L. B. Sutherland, et al. (2007). "Control of stress-dependent cardiac growth and gene expression by a microRNA." Science **316**(5824): 575–579.
Vasudevan, S., Y. Tong, et al. (2007). "Switching from repression to activation: microRNAs can up-regulate translation." Science **318**(5858): 1931-4.

Vasudevan, S., Y. Tong, et al. (2008). "Cell-cycle control of microRNA-mediated translation regulation." Cell Cycle **7**(11).
Verzi, M. P., D. J. McCulley, et al. (2005). "The right ventricle, outflow tract, and ventricular septum comprise a restricted expression domain within the secondary/anterior heart field." Dev. Biol. **287**(1): 134–145.
Viswanathan, S. R., G. Q. Daley, et al. (2008). "Selective blockade of microRNA processing by Lin28." Science **320**(5872): 97-100.
Walsh, E. C. and D. Y. Stainier (2001). "UDP-glucose dehydrogenase required for cardiac valve formation in zebrafish." Science **293**(5535): 1670-3.
Wienholds, E., W. P. Kloosterman, et al. (2005). "MicroRNA expression in zebrafish embryonic development." Science **309**(5732): 310–311.
Wienholds, E., M. J. Koudijs, et al. (2003). "The microRNA-producing enzyme Dicer1 is essential for zebrafish development." Nat. Genet. **35**(3): 217–218.
Williams, A. E., S. A. Moschos, et al. (2007). "Maternally imprinted microRNAs are differentially expressed during mouse and human lung development." Dev Dyn **236**(2): 572-80.
Williams, A. E., M. M. Perry, et al. (2007). "microRNA expression in the aging mouse lung." BMC Genomics **8**: 172.
Wu, L., J. Fan, et al. (2006). "MicroRNAs direct rapid deadenylation of mRNA." Proc Natl Acad Sci U S A **103**(11): 4034-9.
Yang, B., H. Lin, et al. (2007). "The muscle-specific microRNA miR-1 regulates cardiac arrhythmogenic potential by targeting GJA1 and KCNJ2." Nat. Med. **13**(4): 486–491.
Yang, W., T. P. Chendrimada, et al. (2006). "Modulation of microRNA processing and expression through RNA editing by ADAR deaminases." Nat. Struct. Mol. Biol. **13**(1): 13–21.
Yekta, S., I. H. Shih, et al. (2004). "MicroRNA-directed cleavage of HOXB8 mRNA." Science **304**(5670): 594–596.
Yelbuz, T. M., K. L. Waldo, et al. (2002). "Shortened outflow tract leads to altered cardiac looping after neural crest ablation." Circulation **106**(4): 504-10.
Yi, R., Y. Qin, et al. (2003). "Exportin-5 mediates the nuclear export of pre-microRNAs and short hairpin RNAs." Genes Dev. **17**(24): 3011–3016.
Yu, B., Z. Yang, et al. (2005). "Methylation as a crucial step in plant microRNA biogenesis." Science **307**(5711): 932-5.
Zamore, P. D., T. Tuschl, et al. (2000). "RNAi: double-stranded RNA directs the ATP-dependent cleavage of mRNA at 21 to 23 nucleotide intervals." Cell **101**(1): 25-33.
Zhao, Y., J. F. Ransom, et al. (2007). "Dysregulation of cardiogenesis, cardiac conduction, and cell cycle in mice lacking miRNA-1-2." Cell **129**: 303–317.
Zhao, Y., J. F. Ransom, et al. (2007). "Dysregulation of cardiogenesis, cardiac conduction, and cell cycle in mice lacking miRNA-1-2." Cell **129**(2): 303-17.
Zhao, Y., E. Samal, et al. (2005). "Serum response factor regulates a muscle-specific mircroRNA that targets *Hand2* during cardiogenesis." Nature **436**: 214–220.
Zhao, Y. and D. Srivastava (2007). "A developmental view of microRNA function." Trends Biochem. Sci. **32**: 189–197.

Figure Legends

Figure 1-1

Cardiac development in mouse and human. Development of the heart in mouse and human embryos includes contributions from at least three progenitor populations: first heart field (also know as primary heart field or PHF), which primarily contributes cells to the left ventricle and atria; second heart field (SHF), which descends through the pharyngeal arches into the heart around Day 21 of human embryonic development to form the right ventricle and proximal outflow tract; and the cardiac neural crest (CNC) which forms the distal outflow tract. Figure by Kimberly Cordes.

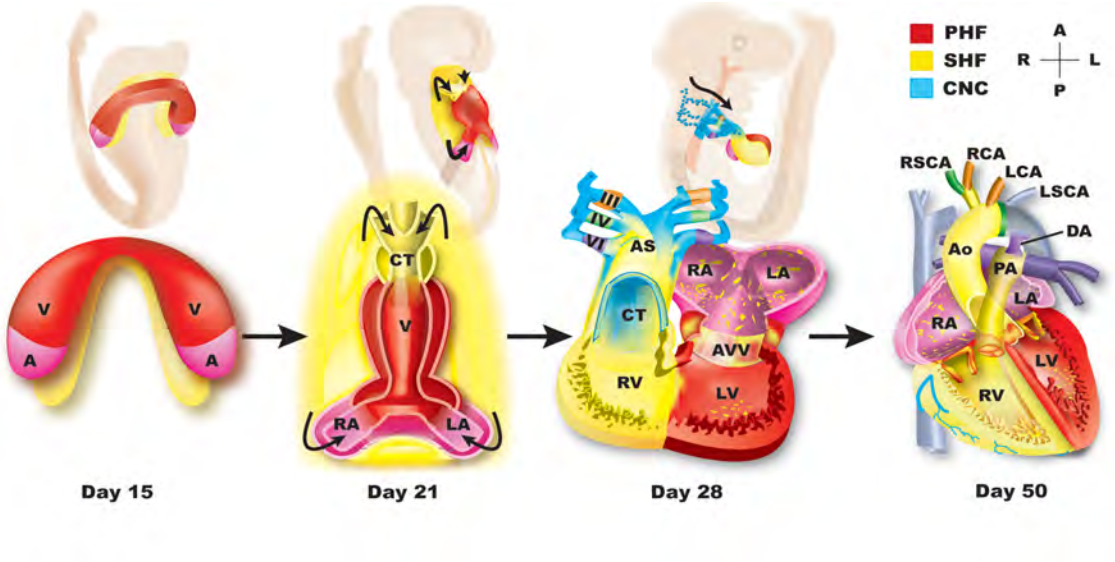
PHF
SHF
CNC
A
R
L
P
V
V
A
A
CT
V
RA
LA
III
IV
VI
AS
RA
LA
CT
AVV
RV
LV
RSCA
RCA
LCA
LSCA
DA
Ao
PA
LA
RA
LV
RV
Day 15
Day 21
Day 28
Day 50

Figure 1-2

miRNA biogenesis. miRNA genes are transcribed by RNA polymerase III into long primary miRNA (pri-miRNA) precursors. These pri-miRNAs are cleaved in the nucleus by a protein complex that includes Drosha and DGCR8 to produce 70-80 nucleotide pre-miRNAs. Pre-miRNAs are exported from the nucleus by Exportin5-RanGTP. Once in the cytoplasm, pre-miRNAs undergo another cleavage by a complex including Dicer. The mature miRNA then remains bound in Dicer, and the RNA-induced silencing complex (RISC) of proteins is assembled. The active RISC can then inhibit mRNA translation, or trigger mRNA degradation by deadenylation or nuclease cleavage. Figure by Kimberly Cordes.

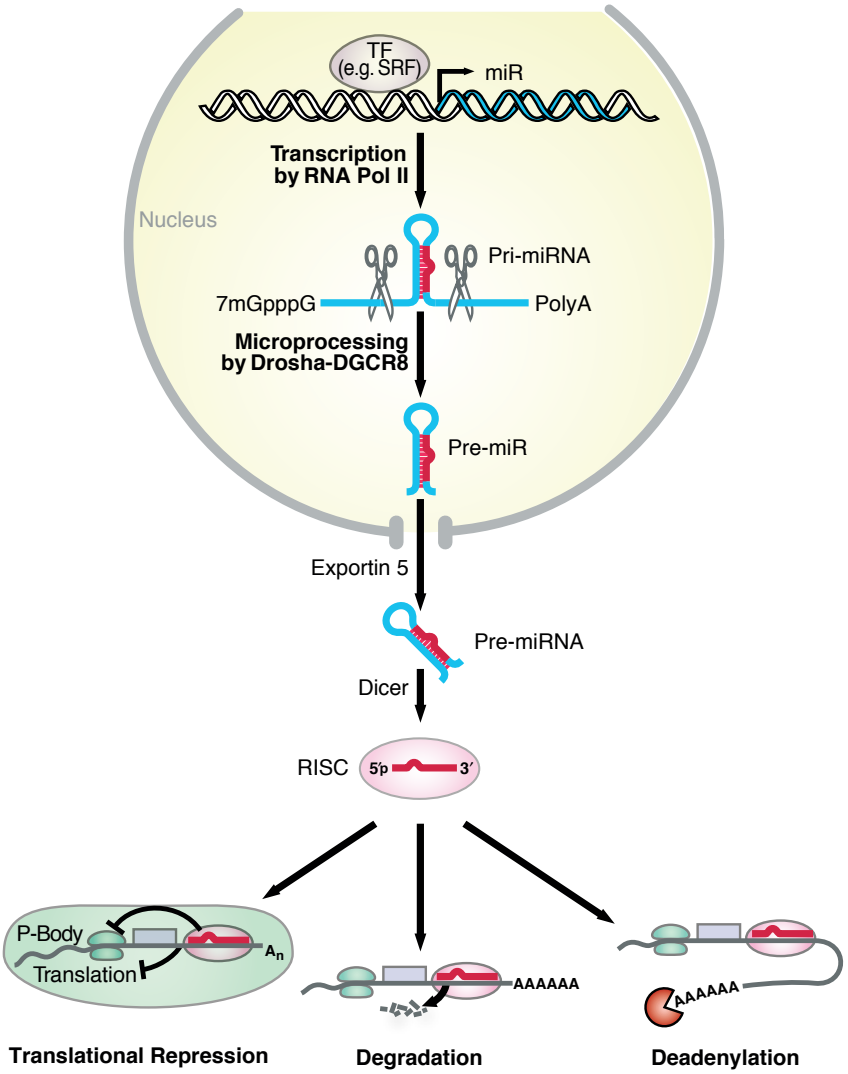
TF
(e.g. SRF)
miR
Transcription
by RNA Pol II
Nucleus
Pri-miRNA
7mGpppG
PolyA
Microprocessing
by Drosha-DGCR8
Pre-miR
Exportin 5
Pre-miRNA
Dicer
RISC
5′p
3′
P-Body
Translation
An
AAAAAA
AAAAAA
Translational Repression
Degradation
Deadenylation

Chapter Two:

miR-202* Is Necessary for Cardiac Patterning

Summary

Organ patterning during embryonic development requires precise temporal and spatial regulation of protein activity. microRNAs (miRNAs), small non-coding RNAs that typically inhibit protein expression, are broadly important for proper development, but their individual functions during organogenesis are largely unknown. We report that miR-138 is expressed in specific domains in the zebrafish heart and is required to establish appropriate chamber-specific gene expression patterns. Disruption of miR-138 function led to ventricular expansion of gene expression normally restricted to the atrio-ventricular valve region, and ultimately to disrupted ventricular cardiomyocyte morphology and cardiac function. Temporal-specific knockdown of miR-138 by antagomiRs showed miR-138 function was required during a discrete developmental window, 24-34 hours post-fertilization (hpf). miR-138 functioned partially by repressing the retinoic acid synthesis enzyme, aldehyde dehydrogenase-1a2, in the ventricle. This activity was complemented by miR-138-mediated ventricular repression of the gene encoding versican (*cspg2*), which is positively regulated by retinoic-acid signaling. Our findings demonstrate that miR-138 helps establish discrete domains of gene expression during cardiac morphogenesis by targeting multiple members of a common pathway, and also establishes the use of antagomiRs in fish for temporal knockdown of miRNA function.

Introduction

Most organs are composed of cells of similar origin that develop divergent patterns of gene expression and functional properties necessary for myriad biological outcomes. The heart has been a particularly informative model for such organ patterning, with numerous transcriptional networks that establish chamber or domain-specific gene expression and function (Srivastava 2006). In vertebrates, the linear heart tube forms in a highly conserved process from the migration and fusion of bilateral cardiac progenitor fields at the midline, followed by cardiac looping to form an s-shaped heart and further cellular differentiation. Distinct atrial and ventricular chambers with unique physiological and electrical properties arise, separated by a discrete domain known as the atrioventricular canal (AVC) (Stainier 2001; Beis, Bartman et al. 2005). The AVC gives rise to the valves that ensure unidirectional flow of blood. In mammals, each chamber and valve becomes septated resulting in a four-chambered heart.

Transcriptional networks that establish chamber-specific gene expression are highly conserved across species ranging from zebrafish to humans (1). Zebrafish have proven to be particularly informative for studying these early patterning networks due to the relatively simple two-chambered heart and their ability to develop even in the absence of a functioning heart. Ultimately, the atrial and ventricular chambers express distinct *myosin* genes (Yelon, Horne et al. 1999), while genes such as *cspg2*, encoding versican, and *notch1b* are restricted to the AVC (Walsh and Stainier 2001).

In addition to transcriptional control of gene expression, post-transcriptional regulation through small non-coding RNAs is emerging as a frequently employed cellular mechanism to titrate activity of key regulatory pathways. The class of small, highly-conserved non-coding RNAs known as microRNAs (miRNAs) function to fine-tune gene expression during development and in some cases can function as major

switches of gene programs (Zhao and Srivastava 2007). miRNA precursors, known as primary miRNA (pri-miRNA) are transcribed by RNA polymerase II and processed into ~70-nucleotide (nt) hairpins by an enzyme complex containing Drosha (Lee, Ahn et al. 2003). These pre-miRNA forms are exported from the nucleus by Exportin5 and cleaved by Dicer to make biologically-active 20-25-nt mature miRNAs (Hutvagner, McLachlan et al. 2001; Yi, Qin et al. 2003). Sequence-specific interaction of the mature miRNA with mRNA targets, typically involving the 5' end of the miRNA known as a "seed sequence", can result in translational repression or mRNA degradation. (Hutvagner, McLachlan et al. 2001; Lee, Ahn et al. 2003; Gregory, Chendrimada et al. 2005).

We and others previously reported that miR-1 regulates gene expression and muscle differentiation during mouse and fly cardiogenesis (Kwon, Han et al. 2005; Sokol and Ambros 2005; Zhao, Samal et al. 2005; Chen, Mandel et al. 2006; Zhao, Ransom et al. 2007), however evidence for individual miRNAs in patterning distinct domains of the heart has been lacking (Bernstein, Kim et al. 2003; Wienholds, Koudijs et al. 2003; Giraldez, Cinalli et al. 2005; Harfe, McManus et al. 2005; Harris, Zhang et al. 2006). Here, we show that the highly conserved miRNA, miR-138, helps establish discrete domains of gene expression required for normal cardiac morphogenesis and does so by directly repressing multiple members of a common pathway involving retinoic acid synthesis. In addition, we demonstrate the utility of antagomiR technology in zebrafish to delineate developmental windows of miRNA function.

Results

miR-138 is expressed in the zebrafish heart and is required for normal cardiogenesis.

We used zebrafish as a model to investigate regulation of chamber-specific gene expression and cardiac patterning by miRNAs (Glickman and Yelon 2002). *In situ* hybridization studies in zebrafish showed restricted cardiac expression of many miRNAs, including miR-138 (Wienholds, Kloosterman et al. 2005), which is 100% conserved from fugu to humans (Fig. 2-S1). Further *in situ* hybridization analysis suggested that cardiac expression of miR-138 was localized to ventricular cardiomyocytes (Fig. 2-1A). To determine whether miR-138 was restricted to cardiac muscle or was also expressed in endothelial and endocardial cells, we isolated these two cell types from 48 hpf transgenic fish expressing GFP driven by the myocardial- or endothelial-specific enhancers of *cmlc2* or *flk1*. Mature miR-138 was enriched in cardiomyocytes, but was not detected in the *flk1*-gfp^{+} population (Fig. 2-1B).

We injected 2-4 ng of a 17-nt morpholino complementary to the mature miR-138 sequence into 1-2-cell embryos to examine miR-138 requirement during cardiac development. At 36 hpf, cardiac function of fish injected with miR-138-specific morpholino (miR-138$^{mo\text{-}1}$) was indistinguishable from controls. At 48 hpf, blood circulation appeared unaffected in the miR-138$^{mo\text{-}1}$ fish, but pericardial edema, reflecting cardiac dysfunction, and abnormal looping between the atrial and ventricular chambers were obvious in 60-80% of embryos (Fig. 2-1C,D). No other gross morphological defects were present throughout the embryo. Control embryos injected with a 17-nt morpholino scrambled in the region complementary to the 2-7-nt "seed region" of the miRNA (miR-138^{scr}) were unaffected. miR-138$^{mo\text{-}1}$ fish survived to 72-96 hpf. Blood vessel formation at 24-48 hpf, visualized using the

Tg(flk1:EGFP)^{s843} line, which expresses GFP in endothelial cells (Beis, Bartman et al. 2005), was unaffected by morpholino injection (Fig. 2-S2).

miR-138 is required for cardiac maturation and patterning in zebrafish.

Confocal microscopy of miR-138^{mo-1} fish revealed defects in elongation of ventricular cardiomyocytes and in cardiac looping at 48 hpf (Fig. 2-1,E-H). About 60% of embryos analyzed by confocal microscopy had myocardial cells along the outer curvature of the ventricle that failed to elongate and remained in a primitive, rounded state typical of less differentiated myocytes (n=45; Fig. 2-1,E-G). Ventricular cardiomyocytes normally become elongated by 48 hpf, while myocytes that normally persist around the AVC remain in the more rounded immature state (Auman, Coleman et al. 2007). Blood flow and contractility, which are important stimuli for cardiomyocyte maturation (Auman, Coleman et al. 2007), appeared grossly intact at 48 hpf. A second, 31-nt morpholino against the pri-miR-138 produced a similar defect, suggesting that the morpholino–induced effects were specifically due to downregulation of miR-138 (Fig. 2-1H). Less commonly (~15%), an elongated AVC domain occurred between the atrium and ventricle (Fig. 2-1I).

To determine whether cardiac patterning was affected by loss of miR-138, we performed *in situ* hybridization to detect chamber-specific genes. At 24 hpf, *cmlc2* mRNA expression, which marks all cardiomyocytes (Yelon, Horne et al. 1999), was similar in wild-type and miR-138^{mo-1} fish (Fig. 2-S3A,B). The atrial and ventricular-specific markers, *amhc* and *vmhc,* respectively, were expressed in appropriate domains at 48 hpf, suggesting normal gross chamber-specification and initial differentiation (Fig. 2-2,A-D) (Yelon, Horne et al. 1999; Berdougo, Coleman et al. 2003). However, genes normally restricted to the AVC region, including *cspg2* and *notch1b* (Walsh and Stainier 2001)*,* were ectopically expressed in the ventricle of embryos injected with miR-138^{mo-1} (Fig. 2-2,E-H), but not miR-138^{scr} (Fig. 2-S3,C-F)

Expanded *cspg2* and *notch1b* expression was also observed in fish treated with the 31-nt morpholino (data not shown). Versican, the protein encoded by *cspg2*, and Notch1 are involved in valvulogenesis in various animal models (6). Persistence of *cspg2* and *notch1b* transcripts in the ventricle of miR-138^{mo-1} zebrafish suggests that miR-138 restricts the valve-forming domain by repressing AVC gene expression in the ventricle.

miR-138 is required during a distinct temporal window of cardiac development.

Cholesterol-conjugated antisense oligonucleotides, called antagomiRs, can be used to inhibit miRNAs in cell culture and mice where they broadly diffuse into most cells (Krutzfeldt, Rajewsky et al. 2005). We hypothesized that antagomiRs could be used to decrease miRNA activity in fish simply upon their addition to fish water, offering an opportunity to dissect temporal miRNA function in fish. As a proof of concept, we tested antagomiRs targeting miR-451, a miRNA that was previously reported to regulate red blood cell maturation in fish using conventional miR-451 morpholino knockdown methods (Dore, Amigo et al. 2008). Addition of miR-451 antagomiR (miR-451^{am}) to the water of transgenic fish containing the red blood cell-specific *gata1* enhancer upstream of red fluorescent protein (RFP) resulted in an absence of RFP^{+} red blood cells, recapitulating the reported effects of miR-451mo (Beis, Bartman et al. 2005) (Fig 2-S4,A-B). Endothelial cells of the vasculature were intact as marked by *flk1*:EGFP. These findings validated the use of antagomiRs in fish water to knockdown miRNA function.

To determine the developmental window during which miR-138 was required, zebrafish were treated with miR-138 antagomiR (miR-138^{am}) starting at varying times and collected at 72 hpf. Addition of 2-20 μM of miR-138^{am} from 24, 30 or 34 hpf decreased mature miR-138 to levels observed upon injection of the 31-nt

morpholino against pri-miR-138 (Fig. 2-3A). Decreased levels of mature miR-138 were observed up to 5 days after treatment at 24 hpf (Fig. 2-S4C). Scrambled antagomiR did not affect miR-138 levels. Exposure of fish to miR-138^{am} between 24-72 hpf resulted in defects similar to those observed upon miR-138^{mo-1} injection, including pericardial edema and altered myocardial cell shape (83% *vs* 13% with PBS alone, n=106) (Fig. 2-3,B-E). Scrambled antagomiR had similar effects as PBS alone. Treatment from 24 hpf also resulted in expansion of *cspg2* mRNA expression into the ventricle, similar to that seen in miR-138^{mo-1} embryos (Fig. 2-3F,G). After 30 hpf, 46% (n=88) of treated fish showed cardiac defects, compared to 9% of embryos treated with a scrambled antagomiR or 10% of PBS-treated embryos. By 34 hpf (n=88), embryos were no longer susceptible to miR-138^{am}, although the knockdown was still effective. Thus, miR-138 is required between 24 and 34 hpf, which corresponds to the time of early cardiac looping in the fish, but is dispensable thereafter.

miR-138 targets *aldh1a2* and *cspg2* in the developing zebrafish heart.

Complimentarity between a miRNA and its target mRNAs, as well as accessibility of the binding site within the 3´UTR of the mRNA, are both important factors in predicting miRNA targets (Zhao, Samal et al. 2005; Zhao, Ransom et al. 2007). We used a bioinformatics approach incorporating these and other parameters (K. Ivey, Y. Zhao, & D. Srivastava, unpublished) to predict mRNA targets of miR-138, and tested 8 potential targets. Among these, *aldh1a2*, encoding retinoic acid dehydrogenase (Raldh2), had a highly conserved miR-138 binding site (Fig. 2-4A). Raldh2 is involved in retinoic acid (RA) synthesis, which is required for early chamber specification and anterior-posterior cardiac patterning in mouse, chick, and zebrafish, and is important for myocardial maturation (Stainier and Fishman 1992; Xavier-Neto, Shapiro et al. 2000). To test whether miR-138 post-transcriptionally repressed

aldh1a2 by directly targeting the 3'UTR, we cloned the zebrafish *aldh1a2* 3´UTR sequence containing the putative miR-138 binding site downstream of a luciferase reporter. The 3´UTR sequence inhibited luciferase activity in response to miR-138, but not miR-1, for which there was not a predicted binding site (Fig. 2-4A, data not shown). Point mutations in the miR-138 binding site, located where nucleotides 2-7 of the miRNA are predicted to bind, abolished repression, indicating that miR-138 can directly target this binding site in the 3'UTR of *aldh1a2*.

Injection of pri-miR-138 into fish decreased and exposure to miR-138 antagomiR increased endogenous *aldh1a2* mRNA levels, demonstrating regulation of *aldh1a2* by miR-138 *in vivo* (Fig. 2-4B). In wild-type hearts, Raldh2 protein was enriched in the AVC region, but hardly detectable in the remaining heart tube (Fig. 2-4C). In contrast, Raldh2 protein expression was expanded into the ventricle of miR-138^{am} embryos, and the area of cardiac Raldh2 immunostaining was increased fivefold, consistent with it being a direct target normally repressed in the ventricle (Fig. 2-4D, 2-S5A). AntagomiR treatment of embryos transgenically expressing GFP in endothelial cells or cardiomyocytes revealed that Raldh2 protein in the AVC was found in endothelial cells, while the Raldh2 aberrantly expressed in the ventricle was within cardiomyocytes (Fig. 2-S5B, C). *In situ* hybridization analysis of Raldh2 mRNA also revealed expansion of the mRNA expression in the ventricle of miR-138^{mo-1} embryos compared to controls (Fig. 2-S5D, E).

While it is likely that many miR-138 targets mediate its effects on cardiac patterning and gene expression, we sought to determine to what degree RA signaling may contribute to the miR-138 knockdown phenotype. Exogenous RA administered 24-48 hpf caused expansion of *cspg2* expression into the ventricle, similar to that observed in miR-138^{mo-1} embryos (Fig. 2-4,E-G), consistent with increased RA signaling in the ventricle contributing to ventricular *cspg2* expression. Conversely, inhibiting RA signaling with 4-(diethylamino)benzaldehyde (DEAB) (Perz-Edwards,

Hardison et al. 2001) between 24-48 hpf attenuated the miR-138 knockdown phenotype, rescuing the expanded AVC defect (Fig. 2-4,H-J), suggesting that the increased RA production likely contributed to the expansion of the AVC region in miR-138^{mo-1} fish.

Curiously, inhibition of RA signaling in miR-138^{mo-1} embryos did not rescue aberrant ventricular expression of *cspg2* or *notch1b* (Fig. 2-4,K-M and data not shown), indicating that they are affected by miR-138, independent of altered RA signaling and raising the possibility they may also be direct targets of miR-138. The *notch1b* 3′UTR did not contain any miR-138 binding sites and was not responsive to miR-138 (Fig. 2-S6). Because the 3′-UTR of zebrafish *cspg2* has not been annotated, we examined the mouse *cspg2* 3′UTR, given the 100% conservation of zebrafish and mouse miR-138. Like *aldh1a2*, we found a miR-138 binding site in the *cspg2* 3′UTR that was responsive to miR-138 (Fig. 2-5A). Introduction of miR-138 into mouse NIH-3T3 cells decreased endogenous *cspg2* mRNA and protein accumulation by ~40% (Fig. 2-5B,C). Furthermore, miR-138 RNA injection into zebrafish embryos decreased endogenous *cspg2* mRNA levels 10-fold (Fig. 2-5D). Treatment with miR-138 antagomiR increased endogenous *cspg2* mRNA levels eightfold while scrambled antagomiR had no effect. Thus, miR-138 not only restricts Versican expression to the AVC region by regulating retinoic acid synthesis, but also directly represses *cspg2* in the ventricle.

Discussion

We have found that miR-138 regulates a network of developmental signals by repressing AVC-specific transcripts in the developing ventricle. This ultimately contributes to ventricular cardiomyocyte maturation, and thereby aids in establishing the distinct identity of cardiac structures. Specifically, miR-138 represses RA signaling in the ventricles and reinforces its influence on this pathway by negatively regulating *cspg2*, which is downstream of RA and is AVC-specific (Fig. 2-5E). Other yet unknown genes regulated by miR-138 may also be important to this process. These results indicate that miR-138 functions similarly to miR-430, which clears residual maternal mRNAs from the developing zebrafish embryo (Giraldez, Cinalli et al. 2005). This is an elegant example of how miRNA-based networks can refine discrete patterns of gene expression during organogenesis, controlling the formation of functionally distinct domains.

The ability of DEAB to rescue the extended AVC phenotype present in some of the miR-138mo embryos suggests that AVC patterning is sensitive to RA signaling. During migration of the bilateral heart fields early in development there is an anterior-posterior gradient of RA signaling generated by the posterior mesoderm which drives cardiac progenitors to an atrial fate (Stainier and Fishman 1992). Raldh2, which converts retinaldehyde to retinoic acid, is expressed early in mouse development and its targeted deletion results in cardiac defects by embryonic day 9.5, including lack of looping and single chamber morphology (Niederreither, Subbarayan et al. 1999). The looping defect in Raldh2 mutants is rescued by exogenous treatment of retinoic acid. In addition to these known roles of RA signaling in early cardiac patterning, we have shown that restricted AVC expression of Raldh2 at 48hpf is also necessary for proper ventricular development. Ectopic ventricular Raldh2 in miR-138mo embryos may contribute to the mis-patterning of the AVC and ventricle via alterations in amount and distribution of RA.

In contrast, the observed defects in myocardial maturation, which were not rescued by DEAB, may be influenced by increased expression of Versican and other targets that have not yet been identified. miR-138 affected *cspg2* expression through RA signaling and by targeting it directly, thereby repressing AVC gene expression in the ventricle via multiple avenues. However, the degree to which *cspg2* or *notch1b* upregulation contributes to the cardiomyocyte maturation defect in miR-138mo embryos remains unknown, as knockdown of *cspg2* yielded early gastrulation defects, precluding such studies. Knockdown of miRNA targets at later developmental time points, as will become possible with caged morpholinos and other evolving technologies, could allow further dissection of each target's contribution to the miR-138 knockdown phenotype.

Finally, our finding that antagomiRs can regulate zebrafish miRNA function simply by addition to the environment will allow temporal resolution of miRNA function. Current methods cannot determine temporally specific roles of miRNAs (Nasevicius and Ekker 2000), which is particularly important when studying genes required for early development that may also have later physiologic functions. Use of antagomiRs in this model system bypasses these hurdles. Future studies of miRNAs in zebrafish will benefit from this temporal resolution. It will be interesting to determine if this method may also prove to be applicable to mRNA knockdown.

Methods

Zebrafish lines. *wt* AB and transgenic *Tg(myl7:HRAS-mEGFP)*^{s843}, *Tg(flk1:EGFP)* ^{s843} and *Tg(flk1:EGFP, gata1:RFP)* ^{s843} zebrafish (D'Amico, Scott et al. 2007) were raised under standard laboratory conditions at 28°C (Westerfield 2000).

Microinjection. An approximately 350 nt pri-miR-138 fragment was cloned from mouse cDNA and ligated into the pCR-II vector. RNA was made via *in vitro* transcription with the SP6 promoter. Embryos were injected at the 1–2-cell stage with 2–5 ng of miR-138 MO (5´-GAUUCACAACACCAGCU-3´, Integrated DNA Technologies (IDT)), 2–5 ng of scrambled MO (5´-GAUUGGAAACACCAGCU-3´, IDT), 2–5 ng pri-miR-138 MO (5´-GTGACATCGGCCTGATTCACAACACCAGCTG-3´, GeneTools), or 100-200 pg of *pri-miR-138-2* RNA. The embryos were maintained at 28ºC until harvesting.

Confocal analysis. Embryos were fixed in 2% paraformaldehyde (PFA) overnight, embedded in 4% low-melt agarose, and cut into 150-µm sections with a Leica VT1000S vibratome. Images were acquired with a Zeiss LSM5 Pascal confocal microscope.

AntagomiR treatment. All zebrafish embryos were manually dechorionated and treated with 2-20 µM antagomiR. AntagomiR targeting miR-451 (Dharmacon) was added at 12-24 hpf, and embryos were examined at 32-60 hpf. AntagomiR miR-138 (5´-GAUUCACAACACCAGCU-3´, IDT), scrambled antagomiR (5´-GAUUGGAAACACCAGCU-3´, IDT), or PBS were added to water at 24, 30 or 34 hpf and visualized at 72 hpf. Due to variability between preparations, antagomiRs were

assayed for efficacy by injection into 1-2 cell embryos before exogenous use. Phenoype results were averaged from four experiments.

Immunohistochemistry. Embryos were fixed for 1 h at room temperature in 4% PFA, incubated in 20% sucrose/PBS overnight, embedded in OCT, and sectioned using a cryostat. Sections were washed in PBS with 0.05% Triton, and incubated with rabbit anti-Raldh2 antibody (generous gift of Dr. Peter McCaffery) overnight at a 1:200 dilution. This antibody has previously been demonstrated to be specific for raldh2 protein in zebrafish (Prabhudesai, Cameron et al. 2005). The embryos were then incubated in secondary antibody (1:200 Alexa Fluor 574 conjugated goat anti-rabbit antibody (Molecular Probes)) overnight and washed. Images were acquired with a Zeiss LSM5 Pascal confocal microscope.

In situ hybridization. Probes against miR-138 (Exiqon), *cmlc2*(Yelon, Horne et al. 1999)*, amhc*(Berdougo, Coleman et al. 2003)*, vmhc*(Yelon, Horne et al. 1999)*, cspg2*(Walsh and Stainier 2001)*, notch1b*(Walsh and Stainier 2001)*,* and *aldh1a2* were used. miR-138 *in situ* hybridization was performed according to published protocols (Exiqon, Netherlands). Probes against mRNAs were synthesized, and in situ hybridizations were performed as described (Aanstad and Whitaker 1999).

Luciferase assay. Target prediction developed in the Srivastava laboratory was used to bioinformatically identify potential targets of miR-138. 428 nucleotides (1632-2058, NM_131850) of *Danio rerio aldh1a2* and 280 nucleotides (10755-11032, NM_001081249) of *Mus musculus cspg2* 3′-UTRs predicted to contain miR-138 binding sites were cloned into the pGL3 vector (Promega). Point mutations of the binding sites were generated using QuickChange II PCR (Stratagene). pri-miR-138-2 was subcloned into the pSilencer-3.1 vector (Ambion). Renilla-encoding vector

was used as a transfection control. Cos-1 cells were transfected with 350 ng miR-138, 150 ng of CMV-luciferase and 50 ng of CMV-renilla constructs with Fugene (Roche), and cells were harvested after 48 hours. Luciferase and renilla activity were assayed using the Dual-Reporter Assay (Promega). Results shown are from triplicate experiments.

Transient transfection. NIH3T3 mouse fibroblasts were grown in DMEM supplemented with 5% calf serum and penicillin/streptomycin (Gibco). Cells were transfected with 1.5 µg GFP, miR-1 or miR-138 constructs with the nucleofection program U-30 (Amaxa). After 20 hours, cells were collected directly in Trizol (Invitrogen). Transfection efficiency was above 95%.

Quantitative real-time RT-PCR. RNA was prepared from whole embryos injected with pre-miR-138-2, the anterior portion of embryos treated with antagomiRs, or from NIH3T3 mouse fibroblasts with Trizol (Invitrogen). For mRNA qRT-PCR, cDNA was reverse transcribed using an oligo(dT) primer. Custom primers for *Danio rerio cspg2* and *alhla2*, and inventoried primers for *Mus musculus cspg2, gapdh* and *aldh1a2* were used for Taqman-based real-time RT-PCR (Applied Biosystems). For miRNA qRT-PCR, cDNA was reverse transcribed fron 10 ng of total RNA using the Taqman microRNA Reverse Transcription Kit (Applied Biosystems). miR-26a was used as an endogenous control. Results represent least three experiments.

Pharmocological treatment. Embryos were dechorionated and treated with retinoic acid (Sigma) at a final concentration of 0.1–1 µM or DEAB (Sigma) diluted to a final concentration of 25 µM, both with a final concentration of 0.25% DMSO. The embryos were maintained at 28ºC until harvesting.

Statistical Analysis. Results from at least three trials were averaged and the 95% confidence interval calculated and plotted as error bars. Significance was determined using the unpaired student t-test.

ACKNOWLEDGEMENTS

We would like to thank A. Muth, P. Aanstad, C. Shin and all members of the Srivastava and Stainier labs for assistance, invaluable support and discussion. L. Prentice (UCSF) processed frozen sections for immunohistochemistry. Bioinformatics analysis of zebrafish *cspg2* gene was performed by S. Chatterji and L. Pachter. G. Howard provided editorial assistance and B. Taylor assisted with graphics and manuscript preparation. Support for this work came from the American Heart Association (AHA) Western Affiliates (S.U.M.), Helen Hay Whitney Foundation (P.J.S), US National Institutes of Health (HL-54737 (D.Y.R.S.)), Packard Foundation (D.Y.R.S.). D.S. was supported by grants from the NHLBI/NIH, AHA, March of Dimes Birth Defects Foundation and the California Institute of Regenerative Medicine.

References

Aanstad, P. and M. Whitaker (1999). "Predictability of dorso-ventral asymmetry in the cleavage stage zebrafish embryo: an analysis using lithium sensitivity as a dorso-ventral marker." Mech Dev **88**(1): 33-41.

Auman, H. J., H. Coleman, et al. (2007). "Functional modulation of cardiac form through regionally confined cell shape changes." PLoS Biol **5**(3): e53.

Beis, D., T. Bartman, et al. (2005). "Genetic and cellular analyses of zebrafish atrioventricular cushion and valve development." Development **132**(18): 4193–4204.

Berdougo, E., H. Coleman, et al. (2003). "Mutation of weak atrium/atrial myosin heavy chain disrupts atrial function and influences ventricular morphogenesis in zebrafish." Development **130**(24): 6121-9.

Bernstein, E., S. Y. Kim, et al. (2003). "Dicer is essential for mouse development." Nat. Genet. **35**(3): 215–217.

Chen, J. F., E. M. Mandel, et al. (2006). "The role of microRNA-1 and microRNA-133 in skeletal muscle proliferation and differentiation." Nat. Genet. **38**(2): 228–233.

D'Amico, L., I. C. Scott, et al. (2007). "A mutation in zebrafish hmgcr1b reveals a role for isoprenoids in vertebrate heart-tube formation." Curr Biol **17**(3): 252-9.

Dore, L. C., J. D. Amigo, et al. (2008). "A GATA-1-regulated microRNA locus essential for erythropoiesis." Proc Natl Acad Sci U S A **105**(9): 3333-8.

Giraldez, A. J., R. M. Cinalli, et al. (2005). "MicroRNAs regulate brain morphogenesis in zebrafish." Science **308**(5723): 833–838.

Glickman, N. S. and D. Yelon (2002). "Cardiac development in zebrafish: coordination of form and function." Semin Cell Dev Biol **13**(6): 507-13.

Gregory, R. I., T. P. Chendrimada, et al. (2005). "Human RISC couples microRNA biogenesis and posttranscriptional gene silencing." Cell **123**(4): 631–640.

Harfe, B. D., M. T. McManus, et al. (2005). "The RNaseIII enzyme Dicer is required for morphogenesis but not patterning of the vertebrate limb." Proc. Natl. Acad. Sci. USA **102**(31): 10898–10903.

Harris, K. S., Z. Zhang, et al. (2006). "Dicer function is essential for lung epithelium morphogenesis." Proc. Natl. Acad. Sci. USA **103**(7): 2208–2213.

Hutvagner, G., J. McLachlan, et al. (2001). "A cellular function for the RNA-interference enzyme Dicer in the maturation of the let-7 small temporal RNA." Science **293**(5531): 834–838.

Krutzfeldt, J., N. Rajewsky, et al. (2005). "Silencing of microRNAs in vivo with 'antagomirs'." Nature **438**(7068): 685-9.

Kwon, C., Z. Han, et al. (2005). "MicroRNA1 influences cardiac differentiation in Drosophila and regulates Notch signaling." Proc. Natl. Acad. Sci. USA **102**(52): 18986–18991.

Lee, Y., C. Ahn, et al. (2003). "The nuclear RNase III Drosha initiates microRNA processing." Nature **425**(6956): 415–419.

Nasevicius, A. and S. C. Ekker (2000). "Effective targeted gene 'knockdown' in zebrafish." Nat Genet **26**(2): 216-20.

Niederreither, K., V. Subbarayan, et al. (1999). "Embryonic retinoic acid synthesis is essential for early mouse post-implantation development." Nat Genet **21**(4): 444-8.

Perz-Edwards, A., N. L. Hardison, et al. (2001). "Retinoic acid-mediated gene expression in transgenic reporter zebrafish." Dev Biol **229**(1): 89-101.

Prabhudesai, S. N., D. A. Cameron, et al. (2005). "Targeted effects of retinoic acid signaling upon photoreceptor development in zebrafish." Dev Biol **287**(1): 157-67.
Sokol, N. S. and V. Ambros (2005). "Mesodermally expressed *Drosophila* microRNA-1 is regulated by Twist and is required in muscles during larval growth." Genes Dev. **19**(19): 2343–2354.
Srivastava, D. (2006). "Making or breaking the heart: From lineage determination to morphogenesis." Cell **126**: 1037–1048.
Stainier, D. and M. Fishman (1992). "Patterning the zebrafish heart tube: acquisition of anteroposterior polarity." Dev. Biol. **153**(1): 91–101.
Stainier, D. Y. (2001). "Zebrafish genetics and vertebrate heart formation." Nat Rev Genet **2**(1): 39-48.
Walsh, E. C. and D. Y. Stainier (2001). "UDP-glucose dehydrogenase required for cardiac valve formation in zebrafish." Science **293**(5535): 1670-3.
Westerfield, M. (2000). The zebrafish book. Aguide for the laboratory use of zebrafish (Danio rerio). Eugene, University of Oregon Press.
Wienholds, E., W. P. Kloosterman, et al. (2005). "MicroRNA expression in zebrafish embryonic development." Science **309**(5732): 310–311.
Wienholds, E., M. J. Koudijs, et al. (2003). "The microRNA-producing enzyme Dicer1 is essential for zebrafish development." Nat. Genet. **35**(3): 217–218.
Xavier-Neto, J., M. D. Shapiro, et al. (2000). "Sequential programs of retinoic acid synthesis in the myocardial and epicardial layers of the developing avian heart." Dev Biol **219**(1): 129-41.
Yelon, D., S. A. Horne, et al. (1999). "Restricted expression of cardiac myosin genes reveals regulated aspects of heart tube assembly in zebrafish." Dev Biol **214**(1): 23-37.
Yi, R., Y. Qin, et al. (2003). "Exportin-5 mediates the nuclear export of pre-microRNAs and short hairpin RNAs." Genes Dev. **17**(24): 3011–3016.
Zhao, Y., J. F. Ransom, et al. (2007). "Dysregulation of cardiogenesis, cardiac conduction, and cell cycle in mice lacking miRNA-1-2." Cell **129**: 303–317.
Zhao, Y., E. Samal, et al. (2005). "Serum response factor regulates a muscle-specific mircroRNA that targets *Hand2* during cardiogenesis." Nature **436**: 214–220.
Zhao, Y. and D. Srivastava (2007). "A developmental view of microRNA function." Trends Biochem. Sci. **32**: 189–197.

Figure Legends

Figure 2-1.

miR-138 is required for cardiac development. (*A*) Oblique view of 72 hpf fish after *in situ* hybridization showing expression of miR-138 in ventricular cardiomyocytes marked by blue staining. (*B*) qRT-PCR analysis of mature miR-138 expression at 48 hpf in cardiomyocytes (cmlc2), endothelial cells (flk1) or whole embryo demonstrated enrichment of miR-138 in cardiomyocytes. Mature miR-138 was not detected (nd) in endothelial cells. **(***C,D***)** Fish embryos injected with miR-138 scrambled control oligo (scr) (*C*) or miR-138 morpholino (mo-1) **(***D***)** showing pericardial edema (asterisk); arrowhead indicates heart. (*E-I***)** Representative confocal analysis of transgenic *Tg(myl7:HRAS-mEGFP)*^{s843} uninjected embryos (*E*) or embryos injected with 17-nt miR-138^{scr} **(***F***)**, 17-nt miR-138$^{mo\text{-}1}$ **(***G***)**, or a second 31-nt miR-138$^{mo\text{-}2}$ oligo **(***H*). Insets show single z-stack images of outer curvature ventricular myocytes which normally elongate with maturation (*E,F*) but remained rounded in the miR-138$^{mo\text{-}1}$ embryos (*G,H*). (*I*) Confocal image of elongated atrioventricular canal (avc) upon miR-138$^{mo\text{-}1}$ injection. (e, eye; y, yolk sac; a, atrium; v, ventricle).

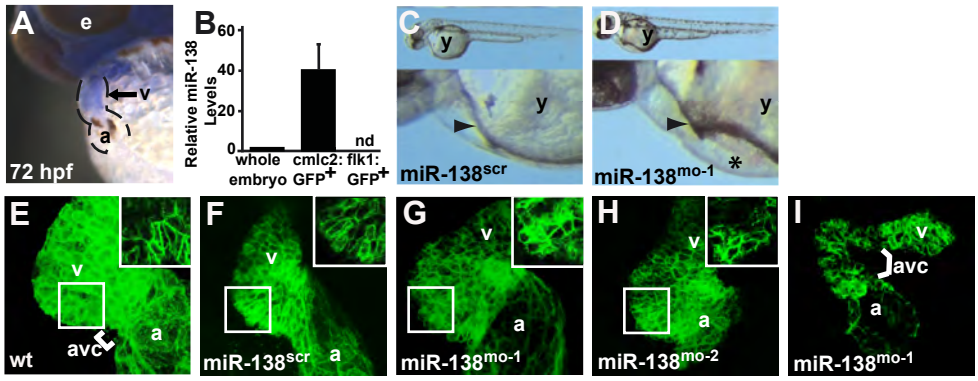
A
e
v
a
72 hpf
B
Relative miR-138 Levels
60
40
20
0
whole embryo
cmlc2: GFP+
flk1: GFP+
nd
C
y
y
miR-138scr
D
y
y
miR-138mo-1
*
E
v
a
avc
wt
F
v
a
miR-138scr
G
v
a
miR-138mo-1
H
v
a
miR-138mo-2
I
v
avc
a
miR-138mo-1

Figure 2-2.

miR-138 knockdown leads to expansion of atrioventricular canal-specific gene expression into the ventricle. (*A-H*) Ventral views of 48 hours post fertilization (hpf) embryos after mRNA in situ hybridization focusing on head (h) and heart (dotted lines) regions. Atrial **(***A***,** *B***)** and ventricular **(***C,D***)** markers were similar in wild-type (wt) **(***A,C***)** and miR-138$^{mo\text{-}1}$ embryos **(***B,D***)**. Expression of atrioventricular canal (avc)-specific markers *cspg2* **(***E,F***)** and *notch1b* **(***G,H***)** expanded into the ventricles (v) in miR-138$^{mo\text{-}1}$ embryos **(***F,H***)** compared to wild type embryos (*E,G*). (a, atrium; amhc, atrial myosin heavy chain; vmhc, ventricular myosin heavy chain).

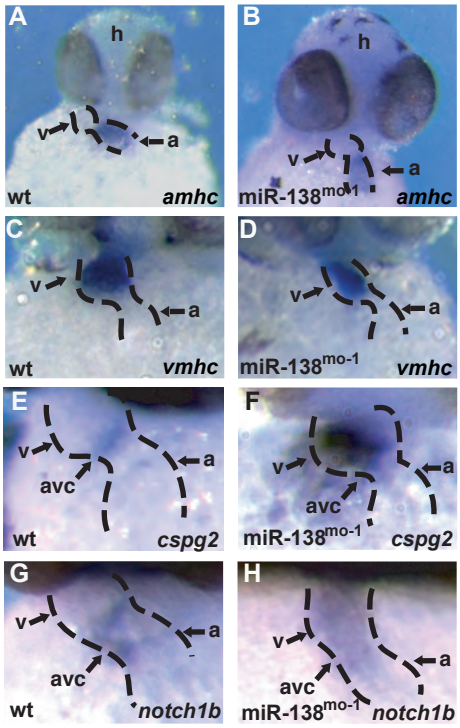
A
h
v
a
wt
amhc
B
h
v
a
miR-138mo-1
amhc
C
v
a
wt
vmhc
D
v
a
miR-138mo-1
vmhc
E
v
avc
a
wt
cspg2
F
v
avc
a
miR-138mo-1
cspg2
G
v
a
avc
wt
notch1b
H
v
a
avc
miR-138mo-1
notch1b

Figure 2-3.

Temporal regulation of miRNA function by antagomiRs in zebrafish. (*A*) miR-138 RNA levels detected by qRT-PCR in 72-hpf fish embryos treated with antagomiRs from 24, 30 or 34 hours post fertilization (hpf), or injected with the 31-nt morpholino (MO-2) compared to PBS- or scrambled antagomiR-treated controls. **(***B-D***)** Confocal images of hearts of 72-hpf *Tg(myl7:HRAS-mEGFP)*^{s843} transgenic embryos treated with PBS (*B*), scrambled antagomiR (SCR^{am}) (*C*), or miR-138 antagomiR (miR-138^{am}) (*D*) from 24–72 hpf. GFP revealed rounded myocyte morphology (inset) in miR-138^{am} embryos compared to the normally elongated myocytes seen in controls. (*E*) Pericardial edema indicating cardiac dysfunction and rounded ventricular myocytes reflecting delayed maturation were observed in varying percentages of 72-hpf embryos treated with PBS, SCR^{am}, or miR-138^{am} from the hpf indicated. (*F*,*G*) Ventral view of mRNA *in situ* hybridization to detect *cspg2* expression in hearts of embryos treated with SCR^{am} (*F*) or miR-138^{am} (*G*) showed expansion of *cspg2* into the ventricle of miR-138^{am} embryos; heart is indicated with dotted lines. Results shown are the average of four experiments in (*A***)** and (*E*). (v, ventricle; a, atrium; atrioventricular canal (avc); *, $p<0.05$)

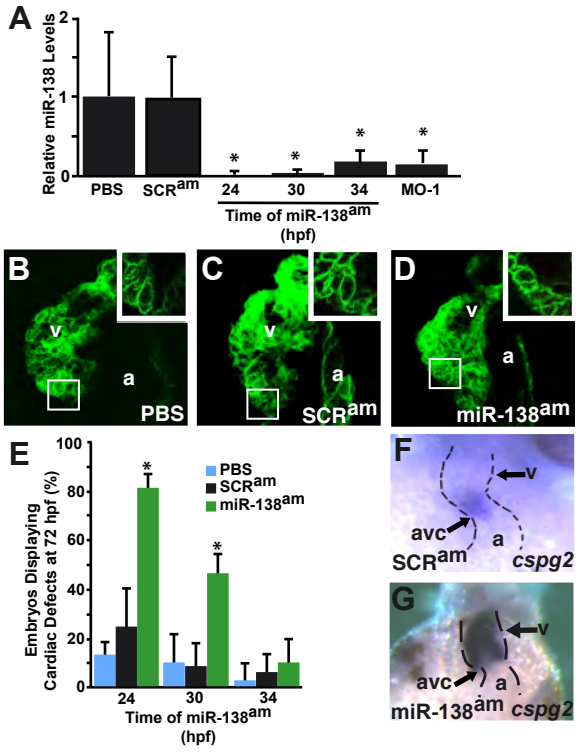
A
Relative miR-138 Levels
2
1
0
PBS
SCRam
24
30
34
MO-1
Time of miR-138am
(hpf)
B
v
a
PBS
C
v
a
SCRam
D
v
a
miR-138am
E
Embryos Displaying
Cardiac Defects at 72 hpf (%)
100
80
60
40
20
0
PBS
SCRam
miR-138am
24
30
34
Time of miR-138am
(hpf)
F
v
avc
a
SCRam
cspg2
G
v
avc
a
miR-138am
cspg2

Figure 2-4.

miR-138 directly targets *aldh1a2,* restricting its expression to the atrioventricular canal. (*A*) miR-138 binding site in zebrafish *aldh1a2* 3´ UTR with complementary nucleotides indicated in red. Luciferase activity in Cos cells upon introduction of wild type or mutated *aldh1a2* 3´ UTR sequences downstream of a CMV-driven luciferase reporter with no miRNA (negative control) or miR-138 is shown. **(***B***)** *aldh1a2* mRNA levels measured by qRT-PCR in embryos injected with pri-miR-138 or treated at 24 hpf with miR-138 antagomiR (miR-138^{am}) or scrambled antagomiR (SCR^{am}). **(***C,D***)** Raldh2 immunohistochemistry on sections of 72-hpf embryos treated with PBS or miR-138^{am} from 24-72 hpf. Ventricular cardiomyocyte expression (arrow) was readily detectable in miR-138^{am} hearts but not in controls, while intensity of staining in the atrioventricular canal (avc) was similar. **(***E-G***)** Ventral view of *cspg2* expression in the heart by mRNA *in situ* hybridization in embryos treated with scrambled morpholino (miR-138^{scr}) (*E*), miR-138^{mo-1} (*F*) or retinoic acid (RA) **(***G***)**; heart is indicated with dotted lines. **(***H-J***)** Confocal images of *myl7-GFP* embryos (48 hpf) treated with vehicle (DMSO) **(***H***)**, miR-138^{mo-1} **(***I***)**, or miR-138^{mo-1} embryos treated with DEAB **(***J***)** showing rescue of the expanded atrioventricular canal (avc) defect with DEAB. (*K-M*) Expansion of *cspg2* mRNA expression from the avc (K) into the ventricle (v) of miR-138^{mo-1} embryos (*L*) was not rescued by DEAB **(***M***).** Results shown represent at least four experiments in (*A*) and (*B*). Error bars indicate 95% confidence intervals. **(**avc, atrioventricular canal; a, atrium; v, ventricle; *, $p<0.05$.)

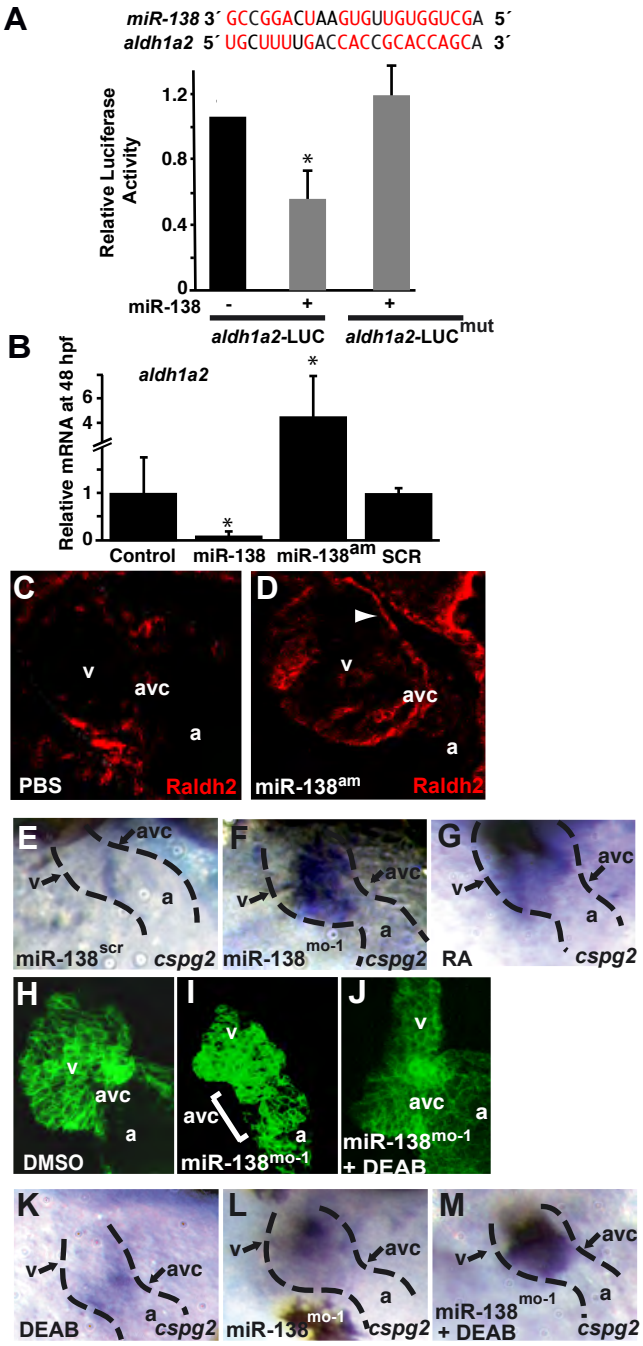
A
miR-138 3´ GCCGGACUAAGUGUUGUGGUCGA 5´
aldh1a2 5´ UGCUUUUGACCACCGCACCAGCA 3´
Relative Luciferase Activity
1.2
0.8
0.4
0
miR-138 - + +
aldh1a2-LUC
aldh1a2-LUCmut
B
aldh1a2
Relative mRNA at 48 hpf
6
4
1
0
Control
miR-138
miR-138am
SCR
C
v
avc
a
PBS
Raldh2
D
v
avc
a
miR-138am
Raldh2
E
avc
v
a
miR-138scr
cspg2
F
avc
v
a
miR-138mo-1
cspg2
G
avc
v
a
RA
cspg2
H
v
avc
a
DMSO
I
v
avc
a
miR-138mo-1
J
v
avc
a
miR-138mo-1
+ DEAB
K
v
avc
a
DEAB
cspg2
L
v
avc
a
miR-138mo-1
cspg2
M
v
avc
a
miR-138mo-1
+ DEAB
cspg2

Figure 2-5.

miR-138 directly targets *cspg2*. (*A*) miR-138 binding site in mouse *cspg2* 3′ UTR with complementary nucleotides indicated in red. Luciferase activity in Cos cells upon introduction of wild type or mutated *cspg2* 3′ UTR sequences downstream of a CMV-driven luciferase reporter with no miRNA (negative control) or miR-138 is shown. **(***B,C***)** Analysis of *cspg2* RNA level assessed by qRT-PCR **(***B***)** and corresponding versican protein by western blot **(***C***)** in mouse NIH3T3 fibroblasts transfected with miR-138. **(***D***)** *cspg2* mRNA levels detected by qRT-PCR in zebrafish embryos injected with miR-138 or treated at 24 hpf with miR-138 antagomiR or scrambled antagomiR. (*E*) Proposed model for the function of miR-138 in regulating chamber-specific gene expression and atrioventricular canal (avc) patterning. miR-138 directly represses retinoic acid (RA) synthesis in the ventricle (v) via *aldh1a2*, which would otherwise induce expression of the avc-specific gene, *cspg2* (versican). Repression of *cspg2* by miR-138 in the ventricle is also accomplished by directly targeting *cspg2*. Results shown in (*A*), (*B*) and (*D*) represent at least four experiments with error bars indicating 95% confidence intervals. (a, atrium; *, $p<0.05$).

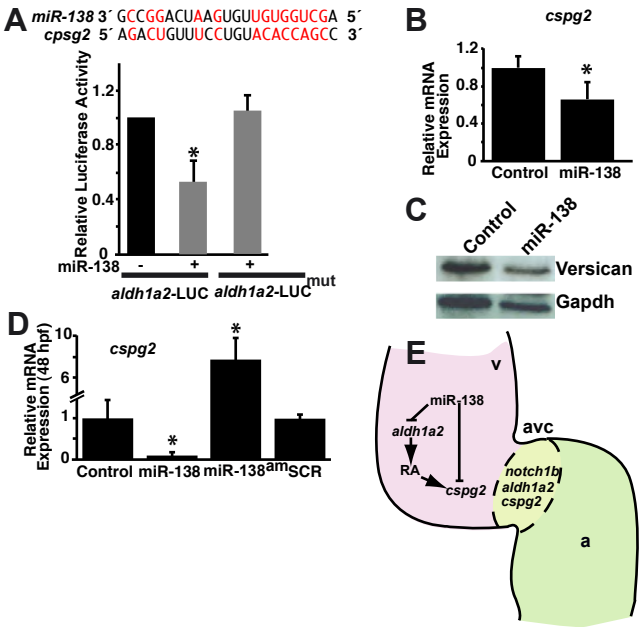
A
miR-138 3´ GCCGGACUAAGUGUUGUGGUCGA 5´
cpsg2 5´ AGACUGUUUCCUGUACACCAGCC 3´
Relative Luciferase Activity
1.2
0.8
0.4
0
miR-138 - + +
aldh1a2-LUC aldh1a2-LUCmut
B
cspg2
Relative mRNA Expression
1.2
0.8
0.4
0
Control miR-138
C
Control
miR-138
Versican
Gapdh
D
cspg2
Relative mRNA Expression (48 hpf)
10
6
1
0
Control miR-138 miR-138amSCR
E
v
miR-138
aldh1a2
RA
cspg2
avc
notch1b
aldh1a2
cspg2
a

Supplemental Figure 2-1

Alignment of mature miR-138 sequence from multiple species. A single copy of the gene is present in most species shown, while two genes encoding miR-138 are found in others, including mouse and human.

		5`	3`
Fugu	miR-138	AGCUGGUGUUGUGAAUC	
Zebrafish	miR-138	AGCUGGUGUUGUGAAUC	
Frog	miR-138	AGCUGGUGUUGUGAAUC	
Opossum	miR-138	AGCUGGUGUUGUGAAUC	
Cow	miR-138	AGCUGGUGUUGUGAAUC	
Mouse	miR-138-2	AGCUGGUGUUGUGAAUC	
	miR-138-1	AGCUGGUGUUGUGAAUC	
Human	miR-138-2	AGCUGGUGUUGUGAAUC	
	miR-138-1	AGCUGGUGUUGUGAAUC	

Supplemental Figure 2-2

miR-138 is not required for vasculogenesis. (*A,B*) *Tg(flk1:EGFP)*^{s843} embryos, where GFP expression at 48 hpf marks endocardial cells and endothelial cells in blood vessels. Blood vessels between the somites and within the head appear similar in control (*A*) and miR-138-morpholino injected fish (*B*). (dv, dorsal vessels; h, head; ht, heart; isv, intersomitic vessels.)

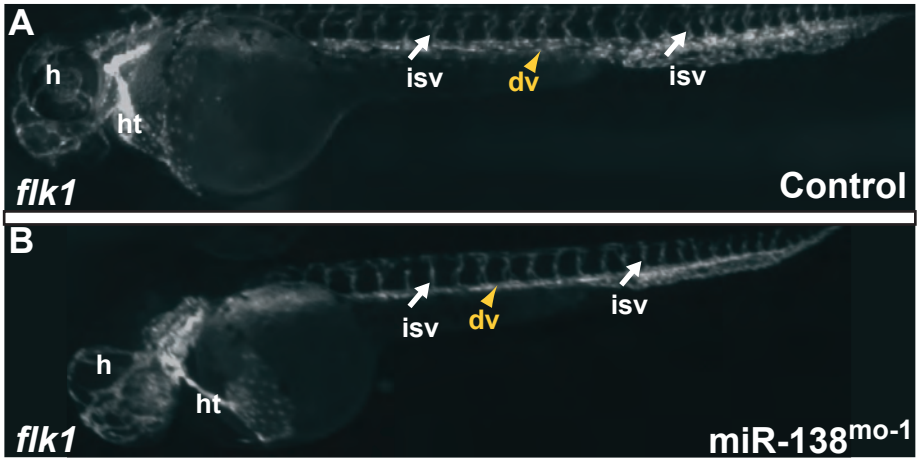
A
h
ht
isv
dv
isv
flk1
Control
B
isv
dv
isv
h
ht
flk1
miR-138mo-1

Supplemental Figure 2-3

miR-138 is not required for early cardiac progenitor specification. (*A,B*) Expression of *cmlc2* in dorsal views at 24 hpf as determined by *in situ* hybridization (purple) in whole-mount embryos indicates that cardiac progenitors are similarly specified in control (*A*) and 138-morpholino injected fish (*B*). (*C-F*) *In situ* hybridization for *cspg2* (*C,D*) and *notch1b* (*E,F*) in wild-type (*C,E*) and miR-138^{scr} fish (*D,F*) demonstrate atrioventricular-specific expression at 48 hpf.

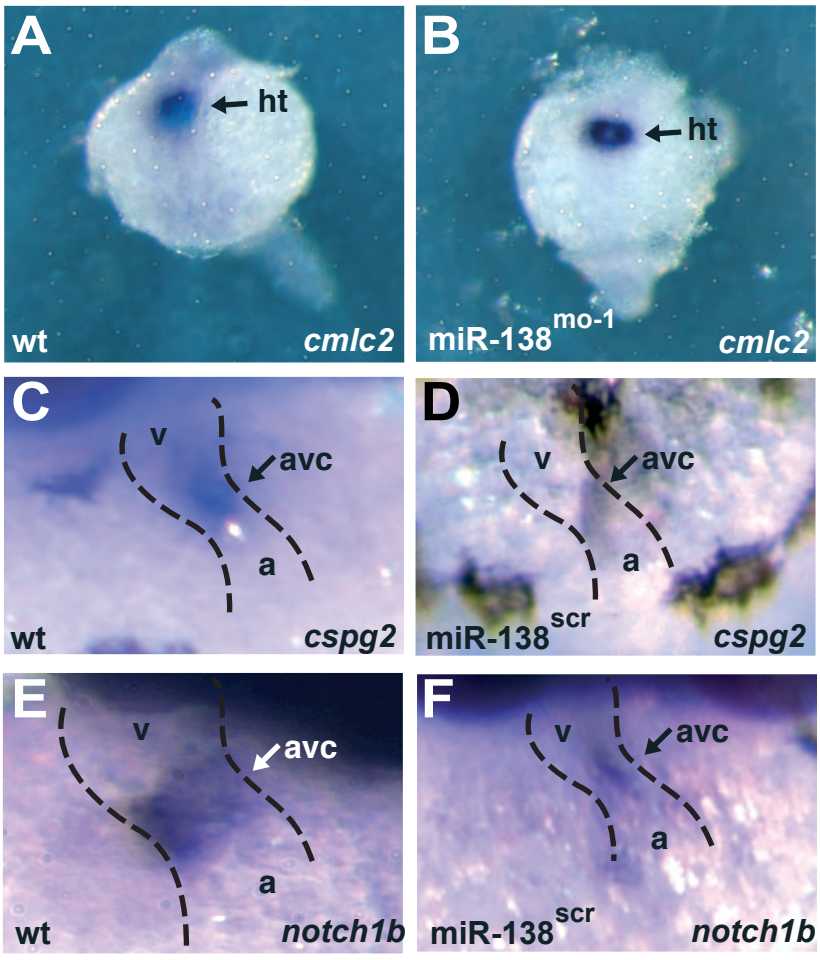
A
ht
wt
cmlc2
B
ht
miR-138mo-1
cmlc2
C
v
avc
a
wt
cspg2
D
v
avc
a
miR-138scr
cspg2
E
v
avc
a
wt
notch1b
F
v
avc
a
miR-138scr
notch1b

Supplemental Figure 2-4

AntagomiRs effectively knockdown miRNA in zebrafish. (*A,B*) *Tg(flk1:EGFP*^{s843}*; gata1:dsRed)*^{s843} embryos at 32 hpf, where RFP expression marks red blood cells (RBCs) and GFP expression marks endothelial cells. Decreased RBCs are seen in miR-451^{am} embryos (*B*) compared to control antagomiR-treated embryos (*A*). (*C*) qRT-PCR analysis of 5 day post fertilization embryos treated with PBS or miR-138 antagomiR demonstrates continued knockdown of miR-138.

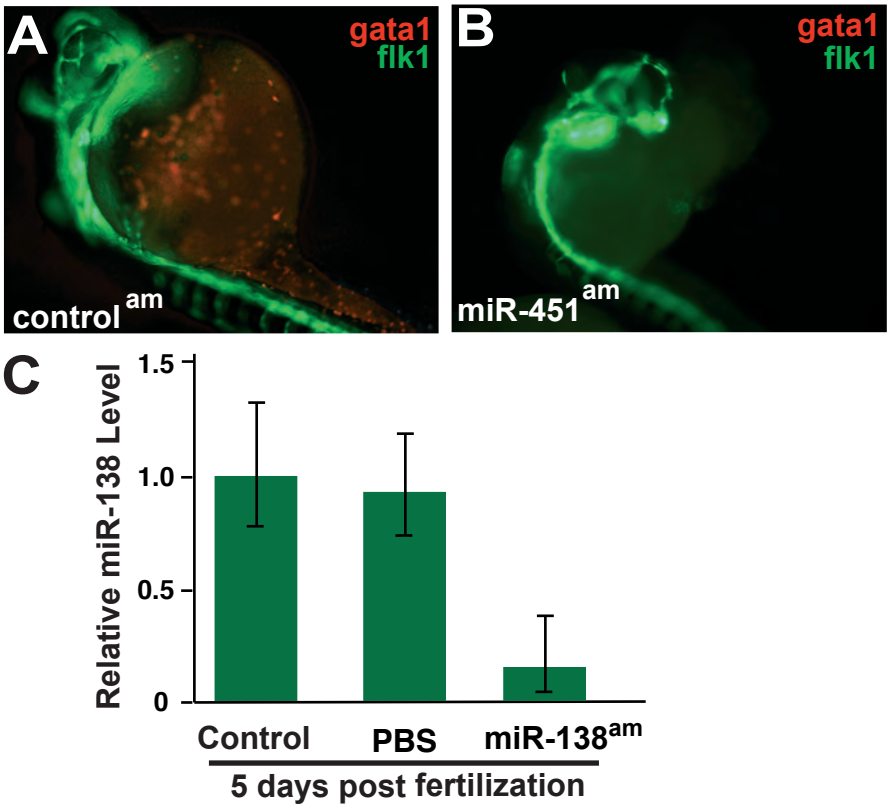
A
gata1
flk1
control am
B
gata1
flk1
miR-451 am
C
Relative miR-138 Level
1.5
1.0
0.5
0
Control
PBS
miR-138am
5 days post fertilization

Supplemental Figure 2-5

miR-138 regulates Raldh2 expression. (*A*) Quantification of Raldh2-positive area in multiple immunohistochemistry sections as represented in Figure 4 c-d. Results shown are the average of 4 slides per group. (*B*-*C*) Immunohistochemistry for Raldh2 protein in miR-138^{am} fish demonstrates Raldh2 expression overlapping with Tg(*flk1*-EGFP)^{s843} (*B*) in the atrioventricular canal (AVC), and raldh2 overlapping with Tg(*cmlc2*-ras-EGFP)^{s843} in the ventricle (*C*). *cmlc2*-ras-EGFP expression is localized to the cell membrane of cardiomyocytes. (*D,E*) *In situ* hybridization for *aldh1a2* demonstrates AVC-restricted expression in control fish (*D*) but expanded ventricular expression in miR-138mo fish (*E*).

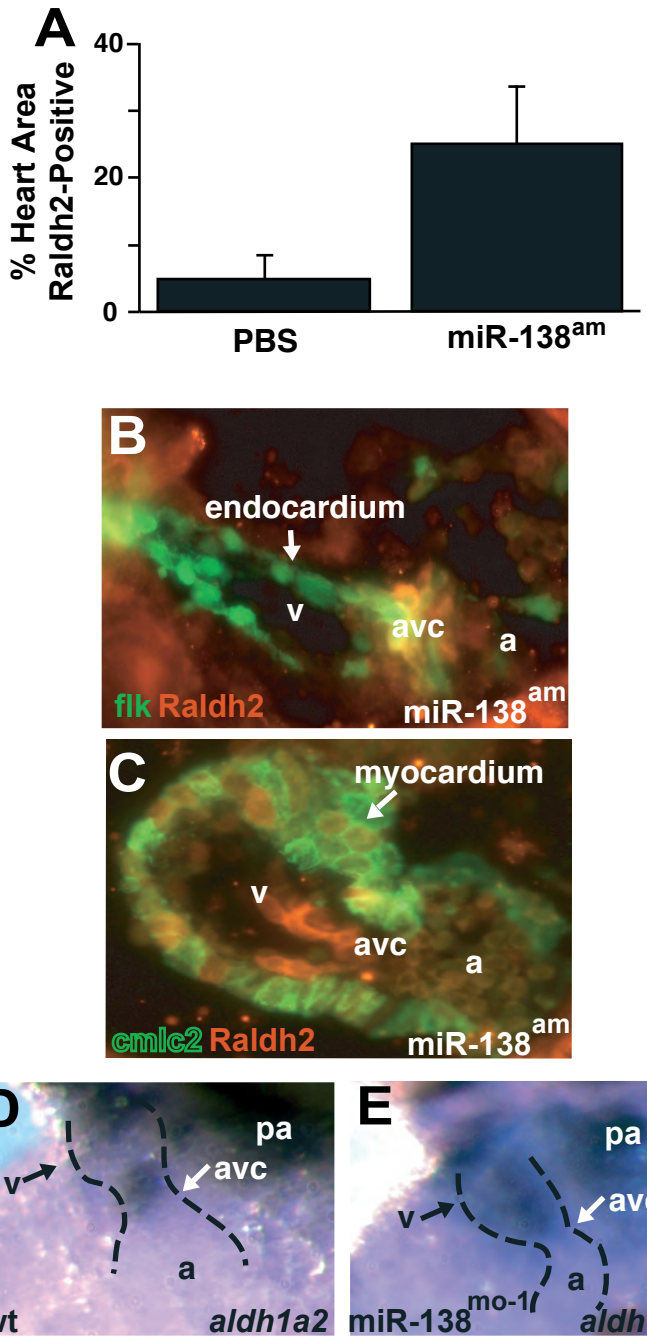
A
% Heart Area Raldh2-Positive
40
20
0
PBS
miR-138am
B
endocardium
v
avc
a
flk Raldh2
miR-138am
C
myocardium
v
avc
a
cmlc2 Raldh2
miR-138am
D
pa
v
avc
a
wt
aldh1a2
E
pa
v
avc
a
miR-138mo-1
aldh1a2

Supplemental Figure 2-6

miR-138 does not directly regulate Notch1b. Luciferase activity upon introduction of *danio rerio notch1b* 3′ UTR sequences downstream of a CMV-driven luciferase reporter. Luciferase activity in Cos cells with miR-138 is shown.

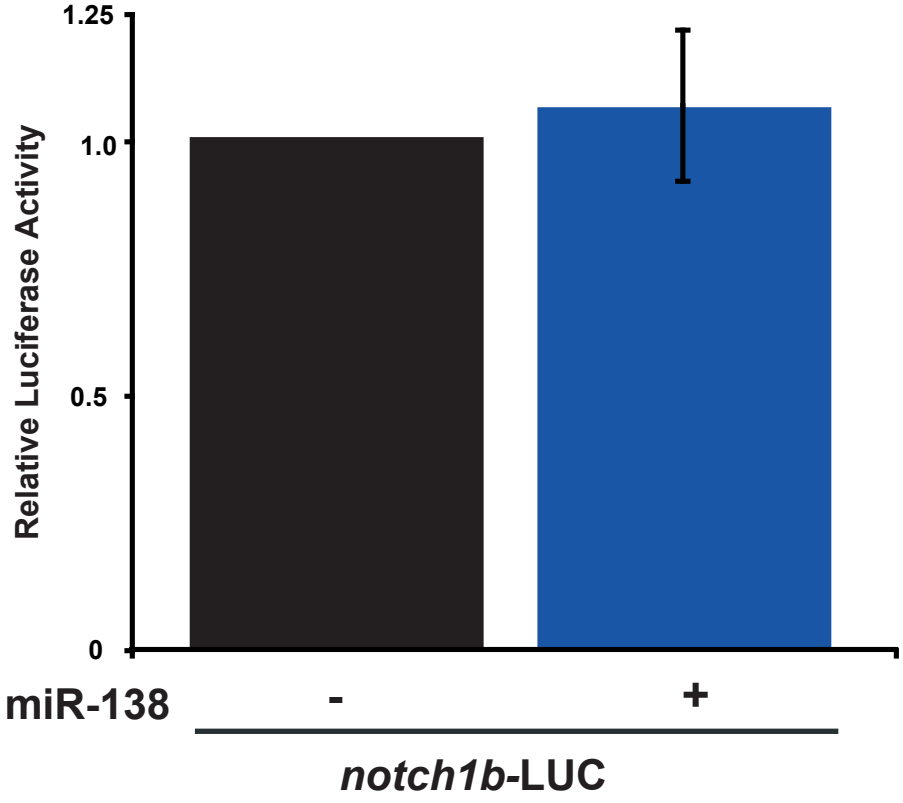
1.25
1.0
0.5
0
Relative Luciferase Activity
miR-138
-
+
notch1b-LUC

Chapter Three:

miR-202* Regulates Left-Right Patterning

Summary

To identify miRNAs regulated during cardiac development, we performed microarray analysis of miRNA expression in cardiac tissues at various stages of mouse embryonic development. We identified one miRNA, miR-202*, to be enriched in the ventricular chambers during late stages of heart development. When miR-202* was inhibited by morpholino during zebrafish development, cardiac development and function were compromised. Specifically, there was a disruption in the laterality of cardiac looping, as well as in synchronization of cardiac conduction. The defects in laterality are likely due in part to direct targeting of the gene *polycystic kidney disease 2, pkd2*; sequence-specific interactions between miR-202* and Pkd2 mRNA result in inhibition in heterologous systems, and downstream genes such as *lefty2* dysregulated in the miR-202* knockdown embryos. These studies are therefore the first demonstration of miRNA involvement in left-right patterning of vertebrates.

Introduction

The heart is the first organ to function during development, and among the first organs to attain left-right asymmetry. As the heart begins to form an initial, linear heart tube arises from lateral plate mesoderm, which then undergoes looping which brings the ventricle to the left of the atrium. Looping breaks the left-right symmetry of the heart, and is regulated by the same pathways that control left-right patterning of the body, such as *pitx2*, *lefty2*, and *southpaw* (Meno, Saijoh et al. 1996; Nonaka, Tanaka et al. 1998; Piedra, Icardo et al. 1998; Ryan, Blumberg et al. 1998; Campione, Steinbeisser et al. 1999). These asymmetrically-expressed genes are downstream of initial embryo patterning events at Kuppfer's node (Bisgrove, Snarr et al. 2005). At the node are motile and immotile cilia, which direct fluid flow in a counterclockwise direction. Pkd2, a calcium channel expressed on epithelial cells including those at Kuppfer's node, may serve as a mechanosensor for the cilia, resulting in calcium ion transients that signal to downstream effectors. Though the timing of the morphological events in left-right patterning is characterized in many organisms, regulation of the key molecular signals for the breaking of left-right symmetry is incompletely understood.

microRNAs (miRNAs) are one class of regulatory molecules known to be necessary for proper cardiac development. miRNAs are small, highly conserved non-coding RNAs (Zhao and Srivastava 2007). Mature miRNAs inhibit gene expression post-transcriptionally by two known mechanisms (Du and Zamore 2005). Binding of the mature miRNA to complimentary sequences in the 3′ untranscribed region (UTR) of mRNA can trigger mRNA degradation or inhibit translation. The best-characterized miRNA in cardiac development is miR-1; studies of miR-1 set a precedent for the importance of miRNAs in directing heart development. Other miRNAs, expressed as the cardiac precursors migrate and mature to form the adult heart, are likely to be instrumental to cardiac specification and differentiation, given the extreme

phenotype observed when miRNA processing is halted in cardiac progenitors (Zhao, Ransom et al. 2007). Mouse embryos that have Cre-mediated excision of the processing domain of *Dicer*, a nuclease necessary for miRNA maturation, within the cardiac precursor population defined by expression of the transcription factor *Nkx-2.5* have cardiac defects not observed in the mice null for *miR-1-2*.

The aim of this study was to identify new miRNAs important in cardiac development, and to characterize the role of one of these miRNAs, miR-202*, in zebrafish cardiac development. Through miRNA microarray of developing mouse hearts we identified many miRNAs expressed during embryonic heart development. Further characterization of the role one miRNA highly expressed in cardiac tissue, miR-202*, during cardiac development in zebrafish has demonstrated its necessity for proper left-right axis formation. This effect may be mediated through its direct target, *pkd2*, known to be upstream of *lefty2* and *southpaw* in left-right patterning. Further characterization of this regulatory interaction will determine whether *pkd2* alone, or other direct targets, mediate this effect.

Results

miRNAs Expression Patterns in the Developing Heart

To identify miRNAs that are enriched in the developing heart, specific regions of heart were microdissected from mouse embryos. At early time points, embryonic day (E) 11.5, E12.5 and E13.5, the derivatives of the first and second heart field were separated by dissection of the outflow tract and right ventricle from the left ventricle and atria. At later time points, E15.5 and E18.5, the left and right ventricles were dissected individually, and the atria collected. Total RNA from these tissues were hybridized on miRNA microarrays against E14 whole embryo RNA, to identify miRNAs enriched in cardiac regions throughout development. Clustering of the microarrays demonstrated a diversity of expression patterns among miRNAs (Fig. 3-S1A). Analysis of those miRNAs with high relative expression in cardiac tissues revealed the known cardiac miRNA, miR-1 (Fig. 3-1A). qRT-PCR analysis showed similar relative enrichment of miR-1 as was seen by microarray (Fig. 3-1B). Other miRNAs in this category include miR-155, a known hematopoietic miRNA (Calame 2007). It is likely that miR-155 appears enriched due to blood cells within the heart tissue collected.

Many patterns of miRNA analysis were evident in the clustered array data. Some, such as miR-182*, were expressed primarily at later stages of heart development. Among the miRNAs with high expression throughout heart development were miR-1 and miR-202*. miR-202* had high expression in the developing heart, and its pattern of expression clustered closely with the expression pattern for miR-1. At the later time points, miR-202* was particularly enriched in the ventricular chambers.

miR-202*, annotated as miR-202-5p in mouse, is a highly conserved miRNA and has been previously described as expressed in adult testes (Michalak and Malone

2008) (Fig. 3-1C). Northern analysis of adult mouse organs demonstrated ubiquitous expression of pri-miR-202*, with mature miR-202* found in the many tissues including testis, thymus, and uterus (Fig. 3-1D). The pre-miR-202* transcript also encodes another identified miRNA, miR-202-3p. Analysis of expression of miR-202-5p and miR-202-3p in embryonic tissues by qRT-PCR showed that miR-202-5p and miR-202-3p are often co-expressed in tissues of the mouse embryo (Fig. 3-S2).

Alterations in miR-202* Levels Cause Abnormal Heart Development

The sequence of miR-202* is highly conserved among species (Fig. 3-1C). We therefore used zebrafish as a model system to test its function during cardiognesis. qRT-PCR analysis of whole fish RNA during embryogenesis revealed high levels of miR-202* within the first day of life, and continued expression out to 96 hours post fertilization (hpf) (Fig. 3-S3A). *In situ* hybridization analysis of miR-202* demonstrated broad expression throughout the embryo at many time points. In agreement with the qRT-PCR results, miR-202* was easily detected at 24 hpf (Fig. 3-2A). Expression levels at 32 hpf remained high by *in situ* hybridization (Fig. 3-2B). Isolation of myocardial cells, or endocardial/endothelial cells, at 48 hpf using the *cmlc2* or *flk1* transgenic reporters, respectively, followed by qRT-PCR for miR-202* demonstrated modest enrichment in myocardial cells compared to whole embryo and strong enrichment in the endocardial/endothelial cell population (Fig. 3-2C). Thus it is likely that the cardiac enrichment observed array is due to high expression of miR-202* in the ventricular endocardium. miR-202, the 3' product, was undetectable in zebrafish samples by qRT-PCR.

Modulation of miR-202* expression by injection of 1-2 ng of a morpholino against the pri-miR-202 sequence in the 1-2 cell zebrafish embryo resulted in cardiac defects. The morpholino was designed to prevent processing of miR-202* without

disrupting the potential expression of miR-202, encoded at the 3' end of the same pre-miRNA transcript in mouse but not observed by qRT-PCR in zebrafish. Analysis of miR-202* levels by qRT-PCR demonstrated reduction by of mature miR-202* expression by 90% following morpholino injection (Fig. 3-2D). These fish displayed pericardial edema in over 50% of injected embryos at 48 hpf, and body edema in a further 15% of injected embryos (Fig. 3-2,E-G). Most miR-202* knockdown embryos with pericardial edema also had defects in cardiac function, with a hypokinetic or akinetic ventricle being the most commonly observed phenotype. However, the vasculature and circulation of miR-202* morphants were comparable to control morphants at 48hpf, indicating that the cardiac dysfunction was unlikely to be secondary to extracardiac disruption of blood flow (Fig. 3-S2B,C). Overexpression of 50-100 pg of miR-202* by injection of a duplex mimic miRNA also resulted in pericardial edema by 48 hpf, with no gross body defects but occasional tail edema (Fig. 3-2H).

Alterations in miR-202* Levels Do Not Affect Cardiac Chamber Patterning

To identify the causes of the visible dysfunction of the heart in miR-202* knockdown embryos, it was important to separate structural from functional etiologies. Proper patterning of cardiac progenitors and subsequent heart chambers specification were assayed via *in situ* hybridization. Early cardiac progenitors, marked at 24 hpf by *cmlc2* expression, appeared intact irrespective of miR-202* modulation (Fig. 3-3,A-C). Similarly, patterning of the atrium and ventricle, as marked by *amhc* and *vmhc* expression, respectively, was unaffected by alterations to miR-202* expression levels (Fig. 3-3,D-I). *Tbx2b* expression, which marks the atrioventricular canal between the two chambers, was also unaltered with knockdown or overexpression of miR-202* (Fig 3-3,J-L).

miR-202* Knockdown Leads to Left-Right Asymmetry Defects

Though the patterning of cardiac progenitors and chambers were unaffected by miR-202* knockdown or overexpression, the structure of the heart was sensitive to miR-202* levels. The mature zebrafish heart loops to the left by 48 hpf, as seen in fluorescence or confocal microscopy (Fig. 3-4A,B). Knockdown of miR-202* resulted in randomization of cardiac looping, with many hearts found unlooped (Fig. 3-4C,D) or looped to the right (Fig. 3-4E,F). Though not a complete randomization, where one third of the embryos would each be left-looped, midline, or right-looped, around 40% of the miR-202* knockdown embryos displayed irregular looping (Fig. 3-4G). Thus the cardiac defects in miR-202* morphant embryos include the structural abnormality of incompletely looped and right-looped hearts.

2:1 AV Block in miR-202* Morphants

To further study the functional abnormalities in the miR-202* knockdown embryos, we sought to separate any cardiac conduction defects from defects in myocardial contractility. Using the *silent heart* (*sih*) mutant line, which is acontractile due to a lack of cardiac Troponin T, we visualized conduction within atrium and ventricle the miR-202* knockdown embryos using *Tg(cmlc2:gCaMP)*^{s878} reporter fish. Notably, the atrial and ventricular chambers are indistinguishable structurally between fish injected with a control or miR-202* morpholino (Fig. 3-5A,B). Analysis of miR-202* knockdown embryos demonstrated defects in cardiac conduction, specifically a 2:1 atrioventricular (AV) block, where the atrium would conduct twice for every ventricular conduction (Fig. 3-5C). This 2:1 AV block was present regardless of bradycardia or tachycardia. This conduction abnormality is likely the cause of the more complex rhythm disturbance first observed in the miR-202* knockdown embryos, which presented with significant hypokinesis, as the

mechanical stress caused by flow disturbances can lead to further functional abnormalities.

miR-202* Targets *Pkd2* and *p38*

Based on the seed sequence of miR-202*, as well as the secondary structure of potential target mRNAs, we used bioinformatics software to predict potential direct targets of miR-202*. From this list 16 mRNA 3'UTRs were cloned and tested for sequence-specific repression by miR-202* compared to a mutant miR-202*. Three targets demonstrated significant repression by miR-202*: *kcna4*, a cardiac potassium channel; *mapk14*, also known as *p38*, a protein kinase important in cell cycle regulation; and *pkd2*, an epithelial calcium channel important in kidney physiology and left-right patterning (Fig. 3-6A). Mutation of 2-3 nucleotides within the miR-202* binding site in the 3'UTR of these genes relieved repression of luciferase activity, demonstrating the sequence-specific regulation of the target mRNAs by miR-202*.

As *pkd2* has a known role in left-right asymmetry, and miR-202* knockdown resulted in randomization of left-right patterning, we studied potential regulation of Pkd2 by miR-202* in zebrafish embryos and in cell culture. Pkd2 mRNA levels were unchanged in 24hpf fish that had been injected with miR-202* morpholino or miR-202* mimic (Fig. 3-S4A). Antibodies to Pkd2 did not detect zebrafish protein by Western, but analysis of Cos-1 kidney cells transfected with miR-202* duplex mimic demonstrated downregulation of the protein (Fig. 3-6B).

Western blot analysis of miR-202* regulation of Mapk14 expression in 26 hpf zebrafish embryos revealed downregulation of Mapk14 upon overexpression of miR-202* and slight upregulation of the protein with knockdown of miR-202* (Fig. 3-6C). Interestingly, the mRNA levels of both zebrafish versions of Mapk14, Mapk14a and Mapk14b, were unchanged with miR-202* morpholino, and actually increased with

miR-202* mimic (Fig. 3-S4B). Given that Mapk14 is a cell cycle activator, increased levels of Mapk14 protein in miR-202* embryos should result in increased proliferation rates. Pulse treatment of zebrafish embryos at 24 hpf with BrdU did result in increased BrdU incorporation in miR-202* knockdown embryos compared to control (Fig. 3-6D,E), while addition of miR-202* mimic decreased BrdU incorporation (Fig. 3-6F). The defects in cardiac function made determination of relative heart size difficult in miR-202* knockdown embryos, so it is not possible to say whether the increased proliferation resulted in hypercellularity. However, there was no gross abnormality in body size in fish with altered levels of miR-202*.

Discussion

This is the first analysis of miRNA expression in heart development to study the expression of hundreds of miRNAs in specific spatial regions throughout mouse embryogenesis. By analyzing miRNA expression throughout mouse cardiac development, we have identified many miRNAs with significant cardiac expression, and demonstrated their spatiotemporal patterns of expression. The expression patterns of few of the miRNAs identified in this screen as being cardiac-enriched have been characterized in any organism; functions have been identified for even fewer. Thus our results here suggest that many more miRNAs have a role in cardiac development. Preliminary experiments targeting a few of these miRNAs, such as miR-140 and miR-182*, did demonstrate abnormal embryogenesis following knockdown of the miRNA in zebrafish embryos (data not shown). Future studies of the miRNAs identified here to be enriched in the developing heart will shed light on the broad role of miRNAs in cardiac development and function.

The complex functional defects observed following knockdown of miR-202* in zebrafish are at least partially explained by the conduction abnormality observed by optical mapping. The hypokinesis of the ventricle seen in non-*sih* fish was likely due to effects of abnormal conduction on cardiac development. As the atrial depolarization occurs twice for every ventricular depolarization in miR-202* morphants, the output of the atrium creates excess pressure in the more slowly beating ventricle, especially prior to formation of the atrioventricular valve at 48-72 hpf. Thus 2:1 AV block leads to inefficient flow of blood, which then leads to increased atrial pressures. These pressure and flow disturbances, in turn, can lead to abnormalities in myocardial maturation and thus further functional defects (Glickman and Yelon 2002).

In contrast to wildtype fish, the *sih* embryos injected with miR-202* morpholino had normally formed chambers, albeit in the context of the immature hearts that result from the complete lack of blood flow in those mutants. This indicates that chamber morphology per se is not altered directly by the knockdown of miR-202*, but instead that the lack of chamber ballooning in miR-202* morphants results from the functional abnormalities, notably the 2:1 AV block.

Previous studies have demonstrated a link between *pkd2* loss-of-function and defects in laterality (Bisgrove, Snarr et al. 2005). These experiments confirmed randomization of organ laterality, and abnormal expression of left-right patterning genes such as *lefty1*, *lefty2*, and *southpaw*. Analysis of these downstream genes is underway in miR-202* morphants. However, it was reported that overexpression of *pkd2* failed to elicit phenotype (Bisgrove, Snarr et al. 2005). This is in contrast to the definite left-right randomization present in miR-202* morphants, which are presumed to have increased expression of Pkd2 protein. One explanation is that miR-202* likely affects the pathway at multiple steps, and these multiple perturbations to patterning result in significant defects that the single dysregulation of *pkd2* could not produce. Alternatively, the relative expression patterns of miR-202* and *pkd2* could produce a pattern of *pkd2* overexpression that has functional consequences, whereas the global overexpression causes no net disruption to laterality.

While it is obvious based on BrdU incorporation that the amount of proliferation is negatively regulated by miR-202*, the overall size of miR-202* knockdown or overexpression embryos was unaltered. Significant reductions in heart size were seen in many cases of miR-202* overexpression (data not shown), but miR-202* knockdown by morpholino failed to significantly change the size of *sih* embryo hearts. Any change in heart size in wildtype embryos with miR-202* knockdown is therefore likely to be secondary to cardiac dysfunction, as mentioned

previously. Thus alterations in miR-202* levels, even when it produces detectibly different levels of Mapk14 protein, fails to cause gross phenotype relating to cell number. The direct regulation of Mapk14 by miR-202*, though occurring in zebrafish embryos, is perhaps balanced by other regulatory mechanisms that increase apoptosis or necrosis, thus maintaining absolute cell number. miR-202* enrichment in the endocarium/endothelium of 48 hpf embryos indicates that signaling between endocarium and myocardium may play a role in the miR-202* morphant phenotype. A pro-apoptotic or anti-proliferative signal originating from the endocardium may balance the increased Mapk14 expression elsewhere.

Finally, the 2:1 AV block evident in the miR-202* knockdown embryos is not yet explained by direct or indirect targets of miR-202*. Kcna4, a potassium channel expressed in cardiac and skeletal muscle, is active in the rapid repolarization phase of contraction. Increased Kcna4 protein could affect cardiac conduction, but the gene is not characterized in zebrafish. Though a few genes associated with disruption of AV-nodal conduction have been identified in humans, genetic and other regulation of conduction between the atria and ventricle remain largely unknown. Perhaps future studies screening for rescue of the 2:1 AV-block seen in the miR-202* morphant fish could produce a list of candidate genes involved in regulation of AV-nodal conduction.

Methods

miRNA Microarray. RNA was extracted from heart tissues dissected from C57Bl6 embryos using Trizol. Samples from heart regions were hybridized against RNA from whole E14 embryo. 1 µg of RNA was used for microRNA array analysis using Exiqon arrays. Array data was normalized, clustered using Cluster (Eisen Lab), and heat map produced using Tree View (Eisen Lab).

miRNA Northern. Nitrocellulose membrane pre-blotted with whole RNA from adult mouse organs (Zyagen) were hybridized with miR-202* probe (Exiqon) end-labeled with ^{32}P.

Zebrafish lines. *wt* AB and transgenic *Tg(cmlc2:gCaMP)*^{s878} (Arnaout, Ferrer et al. 2007), *Tg(myl7:HRAS-mEGFP)*^{s843}, *Tg(flk1:EGFP)* ^{s843} and *Tg(flk1:EGFP, gata1:RFP)* ^{s843} zebrafish (D'Amico, Scott et al. 2007) were raised under standard laboratory conditions at 28°C (Westerfield 2000).

Microinjection. Embryos were injected at the 1–2-cell stage with 2–5 ng pri-miR-202* MO (5´-AAGCAGCATGTCAAAGAGGTATATG-3´, GeneTools), or 100-200 pg of duplex mature miR-202* (5'-AGAAGUAUAUGCAUAGGAAA-3'; 5'-UUCCUAUGCAUAUACUUCUUU-3') or mutant miR-202* (5'-AUGUAACUAUGCAUAGGAAA-3'; 5'-UUCCUAUGCAUAGUUACAUUU-3') (Dharmacon). The embryos were maintained at 28ºC until harvesting.

Confocal analysis. Embryos were fixed in 2% paraformaldehyde (PFA) overnight and embedded in 4% low-melt agarose. Images were acquired with a Zeiss LSM5 Pascal confocal microscope.

In situ hybridization. Probes against miR-202* (Exiqon), *cmlc2* (Yelon, Horne et al. 1999), *amhc* (Berdougo, Coleman et al. 2003), *vmhc* (Yelon, Horne et al. 1999), *cspg2* (Walsh and Stainier 2001), *notch1b* (Walsh and Stainier 2001), and *lefty2* were used. miR-202* *in situ* hybridization was performed according to published protocols (Exiqon, Netherlands). Probes against mRNAs were synthesized, and in situ hybridizations were performed as described (Aanstad and Whitaker 1999).

Optical mapping by wide-field epifluorescence. Individual zebrafish embryos between 48 and 60 hpf were placed on a coverglass. Images were acquired and data analysis was performed as described previously (Arnaout, Ferrer et al. 2007). Isochronal lines at 60-msec intervals were obtained by identifying the maximal spatial gradient for a given time point.

Luciferase assay. Target prediction developed in the Srivastava laboratory was used to bioinformatically identify potential targets of miR-202*. 300-500 nucleotides of *Mus musculus pkd2, kcna4* and *p38* 3′-UTRs predicted to contain miR-138 binding sites were cloned into the pGL3 vector (Promega). Point mutations of the binding sites were generated using QuickChange II PCR (Stratagene). Duplex mature miR-202* or mature miR-202* mutated in the seed sequence were used (Dharmacon). Renilla-encoding vector was used as a transfection control. Cos-1 cells were transfected with 50 pg miR-202* or mutant miR-202*, 350 ng of CMV-luciferase and 50 ng of CMV-renilla constructs with Lipofectamine 2000 (Invitrogen), and cells were harvested after 24 hours. Luciferase and renilla activity were assayed using the Dual-Reporter Assay (Promega). Results shown are from triplicate experiments.

Western Blotting. Cos-1 cells were grown in DMEM supplemented with 10% calf serum and penicillin/streptomycin (Gibco). Cells were transfected with 50 pg Block-IT (Invitrogen), miR-202* or mutant miR-202* duplex with Lipofectamine 2000. After 24 hours, cells were collected directly in RIPA buffer. For fish protein, embryos were injected with 100 pg miR-202* mimic or 2 ng miR-202* morpholino at the 1-cell stage, and collected at 24 hpf in RIPA buffer. After a freeze-thaw cycle, the samples were sonicated. Protein amount were quantified using the Micro BCA kit (Pierce). Primary antibodies against p38 (Promega), Pkd2 (SantaCruz) and Gapdh (Santa Cruz) were used.

Quantitative real-time RT-PCR. RNA was prepared from whole embryos injected with the *pri-miR-202** morpholino or the miR-202* duplex with Trizol (Invitrogen). For mRNA qRT-PCR, cDNA was reverse transcribed using an oligo(dT) primer. Custom primers for *Danio rerio mapk14a* and *mapk14b*, and inventoried primers for *Danio rerio pkd2* and *gapdh2*, were used for Taqman-based real-time RT-PCR (Applied Biosystems). For miRNA qRT-PCR, cDNA was reverse transcribed fron 10 ng of total RNA using the Taqman microRNA Reverse Transcription Kit (Applied Biosystems) or the miSCRIPT system (Qiagen). miR-26a was used as an endogenous control. Results represent least three experiments.

Statistical Analysis. Results from at least three trials were averaged and the 95% confidence interval calculated and plotted as error bars. Significance was determined using the unpaired student t-test.

ACKNOWLEDGEMENTS

We would like to thank J. Huisken and all members of the Srivastava and Stainier labs for assistance, invaluable support and discussion. L. Prentice (UCSF) processed

in situ hybridization sections. Normalization of array data was performed by R. Roydasgupata (UCSF). Support for this work came from the American Heart Association (AHA) Western Affiliates (S.U.M.), Helen Hay Whitney Foundation (P.J.S), US National Institutes of Health (HL-54737 (D.Y.R.S.)), Packard Foundation (D.Y.R.S.). D.S. was supported by grants from the NHLBI/NIH, AHA, March of Dimes Birth Defects Foundation and the California Institute of Regenerative Medicine.

References

Aanstad, P. and M. Whitaker (1999). "Predictability of dorso-ventral asymmetry in the cleavage stage zebrafish embryo: an analysis using lithium sensitivity as a dorso-ventral marker." Mech Dev **88**(1): 33-41.

Arnaout, R., T. Ferrer, et al. (2007). "Zebrafish model for human long QT syndrome." Proc Natl Acad Sci U S A **104**(27): 11316-21.

Berdougo, E., H. Coleman, et al. (2003). "Mutation of weak atrium/atrial myosin heavy chain disrupts atrial function and influences ventricular morphogenesis in zebrafish." Development **130**(24): 6121-9.

Bisgrove, B. W., B. S. Snarr, et al. (2005). "Polaris and Polycystin-2 in dorsal forerunner cells and Kupffer's vesicle are required for specification of the zebrafish left-right axis." Dev Biol **287**(2): 274-88.

Calame, K. (2007). "MicroRNA-155 function in B Cells." Immunity **27**(6): 825-7.

Campione, M., H. Steinbeisser, et al. (1999). "The homeobox gene Pitx2: Mediator of asymmetric left-right signaling in vertebrate heart and gut looping." Development **126**(6): 1225–1234.

D'Amico, L., I. C. Scott, et al. (2007). "A mutation in zebrafish hmgcr1b reveals a role for isoprenoids in vertebrate heart-tube formation." Curr Biol **17**(3): 252-9.

Du, T. and P. D. Zamore (2005). "microPrimer: The biogenesis and function of microRNA." Development **132**(21): 4645–4652.

Glickman, N. S. and D. Yelon (2002). "Cardiac development in zebrafish: coordination of form and function." Semin Cell Dev Biol **13**(6): 507-13.

Meno, C., Y. Saijoh, et al. (1996). "Left-right asymmetric expression of the TGF beta-family member lefty in mouse embryos." Nature **381**(6578): 151–5.

Michalak, P. and J. H. Malone (2008). "Testis-derived microRNA profiles of African clawed frogs (Xenopus) and their sterile hybrids." Genomics **91**(2): 158-64.

Nonaka, S., Y. Tanaka, et al. (1998). "Randomization of left-right asymmetry due to loss of nodal cilia generating leftward flow of extraembryonic fluid in mice lacking KIF3B motor protein." Cell **95**(6): 829–837.

Piedra, M. E., J. M. Icardo, et al. (1998). "Pitx2 participates in the late phase of the pathway controlling left-right asymmetry." Cell **94**(3): 319–324.

Ryan, A. K., B. Blumberg, et al. (1998). "Pitx2 determines left-right asymmetry of internal organs in vertebrates." Nature **394**(6693): 545–551.

Walsh, E. C. and D. Y. Stainier (2001). "UDP-glucose dehydrogenase required for cardiac valve formation in zebrafish." Science **293**(5535): 1670-3.

Westerfield, M. (2000). The zebrafish book. Aguide for the laboratory use of zebrafish (Danio rerio). Eugene, University of Oregon Press.

Yelon, D., S. A. Horne, et al. (1999). "Restricted expression of cardiac myosin genes reveals regulated aspects of heart tube assembly in zebrafish." Dev Biol **214**(1): 23-37.

Zhao, Y., J. F. Ransom, et al. (2007). "Dysregulation of cardiogenesis, cardiac conduction, and cell cycle in mice lacking miRNA-1-2." Cell **129**(2): 303-17.

Zhao, Y. and D. Srivastava (2007). "A developmental view of microRNA function." Trends Biochem Sci **32**(4): 189-97.

Figure Legends

Figure 3-1.

Characterization of miRNA expression in the developing heart. (a) Heat map of miRNA microarray data demonstrating expression patterns of cardiac-enriched miRNA in the first heart field (FHF) and second heart field (SHF) at embryonic day (E) 11.5, E12.5 and E13.5; and in the atria (A), left ventricle (LV) and right ventricle (RV) at E15.5 and E18.5. (b) Comparison of relative abundance of miR-1 by microarray (left) and qRT-PCR quantification (right) demonstrates good agreement of the relative abundance of miR-1 in the heart tissues. (c) Alignment of mature miR-202* sequence from multiple species. The sequence is well conserved, with variation in only a single nucleotide change in at the 3' end of the miRNA. (d) Northern analysis of miR-202* expression in adult mouse tissues demonstrating ubiquitous expression of the pri-miR-202* transcript, and differential processing in specific tissues. Mature miR-202* accumulates most significantly in uterus, thymus and testis of adult animals.

A

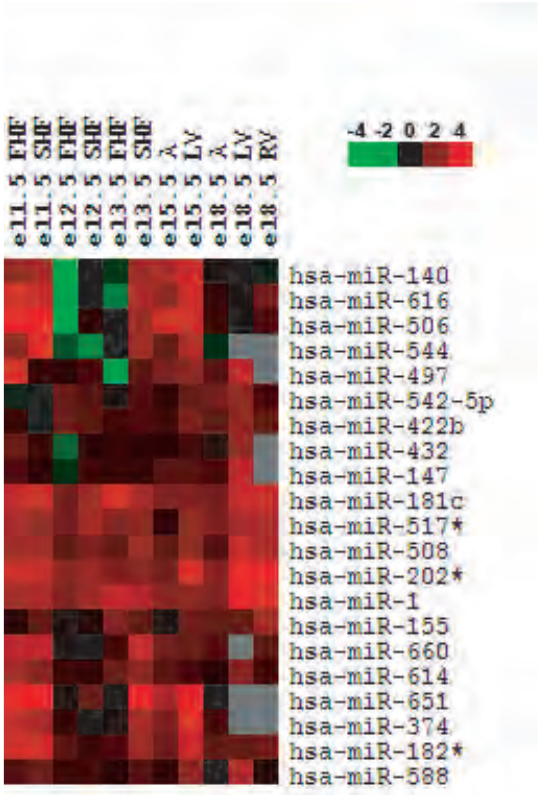

B

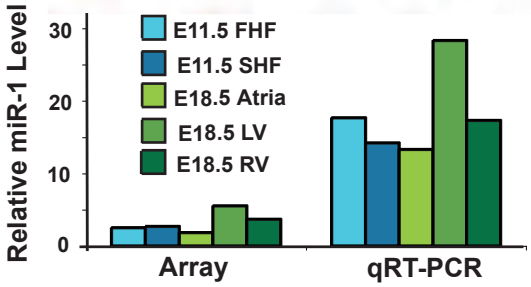

C

hsa-miR-202*	--UUCCUAUGCAUAUACUUCUUUG
mmu-miR-202-5p	--UUCCUAUGCAUAUACUUCUUU
gga-miR-202*	UUUCCUAUGCAUAUACUUCUUU
dre-miR-202*	--UUCCUAUGCAUAUACCUCUUUG
xtr-miR-202*	UUUCCUAUGCAUAUACCUCUUU

D

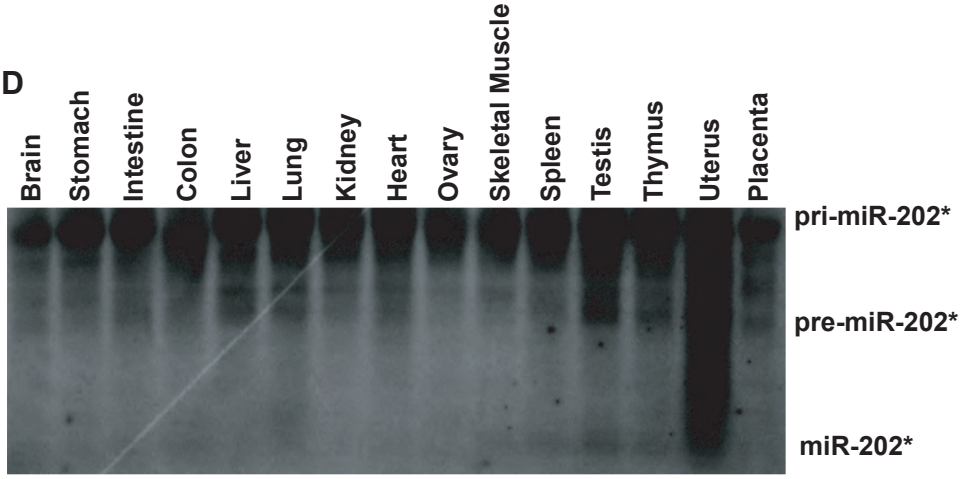

Figure 3-2.

miR-202* is required for cardiac development. (a,b) Oblique view of 24 hpf (a) and 32 hpf (b) zebrafish embryo showing broad expression of miR-202*. (c) qRT-PCR analysis of mature miR-202* expression at 48 hpf in cardiomyocytes (cmlc2), endocardial/endothelial cells (flk1) or whole embryo demonstrated some enrichment of miR-202* in cardiomyocytes, and strong enrichment in endocardial/endothelial cells. Mature miR-202 was not detected. (d) Mature miR-202* levels detected by qRT-PCR in 48-hpf fish embryos injected with control morpholino, miR-202* morpholino (MO) or miR-202* mimic demonstrates robust downregulation of miR-202* by the morpholino, and mild overexpression with injection of mimic. (e-g) Morphology of fish embryos injected with control morpholino (e), miR-202* morpholino (f), or miR-202* mimic (g) showing pericardial edema (asterisk) in f and g. (h) Quantification of pericardial edema observed in the embryos injected with control or miR-202* morpholino compared with uninjected embryos demonstrates a marked increase in pericardial edema at 48hpf with miR-202* morpholino but not other conditions.

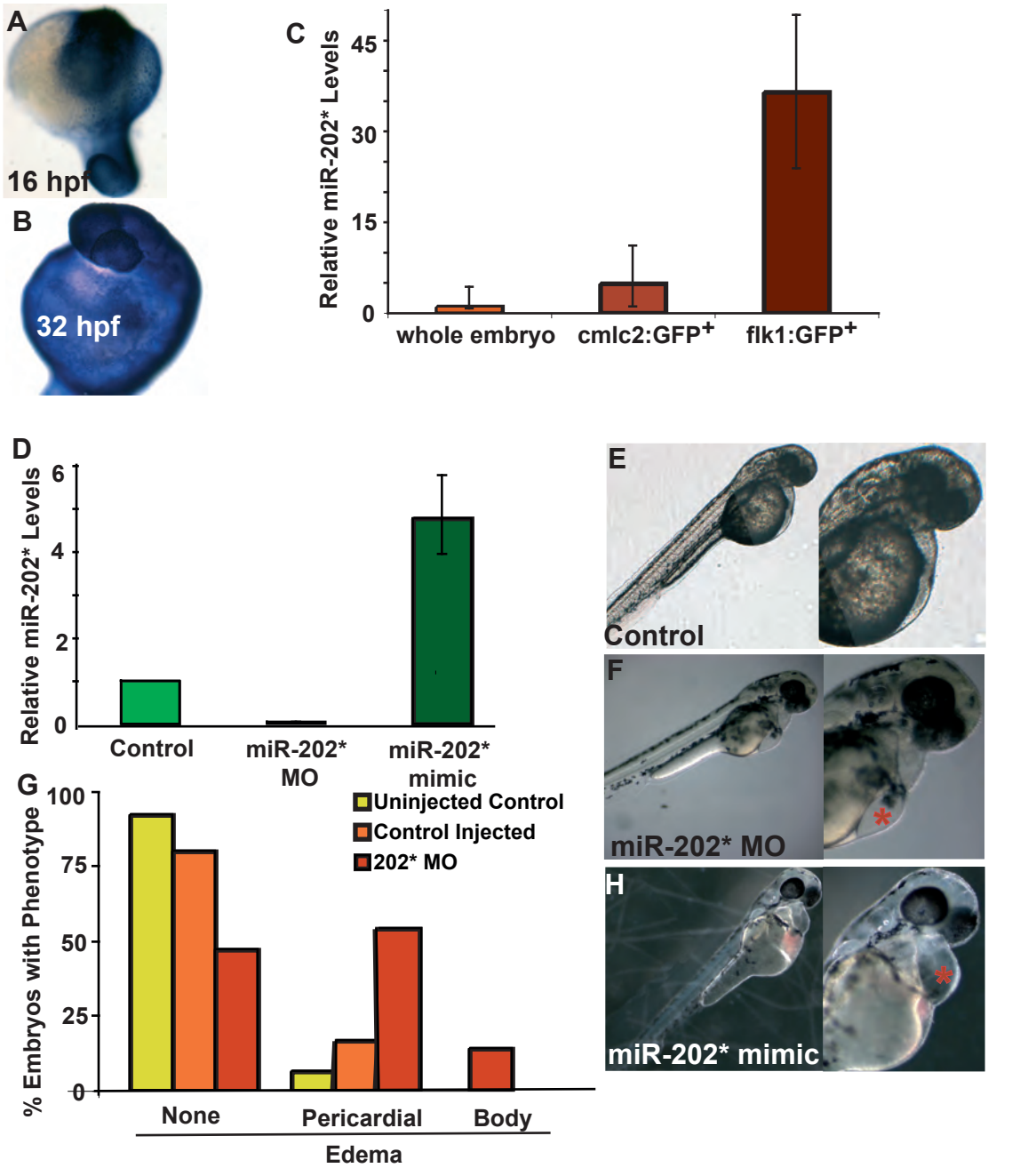
A
16 hpf
B
32 hpf
C
Relative miR-202* Levels
45
30
15
0
whole embryo
cmlc2:GFP+
flk1:GFP+
D
Relative miR-202* Levels
6
4
2
0
Control
miR-202* MO
miR-202* mimic
E
Control
F
miR-202* MO
H
miR-202* mimic
G
% Embryos with Phenotype
100
75
50
25
0
Uninjected Control
Control Injected
202* MO
None
Pericardial Edema
Body

Figure 3-3.

Chamber patterning is not affected by changes in miR-202* expression. (a–c) Expression of *cmlc2* in dorsal views at 24 hpf as determined by *in situ* hybridization (purple) in whole-mount embryos indicates that cardiac progenitors are similarly specified in control (a), 202*-morpholino (b) and miR-202* mimic injected fish (c). Oblique views of 48 hpf embryos demonstrating that atrial (d-f) and ventricular (g-i) markers were similar in control (d,g) and miR-2-2* morpholino (e,h) and miR-202* mimic embryos (f,i). Expression of atrioventricular canal (avc)-specific marker *tbx2b* (j-l) were also similar in control (j), miR-202* morpholino (k) and miR-202* mimic (l) embryos.

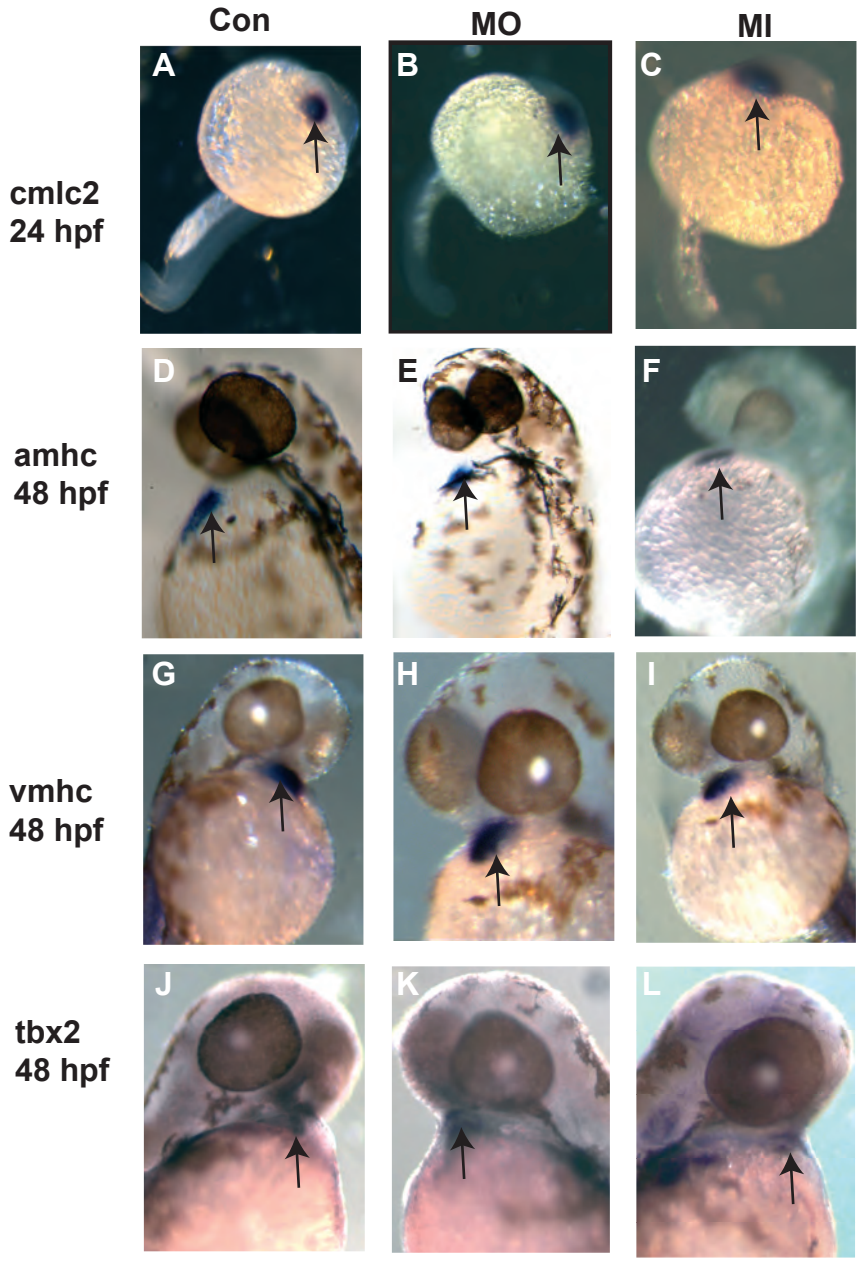
Con
MO
MI
cmlc2
24 hpf
amhc
48 hpf
vmhc
48 hpf
tbx2
48 hpf
A
B
C
D
E
F
G
H
I
J
K
L

Figure 3-4.

Randomization of cardiac looping upon miR-202* knockdown. (a-f) Analysis of transgenic *Tg(myl7:HRAS-mEGFP)*^{s843} embryos injected with miR-202* morpholino by fluorescence (a,c,e) or confocal (b,d,f) microscopy demonstrates that while many hearts are properly looped to the left (a,b), many others are looped to the right (e,f) or remain unlooped (c,d). (g) Quantification of looping direction in miR-202* morphants demonstrates partial randomization of the left-right asymmetry.

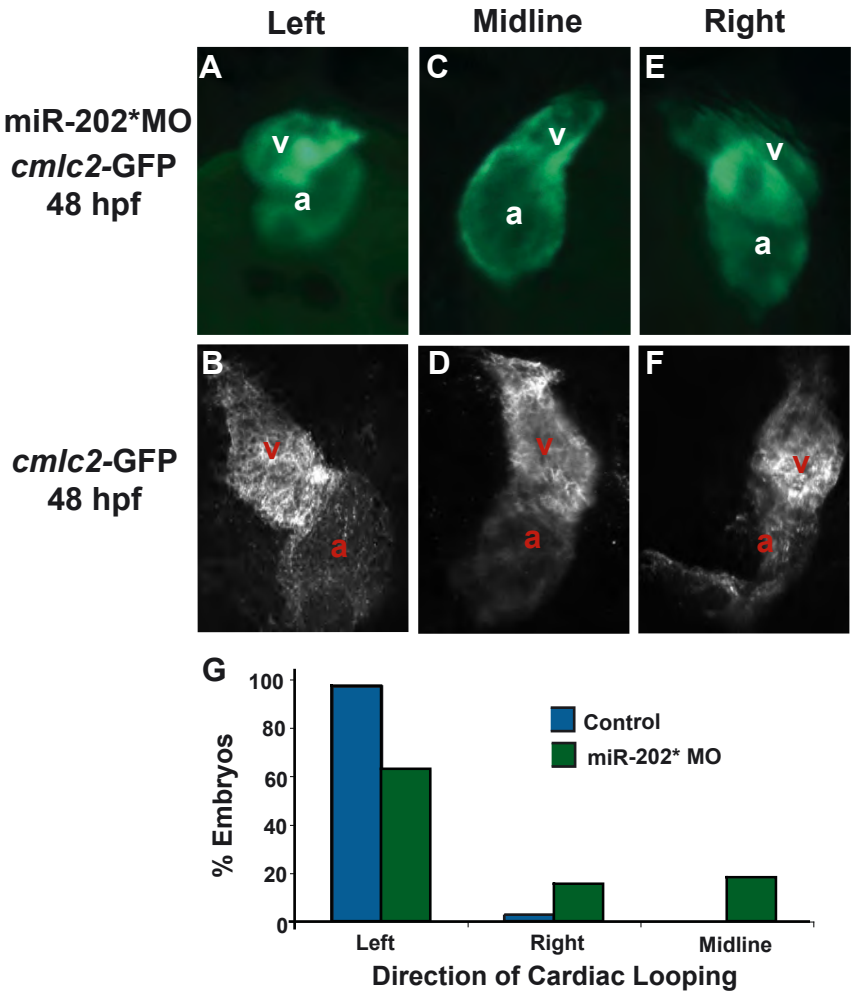
Left
Midline
Right
miR-202*MO
cmlc2-GFP
48 hpf
cmlc2-GFP
48 hpf
A
B
C
D
E
F
v
a
G
% Embryos
100
80
60
40
20
0
Control
miR-202* MO
Left
Right
Midline
Direction of Cardiac Looping

Figure 3-5.

miR-202* morphants have 2:1 AV block. (a,b) Atrial and ventricular chambers of 48 hpf *sih* embryos injected with control (a) or miR-202* (b) morpholinos are similar despite the conduction abnormalities in miR-202* morphants. (c) Visualization of the conduction in miR-202* morphant embryos shows 2:1 atrioventricular block, where the atrium depolarizes twice for every ventricular depolarization.

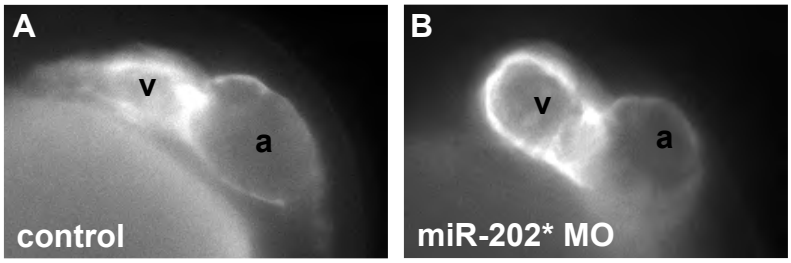
A
v
a
control
B
v
a
miR-202* MO

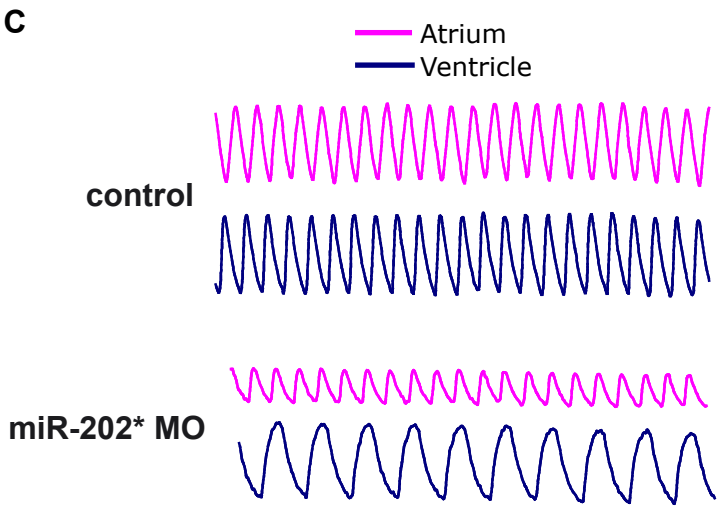
C
Atrium
Ventricle
control
miR-202* MO

Figure 3-6.

miR-202* directly targets Pkd2 and Mapk14 for repression. (a) Luciferase activity upon introduction of endogenous or mutated 3´ UTR sequences downstream of a CMV-driven luciferase reporter. Luciferase activity in Cos cells with miR-202* mimic relative to miR-202* mutant mimic is shown. (b) Pkd2 protein levels in Cos-1 cells are decreased by transfection with miR-202* mimic but not a mutated miR-202* mimic. (c) Western blot for Mapk14 protein in 24 hpf zebrafish embryos injected with control morpholino, miR-202* morpholino, or miR-202* mimic demonstrates *in vivo* regulation of Mapk14. (d-f) Immunohistochemistry for BrdU incorporation in 48 hpf embryos soaked in BrdU 24-26 hpf demonstrates that, compared to control (d), overexpression of miR-202* (e) decreases incorporation of BrdU while knockdown of miR-202* (f) increases BrdU incorporation.

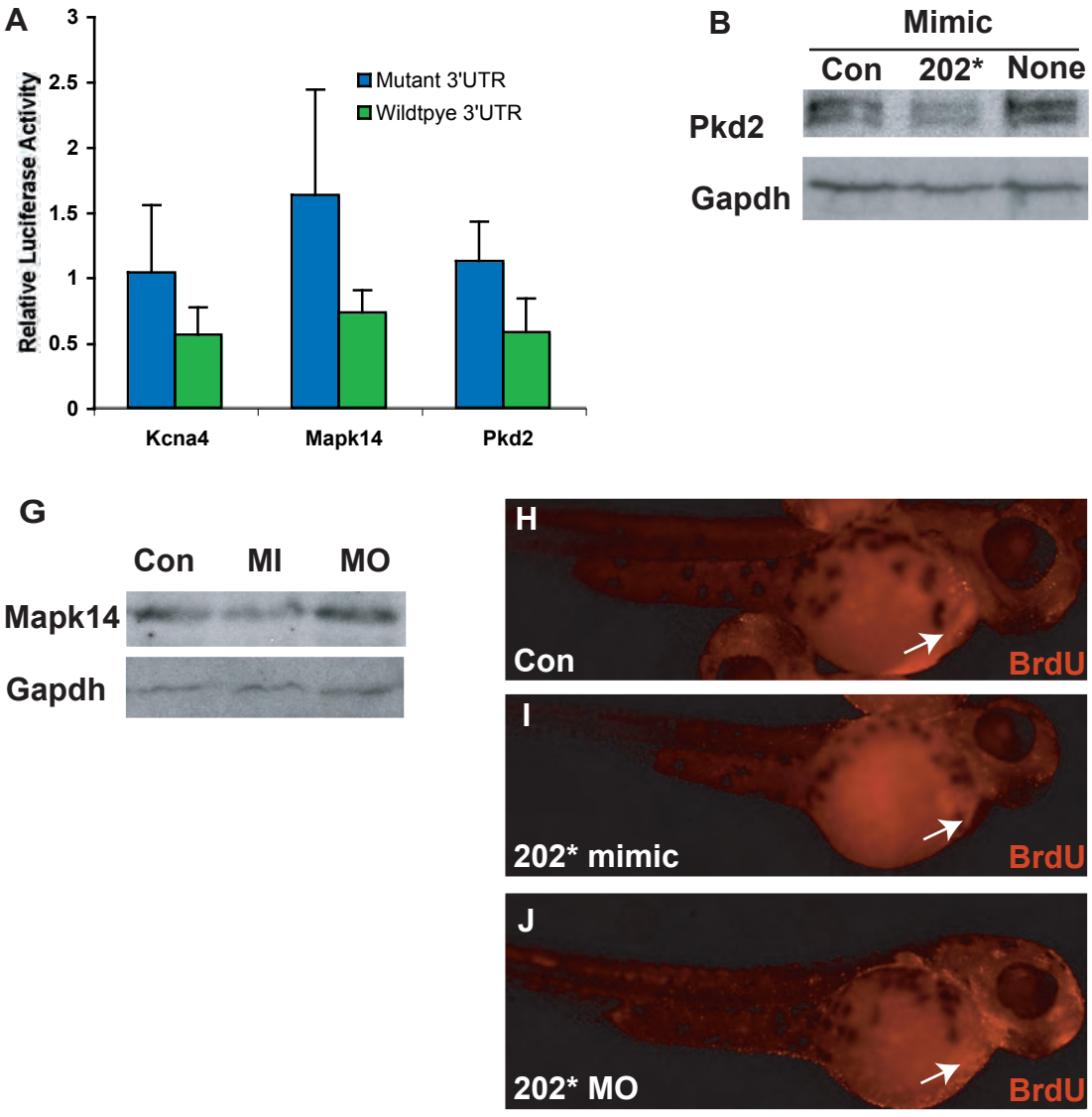
A
Relative Luciferase Activity
3
2.5
2
1.5
1
0.5
0
Mutant 3'UTR
Wildtpye 3'UTR
Kcna4
Mapk14
Pkd2
B
Mimic
Con
202*
None
Pkd2
Gapdh
G
Con
MI
MO
Mapk14
Gapdh
H
Con
BrdU
I
202* mimic
BrdU
J
202* MO
BrdU

Figure 3-S1.

Expression pattern for all miRNAs during mouse cardiac development. Heat map of miRNA microarray data demonstrating expression patterns of all detectable miRNA in the first heart field (FHF) and second heart field (SHF) at embryonic day (E) 11.5, E12.5 and E13.5; and in the atria (A), left ventricle (LV) and right ventricle (RV) at E15.5 and E18.5.

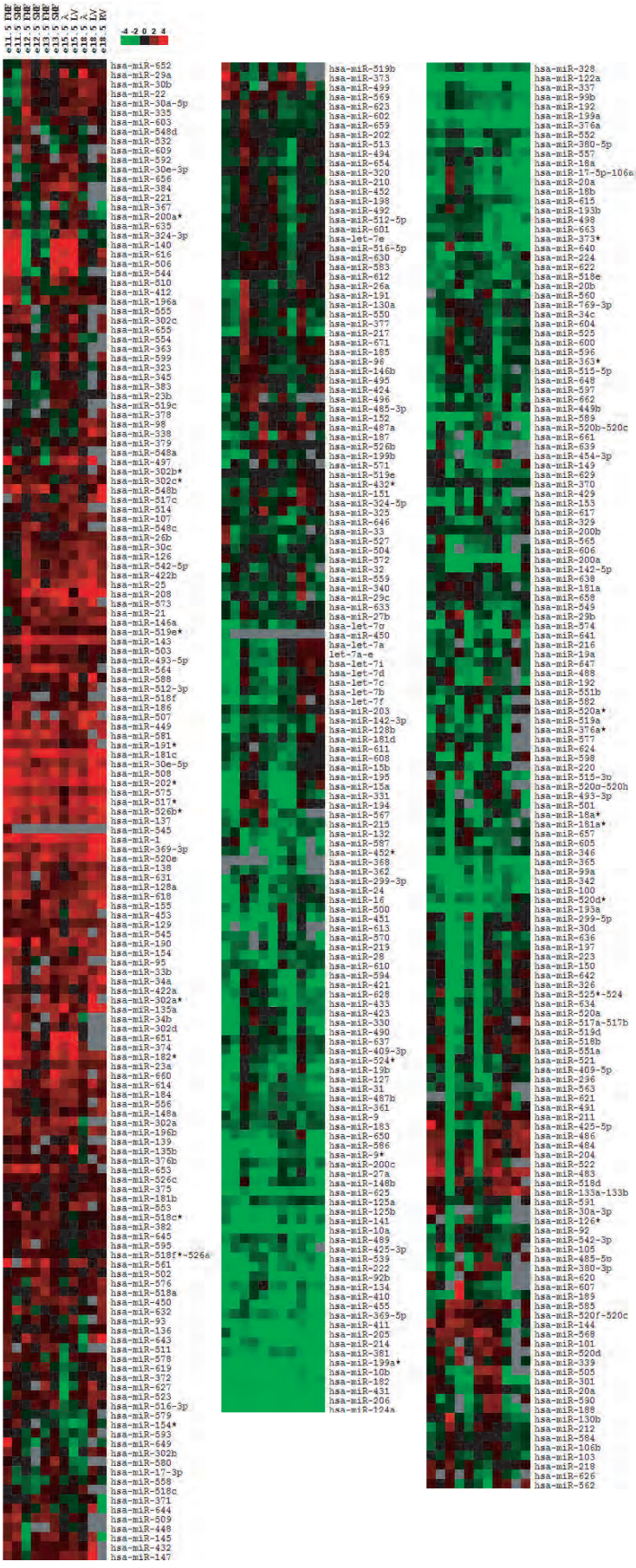
e11.5 DRF
e11.5 SRF
e12.5 DRF
e12.5 SRF
e13.5 DRF
e13.5 SRF
e15.5 A
e15.5 LV
e18.5 A
e18.5 LV
e18.5 RV
-4 -2 0 2 4
hsa-miR-652
hsa-miR-29a
hsa-miR-30b
hsa-miR-22
hsa-miR-30a-5p
hsa-miR-335
hsa-miR-603
hsa-miR-548d
hsa-miR-532
hsa-miR-609
hsa-miR-592
hsa-miR-30e-3p
hsa-miR-656
hsa-miR-384
hsa-miR-221
hsa-miR-367
hsa-miR-200a*
hsa-miR-635
hsa-miR-324-3p
hsa-miR-140
hsa-miR-616
hsa-miR-506
hsa-miR-544
hsa-miR-510
hsa-miR-412
hsa-miR-196a
hsa-miR-555
hsa-miR-302c
hsa-miR-655
hsa-miR-554
hsa-miR-363
hsa-miR-599
hsa-miR-323
hsa-miR-345
hsa-miR-383
hsa-miR-23b
hsa-miR-519c
hsa-miR-378
hsa-miR-98
hsa-miR-338
hsa-miR-379
hsa-miR-548a
hsa-miR-497
hsa-miR-302b*
hsa-miR-302c*
hsa-miR-548b
hsa-miR-517c
hsa-miR-514
hsa-miR-107
hsa-miR-548c
hsa-miR-26b
hsa-miR-30c
hsa-miR-126
hsa-miR-542-5p
hsa-miR-422b
hsa-miR-25
hsa-miR-208
hsa-miR-873
hsa-miR-21
hsa-miR-146a
hsa-miR-519e*
hsa-miR-143
hsa-miR-503
hsa-miR-493-5p
hsa-miR-564
hsa-miR-588
hsa-miR-512-3p
hsa-miR-518f
hsa-miR-186
hsa-miR-507
hsa-miR-449
hsa-miR-581
hsa-miR-191*
hsa-miR-181c
hsa-miR-30e-5p
hsa-miR-508
hsa-miR-202*
hsa-miR-575
hsa-miR-517*
hsa-miR-526b*
hsa-miR-137
hsa-miR-545
hsa-miR-1
hsa-miR-369-3p
hsa-miR-520e
hsa-miR-138
hsa-miR-631
hsa-miR-128a
hsa-miR-618
hsa-miR-155
hsa-miR-453
hsa-miR-129
hsa-miR-545
hsa-miR-190
hsa-miR-154
hsa-miR-95
hsa-miR-33b
hsa-miR-34a
hsa-miR-422a
hsa-miR-302a*
hsa-miR-135a
hsa-miR-34b
hsa-miR-302d
hsa-miR-651
hsa-miR-374
hsa-miR-182*
hsa-miR-23a
hsa-miR-660
hsa-miR-614
hsa-miR-184
hsa-miR-556
hsa-miR-148a
hsa-miR-302a
hsa-miR-196b
hsa-miR-139
hsa-miR-135b
hsa-miR-376b
hsa-miR-653
hsa-miR-526c
hsa-miR-375
hsa-miR-181b
hsa-miR-553
hsa-miR-518c*
hsa-miR-382
hsa-miR-645
hsa-miR-595
hsa-miR-518f*-526a
hsa-miR-561
hsa-miR-502
hsa-miR-576
hsa-miR-518a
hsa-miR-450
hsa-miR-632
hsa-miR-93
hsa-miR-136
hsa-miR-643
hsa-miR-511
hsa-miR-578
hsa-miR-619
hsa-miR-372
hsa-miR-627
hsa-miR-523
hsa-miR-516-3p
hsa-miR-579
hsa-miR-154*
hsa-miR-593
hsa-miR-649
hsa-miR-302b
hsa-miR-580
hsa-miR-17-3p
hsa-miR-558
hsa-miR-518c
hsa-miR-371
hsa-miR-644
hsa-miR-509
hsa-miR-448
hsa-miR-145
hsa-miR-432
hsa-miR-147
hsa-miR-519b
hsa-miR-373
hsa-miR-499
hsa-miR-569
hsa-miR-623
hsa-miR-602
hsa-miR-659
hsa-miR-202
hsa-miR-513
hsa-miR-494
hsa-miR-654
hsa-miR-320
hsa-miR-210
hsa-miR-452
hsa-miR-198
hsa-miR-492
hsa-miR-512-5p
hsa-miR-601
hsa-let-7e
hsa-miR-516-5p
hsa-miR-630
hsa-miR-583
hsa-miR-612
hsa-miR-26a
hsa-miR-191
hsa-miR-130a
hsa-miR-550
hsa-miR-377
hsa-miR-217
hsa-miR-671
hsa-miR-185
hsa-miR-96
hsa-miR-146b
hsa-miR-495
hsa-miR-424
hsa-miR-496
hsa-miR-485-3p
hsa-miR-152
hsa-miR-487a
hsa-miR-187
hsa-miR-526b
hsa-miR-199b
hsa-miR-571
hsa-miR-519e
hsa-miR-432*
hsa-miR-151
hsa-miR-324-5p
hsa-miR-325
hsa-miR-646
hsa-miR-33
hsa-miR-507
hsa-miR-504
hsa-miR-572
hsa-miR-32
hsa-miR-559
hsa-miR-340
hsa-miR-29c
hsa-miR-633
hsa-miR-27b
hsa-let-7g
hsa-miR-450
hsa-let-7a
let-7a-e
hsa-let-7i
hsa-let-7d
hsa-let-7c
hsa-let-7b
hsa-let-7f
hsa-miR-203
hsa-miR-142-3p
hsa-miR-128b
hsa-miR-181d
hsa-miR-611
hsa-miR-608
hsa-miR-15b
hsa-miR-195
hsa-miR-15a
hsa-miR-331
hsa-miR-194
hsa-miR-567
hsa-miR-215
hsa-miR-132
hsa-miR-587
hsa-miR-452*
hsa-miR-368
hsa-miR-362
hsa-miR-299-3p
hsa-miR-24
hsa-miR-16
hsa-miR-500
hsa-miR-451
hsa-miR-613
hsa-miR-570
hsa-miR-219
hsa-miR-28
hsa-miR-610
hsa-miR-594
hsa-miR-421
hsa-miR-628
hsa-miR-433
hsa-miR-423
hsa-miR-330
hsa-miR-490
hsa-miR-637
hsa-miR-409-3p
hsa-miR-524*
hsa-miR-19b
hsa-miR-127
hsa-miR-31
hsa-miR-487b
hsa-miR-361
hsa-miR-9
hsa-miR-183
hsa-miR-650
hsa-miR-586
hsa-miR-9*
hsa-miR-200c
hsa-miR-27a
hsa-miR-148b
hsa-miR-625
hsa-miR-125a
hsa-miR-125b
hsa-miR-141
hsa-miR-10a
hsa-miR-489
hsa-miR-425-3p
hsa-miR-539
hsa-miR-222
hsa-miR-92b
hsa-miR-134
hsa-miR-410
hsa-miR-455
hsa-miR-369-5p
hsa-miR-411
hsa-miR-205
hsa-miR-214
hsa-miR-381
hsa-miR-199a*
hsa-miR-10b
hsa-miR-182
hsa-miR-431
hsa-miR-206
hsa-miR-124a
hsa-miR-328
hsa-miR-122a
hsa-miR-337
hsa-miR-99b
hsa-miR-192
hsa-miR-199a
hsa-miR-376a
hsa-miR-552
hsa-miR-380-5p
hsa-miR-557
hsa-miR-18a
hsa-miR-17-5p-106a
hsa-miR-20a
hsa-miR-18b
hsa-miR-615
hsa-miR-193b
hsa-miR-498
hsa-miR-663
hsa-miR-373*
hsa-miR-640
hsa-miR-224
hsa-miR-622
hsa-miR-518e
hsa-miR-20b
hsa-miR-560
hsa-miR-769-3p
hsa-miR-34c
hsa-miR-604
hsa-miR-525
hsa-miR-600
hsa-miR-596
hsa-miR-363*
hsa-miR-515-5p
hsa-miR-648
hsa-miR-597
hsa-miR-662
hsa-miR-449b
hsa-miR-589
hsa-miR-520b-520c
hsa-miR-661
hsa-miR-639
hsa-miR-454-3p
hsa-miR-149
hsa-miR-629
hsa-miR-370
hsa-miR-429
hsa-miR-153
hsa-miR-617
hsa-miR-329
hsa-miR-200b
hsa-miR-565
hsa-miR-606
hsa-miR-200a
hsa-miR-142-5p
hsa-miR-638
hsa-miR-181a
hsa-miR-658
hsa-miR-549
hsa-miR-29b
hsa-miR-574
hsa-miR-641
hsa-miR-216
hsa-miR-19a
hsa-miR-647
hsa-miR-488
hsa-miR-192
hsa-miR-551b
hsa-miR-582
hsa-miR-520a*
hsa-miR-519a
hsa-miR-376a*
hsa-miR-577
hsa-miR-624
hsa-miR-598
hsa-miR-220
hsa-miR-515-3p
hsa-miR-520g-520h
hsa-miR-493-3p
hsa-miR-501
hsa-miR-18a*
hsa-miR-181a*
hsa-miR-657
hsa-miR-605
hsa-miR-346
hsa-miR-365
hsa-miR-99a
hsa-miR-342
hsa-miR-100
hsa-miR-520d*
hsa-miR-193a
hsa-miR-299-5p
hsa-miR-30d
hsa-miR-636
hsa-miR-197
hsa-miR-223
hsa-miR-150
hsa-miR-642
hsa-miR-326
hsa-miR-525*-524
hsa-miR-634
hsa-miR-520a
hsa-miR-517a-517b
hsa-miR-519d
hsa-miR-518b
hsa-miR-551a
hsa-miR-521
hsa-miR-409-5p
hsa-miR-296
hsa-miR-563
hsa-miR-621
hsa-miR-491
hsa-miR-211
hsa-miR-425-5p
hsa-miR-486
hsa-miR-484
hsa-miR-204
hsa-miR-522
hsa-miR-483
hsa-miR-518d
hsa-miR-133a-133b
hsa-miR-591
hsa-miR-30a-3p
hsa-miR-126*
hsa-miR-92
hsa-miR-542-3p
hsa-miR-105
hsa-miR-485-5p
hsa-miR-380-3p
hsa-miR-620
hsa-miR-607
hsa-miR-189
hsa-miR-585
hsa-miR-520f-520c
hsa-miR-144
hsa-miR-568
hsa-miR-101
hsa-miR-520d
hsa-miR-339
hsa-miR-505
hsa-miR-301
hsa-miR-20a
hsa-miR-590
hsa-miR-188
hsa-miR-130b
hsa-miR-212
hsa-miR-584
hsa-miR-106b
hsa-miR-103
hsa-miR-218
hsa-miR-626
hsa-miR-562

Figure 3-S2.

miR-202-5p and miR-202-3p are co-expressed in late-stage mouse embryos. qRT-PCR analysis of miR-202-5p and miR-202-3p expression in E17.5 mouse embryo demonstrates broad expression of the two miRNAs.

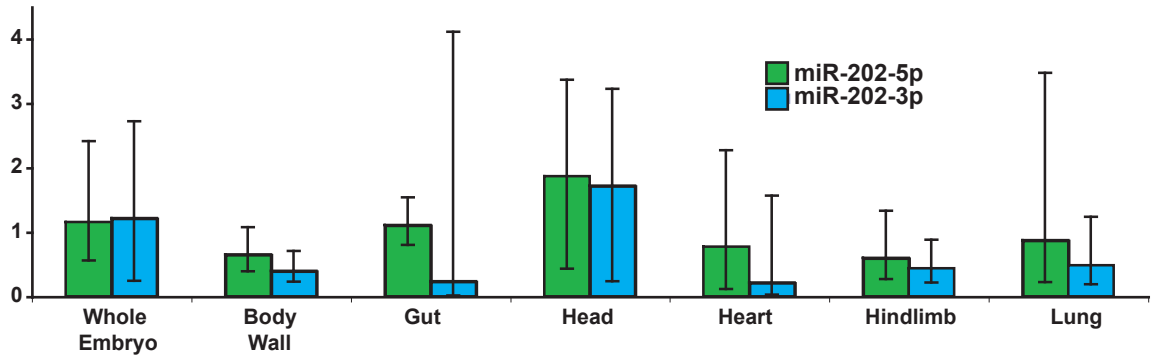
4
3
2
1
0
miR-202-5p
miR-202-3p
Whole Embryo
Body Wall
Gut
Head
Heart
Hindlimb
Lung

Figure 3-S3.

miR-202* is not necessary for vasculogensis. (a) qRT-PCR analysis of miR-202* in zebrafish embryos from 0.5 hpf to 96 hpf demonstrates early expression at high levels. (b,c) Fluorescence microscopy of 48hpf transgenic *Tg(flk1:HRAS-mEGFP)*^{s843} embryos injected with control or miR-202* morpholino demonstrates normal vessel formation in the head and body, with endothelial cells expressing GFP.

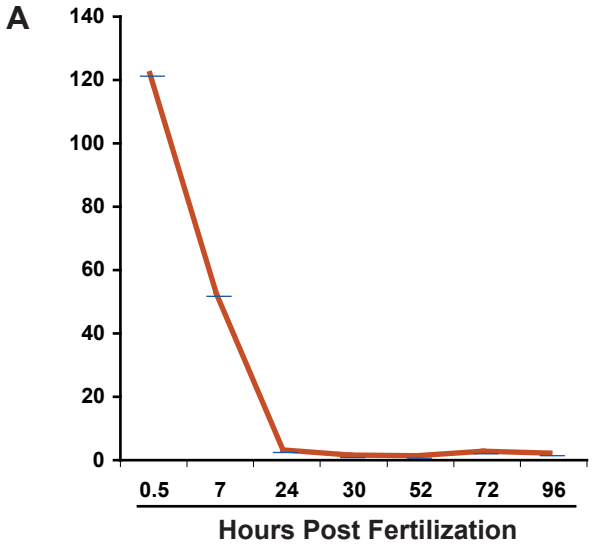
A
140
120
100
80
60
40
20
0
0.5
7
24
30
52
72
96
Hours Post Fertilization

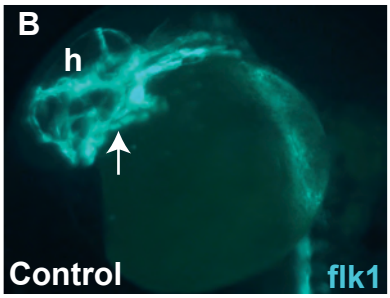
B
h
Control
flk1

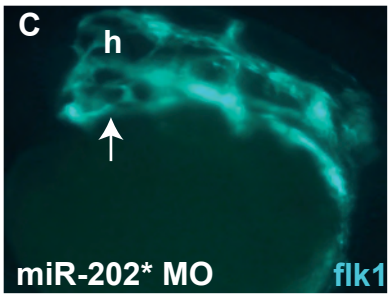
C
h
miR-202* MO
flk1

Figure 3-S4.

miR-202* targets are not altered at the mRNA level. (a) Analysis of *pkd2* RNA level assessed by qRT-PCR in 24 hpf embryos injected with control morpholino, miR-202* morpholino or miR-202* mimic demonstrate no significant change in mRNA levels. (b) Analysis of *mapk14a* and *mapk14b* RNA level assessed by qRT-PCR in 24 hpf embryos injected with control morpholino, miR-202* morpholino or miR-202* mimic demonstrate no significant change in *mapk14a* mRNA levels but a slight increase in *mapk14b* mRNA with miR-202* mimic injection.

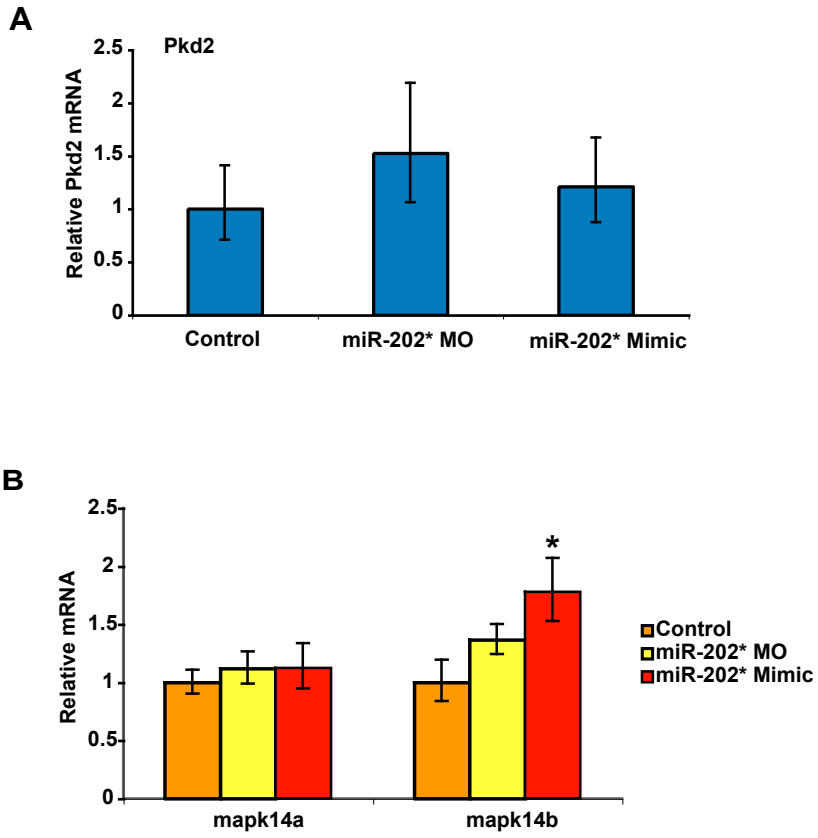
A
Pkd2
Relative Pkd2 mRNA
2.5
2
1.5
1
0.5
0
Control
miR-202* MO
miR-202* Mimic
B
Relative mRNA
2.5
2
1.5
1
0.5
0
*
mapk14a
mapk14b
Control
miR-202* MO
miR-202* Mimic

Chapter Four:

Discussion and Future Directions

Overall, the studies described in this thesis demonstrate the importance of miRNAs in development and function of the vertebrate heart. Whether the role is in early patterning, as seen for miR-138 and miR-202*, or later cardiac function, as is also the case for miR-202*, miRNAs are important regulators of the complex process of heart morphogenesis and function. Future work in the field will inevitably uncover more miRNAs necessary for normal cardiac development and more roles for those that have already been discovered. Important information will be gained from studies of miRNA biology; as the roles of individual miRNAs are elucidated, new features of the biological processes regulated by miRNAs will also be discovered. From this newfound information about miRNAs and the genes they regulate, a more complete understanding of development, and related disease states, will emerge.

Role of Retinoic Acid During Cardiac Looping and Atrioventricular Canal Morphogenesis

Raldh2, which converts retinaldehyde to retinoic acid (RA), is expressed early in mouse development and its targeted deletion from the mouse embryo results in obvious cardiac defects by embryonic day (E) 9.5, including lack of looping and single chamber morphology (Niederreither, Subbarayan et al. 1999; Niederreither, Vermot et al. 2001). This looping defect is rescued by exogenous treatment of retinoic acid. The unlooped heart observed in the *Raldh2*-null mouse embryos was also observed in zebrafish with altered levels of RA; many of the wild-type fish discussed in Chapter 2 that were treated with RA or an inhibitor or retinoic acid signaling, DEAB, had linear heart tubes even at 48-60 hours post fertilization (hpf). Thus, either increased or decreased RA signaling caused a lack of cardiac looping in the zebrafish, indicating that regulation of RA levels within a particular range of concentrations is necessary for normal cardiac looping. Regulation by miR-138 is one mode of controlling RA levels; notably overexpression of miR-138 in zebrafish,

even at 50 pg of miRNA per embryo, resulted in a linear heart tube. Whether the miR-138 overexpression phenotype is due to decreased RA via downregulation of Raldh2 has not yet determined, but rescue experiments using treatment with RA would elucidate a role for RA in the linear heart tube phenotype. For example, if treatment with RA leads to a rescue in cardiac looping in miR-138 overexpression embryos, it would indicate that the overexpression of miR-138 in areas other than the ventricle inhibits RA signaling that is normally necessary for proper looping of the heart.

Though this unlooped heart phenotype was observed in mouse and zebrafish, a source of cardiac RA during looping and atrioventricular (AV) canal morphogenesis had not been identified. Though physiologic roles for RA in heart development are well-characterized during early chamber specification and later signaling from the epicardium, RA was not known to be produced within the heart during cardiac looping and valve morphogenesis. Use of a transgenic reporter demonstrated low retinoic acid activity in the heart at 30 hpf with an increase in activity observed after 48 hpf (Grandel, Lun et al. 2002; Wills, Holdway et al. 2008). Thus Raldh2, identified in Chapter 2 to be expressed in the AV canal of zebrafish at 48hpf, could act as a source of RA during cardiac looping. Expression of Raldh2 in the AV canal at 48hpf suggests that RA may also have a specific role in endocardial cushion formation or epithelial-to-mesenchymal transition (EMT). Future studies of mouse endocardial cushion explants using exogenous RA or RA antagonists, such as DEAB, would be a starting point to determine the role of locally-produced RA in AV canal development. I hypothesize that miR-138 expression in ventricular cardiomyocytes inhibits Raldh2 expression, limiting production of RA to the AV canal. RA within the AV canal may be necessary for the EMT that occurs to the endocardial cushions. Thus treatment of endocardial cushion explants with miR-138 mimic could halt EMT by inhibiting RA signaling, and addition of RA could rescue EMT. By combinatorial

inhibition or addition of miR-138 and RA, the roles of these molecules in endocardial cushion development can be elucidated.

Regulation of Versican by Retinoic Acid

The other demonstrated target of miR-138 discussed in Chapter 2, Versican, is a chondroitin sulfate proteoglycan. Versican is encoded by the gene *cspg2*, which has been shown to be important for cardiac development, especially during outflow tract and AV canal formation. The *heart defect* (*hdf*) mouse mutant described in the 1990s, which has abnormalities in formation of the right-sided heart and cardiac cushions and has embryonic lethality at E10.5, results from disruption of *cspg2* (Yamamura, Zhang et al. 1997; Mjaatvedt, Yamamura et al. 1998). Cleavage of Versican occurs during cardiac cushion morphogenesis starting at E9.5 and continues through E14.5 (Kern, Twal et al. 2006; Kern, Norris et al. 2007). Specifically, non-cleavable Versican promotes cell-cell adhesion and leads to thickening of outflow tract myocardium when added to developing chick embryos. However, the molecular mechanisms downstream of Versican that act to influence endocardial cushion development, and the means by which Versican expression is regulated during development, remain unknown.

The studies of miR-138 function in zebrafish heart demonstrated the importance of robust clearance of Versican mRNA from the ventricle; miR-138 accomplishes this via both direct inhibition of Versican mRNA accumulation in the ventricle, and inhibited production of an upstream signaling molecule, RA. By clearing mRNAs from progenitor cell populations, miRNAs can make the cell environment permissive to new states. For example, clearing of maternal mRNAs by miR-430 allows zebrafish gastrulation to proceed (Giraldez, Cinalli et al. 2005). Alternatively, if a gene needs to remain silenced in order for a cell to differentiate and/or function properly, miRNA can ensure that stochastic misexpression of the

gene does not occur. As RA can act as a transcriptional activator of Versican, miR-138 both directly clears Versican mRNA and targets Raldh2 to prevent stochastic misexpression of Versican in response to errant RA signaling.

Further, the mechanism by which RA upregulates Versican mRNA remains unknown. Previous studies in human monocyte-like THP-1 cells have shown that retinoic-acid responsive PPARγ is able to downregulate the class of metalloproteases known to cleave Versican within cardiac cushions (Worley, Baugh et al. 2003; Torres-Collado, Kisiel et al. 2006). In this model, RA is necessary for PPARγ activity at certain enhancer elements. When RA and PPARγ are co-expressed in these THP-1 cells, it leads to decreased transcription of several genes, including ADAMTS-1. ADAMTS-1, in turn, is known to cleave Versican protein in the carotid artery. This provides an intriguing hypothesis for the upregulation of Versican mRNA by Raldh2 via PPARγ. Though these studies were not in cardiac cells, the molecules involved are broadly expressed. A first study looking at Versican proteolysis in cardiomyocytes and endocardial cells in response to RA treatment could identify whether Versican processing is sensitive to RA. Subsequent analysis of putative PPARγ binding sites near the promoter of *ADAMTS* genes via luciferase assay could see if PPARγ, with or without RA, regulates their expression in cardiac cells.

Role of miRNAs in Cardiac Regeneration

Zebrafish display regenerative potential similar to that seen in amphibians and reptiles. Complete regrowth of a fin is possible after resection, and many of the same signaling pathways involved in fin regeneration are necessary for normal fin development (Poss, Shen et al. 2000; Poss, Shen et al. 2000; Poss, Nechiporuk et al. 2002). Subsequent studies have shown that the zebrafish heart is capable of regeneration following dramatic resection of the ventricle by use of scalpel (Poss,

Wilson et al. 2002). Similarly to tail regeneration, many genes known to be expressed in the heart during development are re-activated during cardiac regeneration.

One gene upregulated in the regenerating zebrafish heart is Raldh2, suggesting a role for RA during heart regeneration. Following resection of the ventricle, robust Raldh2 expression can be detected throughout the damaged heart (Poss, Wilson et al. 2002). The specific role of RA signaling in regeneration has not been elucidated. However, the known roles of Raldh2 and RA in cardiac progenitor specification and chamber patterning suggest that Raldh2 may be aiding in the specification of new cardiac cells and/or the patterning of the repaired heart. Addition or inhibition of RA signaling during regeneration, in a similar manner to the studies in Chapter 2, could be used to ascertain the role of RA during regeneration of the ablated heart. Given the observed role of RA in relation to miR-138, I hypothesize that alteration of RA signaling would impair cardiac regeneration, specifically affecting the maturation and/or patterning. For example, the new cardiomyocytes may fail to elongate with addition of RA, as was seen in the miR-138 knockdown embryos.

Of note, a recent study of zebrafish fin regeneration identified miR-138 as significantly downregulated during the process of regeneration (Yin, Thomson et al. 2008). Characterization of miR-138 levels during cardiac regeneration in zebrafish may reveal a role for miR-138 in regenerative potential, possibly implicating its target, Raldh2, in the process. Such studies have been initiated to determine if miR-138 is similarly regulated during cardiac regeneration, using genetically-controlled ablation of the ventricular myocardium to study cardiac regeneration in larval zebrafish. The ventricle is ablated at 72-96 hpf, and regeneration starts approximately 12 hours post ablation (Neil Chi, personal communication). As miR-138 is known to be expressed in the heart at the time of ablation, and considering

since it represses Raldh2 expression at that time, I hypothesize that miR-138 may be downregulated in the ventricle in response to the regenerative program.

During the process of regeneration is it important to identify both the source of the cells that regenerate the cardiac tissue, as well as the signals that control the regenerative potential. Understanding the biochemical and cellular pathways that are regulated by miRNAs during regeneration will provide insight into the regenerative program. miRNA microarrays can determine which miRNAs are expressed in the regenerating myocardium and endocardium, while mRNA microarray analysis of on the same samples can identify the pathways activated or deactivated during regeneration. However, the role of specific miRNAs and signaling pathways will take longer to elucidate and, given the tissue-specificity of many miRNA and mRNA actions, are likely to involve complex cell-autonomous and non-cell-autonomous mechanisms.

Redundancy of miRNA Regulation

It is interesting to question which functions of miRNAs resulted in their high degree of sequence conservation among species, taking into consideration the more recent observations on miRNA function included in this thesis and other recent work from the Srivastava lab. More examples of a single miRNA targeting multiple mRNA transcripts in the same biological process are emerging in current work. miR-138 targeting both Versican and production of its upstream activator, RA, ensures that Versican expression is fully cleared from the ventricle by 48 hpf. One additional example of coordinate regulation of several regulators of a single biological process is found during zebrafish vascular development. Ongoing studies I have collaborated on in the Srivastava lab, lead by Jason Fish, have identified multiple targets of miR-126 within the angiogenic signaling pathway. Though overexpression of a single target, Spred1, is capable of phenocopying much of the miR-126 knockdown

phenotype in fish, other anti-angiogenic proteins have also been shown to be targets. It has been interesting to see that the overexpression of several of the targets of miR-126 has been able to phenocopy the miR-126 knockdown phenotype, though with varying severity. This is a very robust example of multiple targets related to pro-angiogenic signaling that are regulated by miR-126. miR-126 is also known to be upregulated in many cancer cells (Garzon, Pichiorri et al. 2006; Musiyenko, Bitko et al. 2008; Negrini and Calin 2008; Tavazoie, Alarcon et al. 2008). In the context of a tumor, it may be that miR-126 is able to release any repressive, anti-angiogenic signaling, potentially resulting in increased angiogenesis within tumors.

miRNAs in Human Disease

At the beginning of my graduate training, there was a single miRNA for which ample data was available to conclude that it had a significant role in cardiac development. miR-1 was known to cause defects in cardiac development when overexpressed, and preliminary results in the lab demonstrated that it was also necessary for normal heart development given the phenotype of the miR-1-2 null mouse (Zhao, Samal et al. 2005; Zhao, Ransom et al. 2007). Many projects in the lab, and within other groups, were pursuing the function of miRNAs that were found to be highly expressed or enriched in specific tissues. Over the course of the past three years, as these project have come to fruition, we now can point to dozens of examples of miRNAs necessary for the normal development and function of tissues, organs and organisms.

While many miRNAs have been found to be dysregulated in disease states of humans and model organisms, a mutation in a miRNA coding or regulatory region has not yet been found to be associated with abnormalities in human development. Studies of single nucleotide polymorphisms (SNPs) in humans have demonstrated

that sequence variation in the 3'UTRs of mRNAs can affect the ability of miRNAs to regulate the SNP-containing mRNA (Chen Rajewsky 2006). Ongoing deep sequencing continues to identify novel miRNAs, which will add to the catalog of miRNAs to study in the context of disease. Similarly, as the field begins to study the regulation of miRNA expression, connections between miRNAs and known signaling pathways will be identified, improving our knowledge of miRNA function within characterized biochemical and cellular processes. Most promisingly, as our ability to sequence the genomes of patients improves with regard to efficiency and accuracy, we will be able to better identify mutations outside of protein-coding genes. While many of these mutations will relate to the regulation of mRNAs or other non-miRNA genes, others are likely to be linked to the proper expression of miRNAs. Thus our studies of miRNAs in development and disease will hopefully be translated to increased understanding and improved treatments for human illness. Already it is exciting to think of anti-miR-126 treatment for tumors, thus decreasing tumor angiogenesis and concomitant tumor growth. Perhaps even the antagomiRs employed successfully in Chapter 2 will be able to be used as a therapeutic method to decrease miRNAs in patients.

References

Garzon, R., F. Pichiorri, et al. (2006). "MicroRNA fingerprints during human megakaryocytopoiesis." Proc Natl Acad Sci U S A **103**(13): 5078-83.

Giraldez, A. J., R. M. Cinalli, et al. (2005). "MicroRNAs regulate brain morphogenesis in zebrafish." Science **308**(5723): 833–838.

Grandel, H., K. Lun, et al. (2002). "Retinoic acid signalling in the zebrafish embryo is necessary during pre-segmentation stages to pattern the anterior-posterior axis of the CNS and to induce a pectoral fin bud." Development **129**(12): 2851-65.

Kern, C. B., R. A. Norris, et al. (2007). "Versican proteolysis mediates myocardial regression during outflow tract development." Dev Dyn **236**(3): 671-83.

Kern, C. B., W. O. Twal, et al. (2006). "Proteolytic cleavage of versican during cardiac cushion morphogenesis." Dev Dyn **235**(8): 2238-47.

Mjaatvedt, C., H. Yamamura, et al. (1998). "The Cspg2 gene, disrupted in the hdf mutant, is required for right cardiac chamber and endocardial cushion formation." Dev. Biol. **202**(1): 56–66.

Musiyenko, A., V. Bitko, et al. (2008). "Ectopic expression of miR-126*, an intronic product of the vascular endothelial EGF-like 7 gene, regulates prostein translation and invasiveness of prostate cancer LNCaP cells." J Mol Med **86**(3): 313-22.

Negrini, M. and G. A. Calin (2008). "Breast cancer metastasis: a microRNA story." Breast Cancer Res **10**(2): 203.

Niederreither, K., V. Subbarayan, et al. (1999). "Embryonic retinoic acid synthesis is essential for early mouse post-implantation development." Nat Genet **21**(4): 444-8.

Niederreither, K., J. Vermot, et al. (2001). "Embryonic retinoic acid synthesis is essential for heart morphogenesis in the mouse." Development **128**(7): 1019-31.

Poss, K. D., A. Nechiporuk, et al. (2002). "Mps1 defines a proximal blastemal proliferative compartment essential for zebrafish fin regeneration." Development **129**(22): 5141-9.

Poss, K. D., J. Shen, et al. (2000). "Induction of lef1 during zebrafish fin regeneration." Dev Dyn **219**(2): 282-6.

Poss, K. D., J. Shen, et al. (2000). "Roles for Fgf signaling during zebrafish fin regeneration." Dev Biol **222**(2): 347-58.

Poss, K. D., L. G. Wilson, et al. (2002). "Heart regeneration in zebrafish." Science **298**(5601): 2188-90.

Tavazoie, S. F., C. Alarcon, et al. (2008). "Endogenous human microRNAs that suppress breast cancer metastasis." Nature **451**(7175): 147-52.

Torres-Collado, A. X., W. Kisiel, et al. (2006). "ADAMTS1 interacts with, cleaves, and modifies the extracellular location of the matrix inhibitor tissue factor pathway inhibitor-2." J Biol Chem **281**(26): 17827-37.

Wills, A. A., J. E. Holdway, et al. (2008). "Regulated addition of new myocardial and epicardial cells fosters homeostatic cardiac growth and maintenance in adult zebrafish." Development **135**(1): 183-92.

Worley, J. R., M. D. Baugh, et al. (2003). "Metalloproteinase expression in PMA-stimulated THP-1 cells. Effects of peroxisome proliferator-activated receptor-gamma (PPAR gamma) agonists and 9-cis-retinoic acid." J Biol Chem **278**(51): 51340-6.

Yamamura, H., M. Zhang, et al. (1997). "A heart segmental defect in the anterior-posterior axis of a transgenic mutant mouse." Dev. Biol. **186**(1): 58–72.

Yin, V. P., J. M. Thomson, et al. (2008). "Fgf-dependent depletion of microRNA-133 promotes appendage regeneration in zebrafish." Genes Dev **22**(6): 728-33.
Zhao, Y., J. F. Ransom, et al. (2007). "Dysregulation of cardiogenesis, cardiac conduction, and cell cycle in mice lacking miRNA-1-2." Cell **129**(2): 303-17.
Zhao, Y., E. Samal, et al. (2005). "Serum response factor regulates a muscle-specific mircroRNA that targets *Hand2* during cardiogenesis." Nature **436**: 214–220.

Publishing Agreement

It is the policy of the University to encourage the distribution of all theses and dissertations. Copies of all UCSF theses and dissertations will be routed to the library via the Graduate Division. The library will make all theses and dissertations accessible to the public and will preserve these to the best of their abilities, in perpetuity.

Please sign the following statement:

I hereby grant permission to the Graduate Division of the University of California, San Francisco to release copies of my thesis or dissertation to the Campus Library to provide access and preservation, in whole or in part, in perpetuity.

Sarah Morton — Author Signature

23 June 2008 — Date